ABSTRACT

LAWRENCE, CHARLOTTE ANNE. CubeSats for System Evolvability: A Case Study (Under the direction of Dr. Scott Ferguson and Dr. Mark Pankow.)

The advent of the CubeSat architecture – a low cost option, CubeSats afford designers the opportunity to quickly design, manufacture, and launch a system –increasing civilian access to space. Presently, CubeSats have mostly been used by universities and private institutions to test the technology readiness of a component, or simply to say that they have put something into space. Previous satellite designers have explored the idea of modular satellites but very few have gotten off the ground, and many tried to create designs from scratch. Since the CubeSat architecture follows a prescribed standard and there are many commercially available off the shelf components with which to build these CubeSats, this study investigates the use of the CubeSat architecture as a means to modularize a satellite. A case study was selected and the system was decomposed into subsystems and the primary mission requirements were identified. Then a mathematical model of the resulting mission profiles was generated and these identified driving requirements were adapted into penalty functions for a design parameter optimization to generate viable solutions – where the CubeSat architecture was able to achieve the requirements set forth by a case study of FireSat II from *Space Mission Engineering*. The presented results demonstrate that it is indeed possible to decompose a traditional monolithic satellite into a collection of CubeSats and meet or exceed the specified mission requirements; providing the opportunity for increased data collection, the potential for improving system capabilities, and the ability to respond to new situations. It was also seen that the modular satellite architecture proposed could indeed handle requirement changes placed upon the system through the launch of updated systems. Future work includes the expansion of the mathematical model and the exploration of other possible evolutions of the system.

CubeSats for System Evolvability: A Case Study

by
Charlotte Anne Lawrence

A thesis submitted to the Graduate Faculty of
North Carolina State University
in partial fulfillment of the
requirements for the Degree of
Master of Science

Aerospace Engineering

Raleigh, North Carolina

2017

APPROVED BY:

_____	_____
Dr. Andre Mazzoleni	Dr. Mark Pankow Co-Chair of the Advisory Committee

_____
Dr. Scott Ferguson
Co-Chair of the Advisory Committee

DEDICATION

This thesis would not have been possible without my parents, Lisa and Henry Lawrence, and my younger sister, Abigail Lawrence. Thank you all for always supporting me in all that I do. And Arthur the cat Weasley, king of the kittens, who she stress adopted and is living his best life.

BIOGRAPHY

Charlotte Lawrence completed her Bachelor of Science degree in Mechanical Engineering at Duke University in 2015. Upon graduation, she enrolled at North Carolina State University to pursue a Master of Science degree in Aerospace Engineering. There she joined the System Design and Optimization Lab and began working on her thesis under the joint guidance of Dr. Scott Ferguson and Dr. Mark Pankow.

ACKNOWLEDGEMENTS

The author would like to express her appreciation for her advisors Dr. Scott Ferguson and Dr. Mark Pankow, who went above and beyond in their support over the past two years. The author would also like to thank her lab-mates Gordon Beverly III, Krista Edwards, Anya Flowe, Rachel Hough, Daniel Long, Jaekwan Shin, Samantha White, and Kevin Young for their assistance and support during her tenure in the System Design Optimization Lab.

The author would also like to thank the National Science Foundation for their sponsorship and funding of this project. The work presented in this thesis was funded under the NSF sponsored project Exploring System Evolution: a project whose goals were to is to categorize and understand factors that allow for system evolution, develop methodologies for tracking system evolution and maximizing the evolvability of a complex engineered system, and quantify the tradeoff between cost of evolution capacity and benefits of evolution.

TABLE OF CONTENTS

LIST OF TABLES

LIST OF FIGURES

LIST OF SYMBOLS, ABBREVIATIONS AND NOMENCLATURE

Table of Variables

Symbol	Variable	Value	Usage
A_r	Cross-sectional area in the Ram Direction	--	(4)
A_s	Surface Area the Sunlight is impacting	--	(5)
B	Magnetic Field Strength	--	(2),(3)
C_d	Drag Coefficient	--	(4)
c	Speed of Light		
cp_a	Center of Aerodynamic Pressure	--	(4)
cp_s	Center of Solar Radiation Pressure	--	(5)
cm	Center of Mass of the Spacecraft	--	(4)
D	Spacecraft's Residual Dipole Moment	--	(2)
I_x, I_y, I_z	Moments of Inertia	--	(1),(6)
i_s	Inclination Angle of the Sun onto the orbital plane		(7)
M	Magnetic moment of the earth multiplied by the magnetic constant		(3)
m_i	Mass of the ith component	--	(6)
P	Orbital Period	--	(9)
q	Unitless reflectance factor	--	(5)
R	Radius of the Spacecraft		(1),(3)
R_E	Radius of the Earth		(7)
r_i	Perpendicular distance of the ith component's center of mass to the designated axis		(6)
t_{SH}	Time in Shadow	--	(9)
V	Orbital Velocity	--	(4)
θ	Angle between local vertical and principal Z axis	--	(1)
θ_E	Eclipse Angle	--	(8),(9)
θ_G	Geocentric angle	--	(7),(8)
λ	"unitless function of the magnetic latitude that ranges from 1 at the magnetic equator to 2 at the magnetic poles"		(3)
μ	Earth's Gravitational Constant		(1)
ρ	Atmospheric Density	--	(4)
τ_a	Atmospheric Drag Torque	--	(4)
τ_g	Gravity Gradient Torque	--	(1)
τ_m	Magnetic Field Torque	--	(2)
τ_m	Solar Radiation Pressure Torque	--	(5)
Φ	Solar Constant		(5)
φ	Sun incidence angle	--	(5)

1 INTRODUCTION

Complex engineered systems have a large number of components whose overall structure and behavior is [1] the direct result of the interactions of their components. [2] Additionally, the response of system components change according to their interactions with neighboring components [1]. However, as systems become more complex, there is a greater chance of component failure, resulting in decreased performance or loss of function [3]. In this thesis, a monolithic (integral) architecture will be decomposed into a series of distributed (modular) systems in an attempt to both reduce cost and meet the same initial mission requirements while exhibiting the ability to respond to mission changes.

1.1 Background

In software engineering, a system is considered monolithic if its distinguishable aspects are interwoven [4], and a system is considered distributed if the distinguishable aspects are self-contained [5]. When applying this concept to engineering design and complex engineered systems, integral systems have one function that is realized by many different, connected, components [6]. A modular system is a system in which each component has one particular function [6]. According to Hölttä-Otto and de Weck, a module is "commonly defined as an independent chunk that is *highly coupled within, but only loosely coupled to the rest of the system"* [7].Modular systems can exhibit varying degrees of modularity [7–9], requiring advanced planning and forethought to determine proper module combinations, understand module interactions and the optimal degree of modularity.

One of the main drivers for modularity is changing technology over time. Ideally in a complex engineered system with a modular architecture, modules can be swapped out without impacting the performance of other modules, thus allowing the system to evolve into new configurations. Engineering evolvability is based on the biological idea of evolvability. In biology, evolvability is "the degree to which a biological system can evolve into a diversity of adaptive solutions to future environments."[10] A prime biological example is Darwin's Finches. When Charles Darwin explored the Galapagos Islands he discovered 14 different species of finches that were nearly identical to mainland finches but exhibited different beak shapes. These differences in beaks is an example of adaptive radiation – also known as divergent evolution – in which a single common ancestor slowly developed into different species to fill empty ecological niches and reduce competition for crucial resources. [11] However, complex

engineered system do not have the benefit of organically evolving over thousands of generations, and must be strategically designed to handle these changes.

Previous work has determined that evolution capacity of a complex engineered system was directly related to the excess present in the system. In this excess is defined as the surplus in components or systems once the requirements of the component or system are met. [12] Evolvability allows a system to adapt to new situations. To facilitate this ability, the system should possess standard electrical and mechanical interfaces, an open control structure, and the ability to develop past the original intent of the system. [13] Many of these system facilitators are reminiscent of defining features found in modular architectures.

Traditionally, aerospace systems are designed with weight, safety, cost and reliability as driving influences, resulting in an integral architecture [8,14]. By using integral architectures, aerospace systems generally include higher interaction density and a hierarchical architecture of components, both of which have been shown to limit the evolutionary capability of the system. [15] Previous groups have explored the idea of modular satellites [16–21] with limited success, as their programs died in infancy [16,19,20]. Traditional, integral, satellites are time and cost intensive; it can take years to develop, test, certify, and launch a system. Often, by the time a traditional satellite is launched, the technology on board is out of date, yet there is not enough time or money to certify the new technologies and update the system designs without entering a vicious cycle and delaying launch indefinitely. Creating modular, easy to evolve systems would mean that designers could replace and update their systems in pieces rather than in large, slow, and expensive system overhauls. This has the potential to revolutionize design and innovation of the space industry, as, program directors and/or consumers would be more willing to take risks on new technology if costs decreased. Previous groups have explored the idea of non-traditional satellites architectures with limited success.

One of the first attempts to achieve a non-traditional small satellite architecture was the DARPA F6 Fractionated Space program [22]. It was established to create small satellite swarms that communicated wirelessly, shared resources – power and system information - and flew in formation. The theory driving this program was that clusters of small satellites could reduce costs and increase both system survivability and evolvability [23]. However, guidance and control issues associated with formation flying and wireless communication proved to be a significant challenge and the program was shut down after $200 million in research and development [16]. Yet the motivating factors for pursuing small satellite clusters still hold true.

Realizing the scientific benefits of small satellites requires the reconsideration of design strategies for creating satellite clusters.

The interfaces between the satellites in a swarm are not the only paradigm that must be challenged. A little over a decade after Hurricane Katrina, NASA launched the Cyclone Global Navigation Satellite System (CYGNSS). CYGNSS consists of eight microsatellites (approximately 75 lbs. each) capable of creating images of wind speed intensities and storm surges every few hours [18,19]. Effectively the size of a suitcase, this reduction in satellite size was achieved by using reflected ocean surface roughness signals from the GPS system, rather than having the CYGNSS satellites sense this information. However, while there is a functional decoupling in the mission design, each satellite in the cluster is self-contained – each contains its own power, navigation, propulsion, and sensor packages tied into a central bus architecture. The CYGNSS system is also designed to be launched from a Pegasus XL rocket, as it is too large for existing CubeSat launchers. [24] Pursuing design solutions that can be put into orbit using CubeSat launchers could lead to substantial cost savings and easier orbital access. In the ten years it took to design and launch the CYGNSS system, the United States experienced three additional hurricanes that ranked among the top 5 costliest hurricanes in United States History – amounting to $121.5 billion dollars in damages. [25]

Operationally Responsive Space (ORS) is an Air Force satellite architecture designed for rapid responses. By using plug and play, bus-based architectures, the Air Force is exploring how to decrease design time allows for the ability to create a set of satellites which can be designed and launched quickly to respond to changing needs [20]. The program aims to integrate military capability with networked, autonomous, rapidly produced satellites. The goal of this design is not optimization but agility and dynamic fitness [20]. ORS allows for the construction of a satellite in a few short hours. However even ORS cannot avoid the high cost of launch. Test satellites are around 450 kg, mandating primary payload status and an inherently expensive launch cost [26].

However in 1999 Jordi Puig Suari at California Polytechnic State University, Robert Twiggs at Stanford University, and their teams developed the CubeSat Standard "to provide inexpensive and timely access to space for small payloads." [27] Designed to be complete in "two years or less," [27], CubeSats provides "practical, reliable, and cost-effective launch opportunities." [27] To facilitate this, the CubeSat architecture is standardized [28] and a whole subsection of the space industry has sprung up to meet the needs of aspiring students and companies who desire

to launch their own satellite. Civil, commercial, military, and university developers have all launched CubeSats since 1999 [29], and are continuing to do so and as technology improves, so to do the capabilities of the CubeSats designed and launched. [29] Still a popular architecture, with CubeSat deployments attached to launches through Spring of 2018 [30], CubeSats are self-contained modules that can be combined to form a larger system. This work will use the CubeSat architecture and a sample mission to determine potential performance gains by using this modular architecture in place of a traditional monolithic architecture.

1.2 Selection of FireSat II as a Case Study

When determining the sample mission for the case study examined in this work, two factors were considered: value of mission and level of detail to compare with. FireSat II was selected as the Case Study for this thesis because it met both of these factors. FireSat II is an example mission in *Space Mission Engineering: The New SMAD*, a popular text for those who want to learn about aerospace engineering and aerospace system design. As an example mission, FireSat II has defined mission objectives and requirements to which the proposed alternatives could be compared. With its primary mission objective being to "… detect, identify, and monitor forest fires throughout the United Sates, including Alaska and Hawaii, in near real time and at a low cost," [31] FireSat II provides the opportunity for genuine scientific merit. By selecting a well-documented mission like FireSat II there is ample information for system architecture level comparisons.

Monitoring forest fires is becoming increasingly important. Over the past twenty years, damage from wildfires has increased dramatically – in 1985 2.9 million acres were burned and in 2015 10.1 million were burned [32]. Figure 1.1 was created from data published by the National Interagency Fire Center; it demonstrates that though the number of fires has remained relatively constant over the past 20 years, the amount of land ravaged by these fires has increased dramatically. [33]

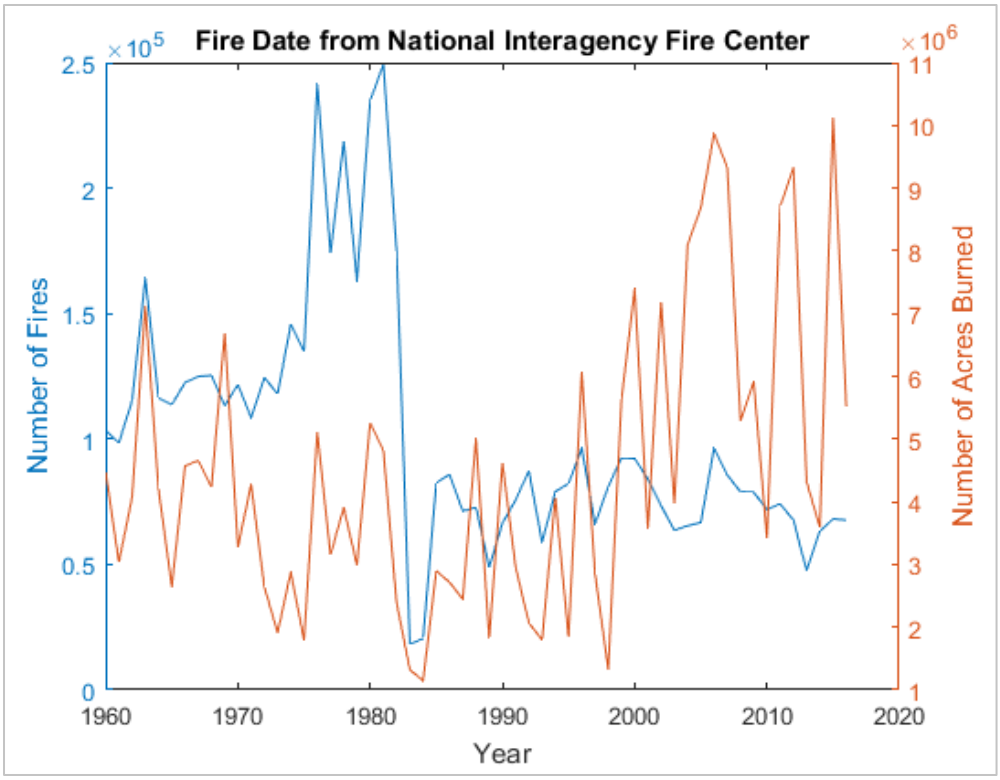

Figure 1.1 – Acres Burned and Number of Fires since 1960, data supplied by the National Interagency Fire Center [33]

Anthropogenic climate change has been identified as one of the driving factors increasing the total area of acres burned. "Climate change contributes to forest fires in a number of ways. Fires kill off trees and other plants that eventually dry and act as the fuel to feed massive wildfires. Global warming also increases the likelihood of the dry, warm weather in which wildfires can thrive."[32] Global warming increases wildfire risk in four ways: longer fire seasons, drier conditions, more fuel for forest fires, and increased frequency of lightning. [34,35] This past year, 2016, was the warmest year on record since the National Oceanic and Atmospheric Administration (NOAA) began tracking global temperatures 137 years ago. It is also the third year in a row that the most recent year has surpassed the previous as the warmest year on record [36].

Despite this, the overall increase in fires since 1980 can be contributed to more than just climate change – the other factors can be attributed to humans themselves. [37] In the past, wildfire fighting organizations have worked to eliminate every fire, however forest fires are crucial part of the environment life cycle and can actually decrease the severity of future fires by eliminating tinder. By constantly putting out fires and performing other fire suppression

tactics, these areas are building up more dry fuel which later fuels even larger fires [38–40]. And thus, by over regulating the forest fires the number and severity of fires has increased [37]. Additionally, humans are the initial cause of 84% of wildfires while lightning only started the remaining 16%. [37] Additionally, fire season is extended by 50 days when human fires considered, [37] thus increasing both the length and severity of the each fire season. Fire season length in a region is defined by the date of the first fire discovery to the date of the last control of a fire. Since 1973, fire season length in the Western United States has increased from 138 days to 222 days. The first discovery of a fire has moved 34 days earlier, and the last controlled fire has occurred 50 days later than average. [40] Figure 1.2 below illustrates the changes in fire season length over time where the length of the fire season is defined as the difference between the first discovery day and the last control day.

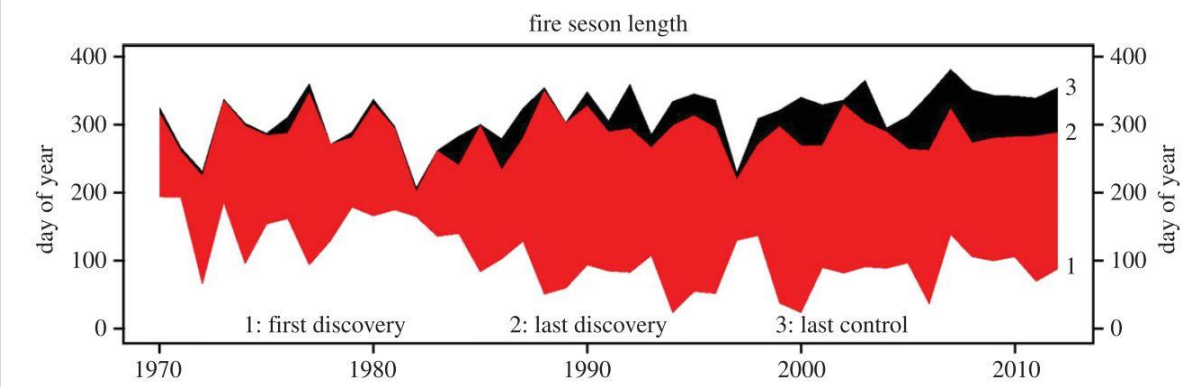

Figure 1.2 – Fire Season Length [40]

With fires starting earlier and ending later, there is great cause for identification and tracking on fires as we move toward longer and more intense seasons. Thus, FireSat II not only provides enough information for system comparison but also provides environmental information with the potential for genuine impact.

This work will look at the FireSat II mission and design a modular system using the CubeSat architecture to meet the same mission requirements. By using a well characterized earth based imaging mission as the test case, this not only provide objectives for a mission, but it also provides a baseline for system architecture comparison for a thorough examination of the benefits and drawbacks of such a system.

1.3 Research Question

Considering previous attempts to create modular satellite systems as well as a the potential for genuine scientific merit, the work in this thesis will create a thorough understanding of the

system characteristics required to decompose a monolithic architecture into a series of distributed systems in order to monitor forest fires by considering the following research question.

What are the performance gains of observing wildfires using a collection of CubeSats instead of a monolithic satellite?

Using the CubeSat architecture as the framework for this mission, a model will be generated to determine potential performance gains by using this modular architecture in place of a traditional monolithic architecture proposed in *Space Mission Engineering*. By selecting a well-documented mission like FireSat II there is ample information for system architecture level comparisons as well as previous iterations of the FireSat design by which the capacity for evolvability for the proposed system can be examined.

Through this research question, a mathematical model of a CubeSat capable of meeting the system requirements of FireSat II will be created. Using this model, potential evolutions can be explored by manipulating the requirements placed on the system.

1.4 Summary of Chapters

The rest of the work done for this thesis is broken down into 4 additional chapters. Chapter 2 decomposes the satellite into its subsystem and identifies the important aspects for creating a mathematical model. Chapter 3 develops the components of the mathematical model and then combines them for evaluation through the use of a genetic algorithm and penalty functions. Chapter 4 implements the model developed in Chapter 3 and examines the implications of manipulating the requirements. And Chapter 5 concludes the research presented in this thesis and provides direction for future work on this topic.

2 SYSTEM DECOMPOSITION

Decomposing complex engineered systems can be a finicky task; determining how and why to divide a system into different subsystems can be frustrating and time consuming and a variety of methods [7,41–43] have been developed to assist in understanding the relationship between different system components. Even with a (relatively) common system like a satellite, different entities define the subsystems in different ways [44–49]. One common breakdown of a satellite results in six subsystems [47]:

- Attitude and Orbit Control System (AOCS) – containing Propulsion, Guidance, Navigation, and Control (GNC), and Attitude Determination and Control (ADC)
- Command and Data Handling (CDH)
- Telemetry, Tracking and Command (TTC)
- Structure and Mechanism (MECH)
- Power
- Payload

Another breaks the satellite down into seven subsystems [49]:

- Propulsion,
- Attitude Determination and Control (ADC)
- Command and Data Handling (CDH)
- Telemetry Tracking and Command (TTC)
- Power
- Mechanical
- Thermal

The primary differences are the inclusion versus exclusion of the payload, and the grouping of varying components that have an impact on orbit. For example, in the first breakdown, ADC and propulsion are combined with GNC to create the AOCS subsystem. In the second breakdown, power and ADC are their own subsystems and GNC is incorporated into ADC. *Space Mission Engineering* uses the second breakdown presented and divides the satellite into seven subsystems. This work follows along with this subsystem breakdown because the primary design drivers of each subsystem are defined within *Space Mission Engineering*, and in doing so offers a springboard for developing a system model of a satellite. In this work, design drivers are defined as the variables which have the largest influence in the final design of the particular

subsystem, while factor are those that are still impactful bit mainly influence or are influenced by the drivers. The following system map, seen in Figure 2.1, and design structure matrix (DSM), seen in Figure 2.2, were created to help visualize the complexity and interactions between the identified variables.

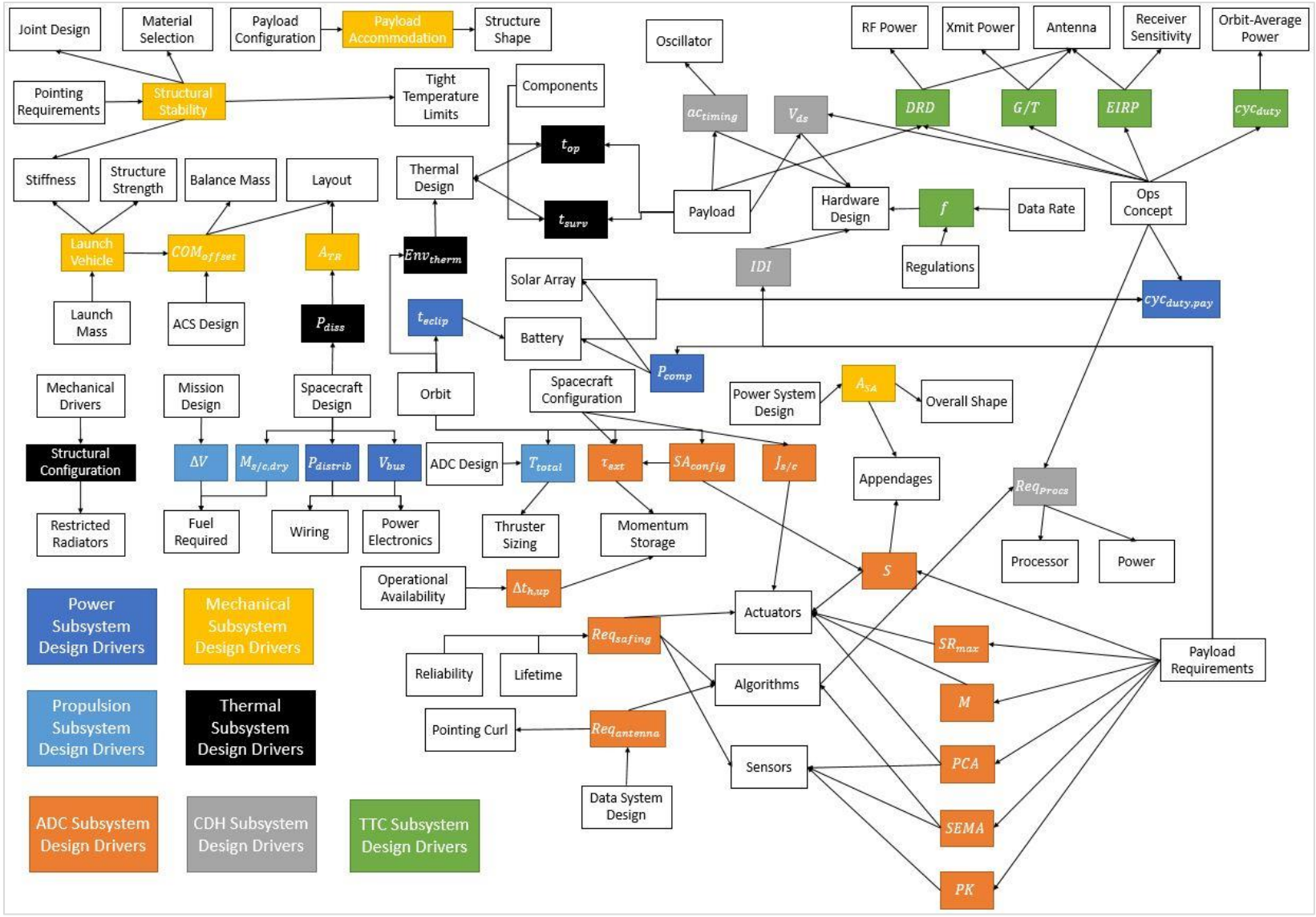

Figure 2.1 – System Map from *Space Mission Engineering*

The seven subsystems mentioned are identified in Figure 2.1 by color. Yellow is the Mechanical Subsystem, black is the Thermal Subsystem, Light Blue and Dark Blue are the Propulsion and Power Subsystems respectively, Orange is the Attitude Determination and Control (ADC) Subsystem, Green is the Telemetry, Tracking and Command (TTC) Subsystem, and Grey is the Command and Data Handling (CDH) Subsystem. This information is also presented in Figure 2.2 below as a Design Structure Matrix (DSM). DSMs provide an alternative method to visualize the interactions between components in a system. In this figure, the black diagonal occurs where the components intersect with themselves and the blue boxes indicate where they interact with other components. Moving along a row shows the output of that particular component, and conversely, going down a column shows the inputs impacting that particular component.

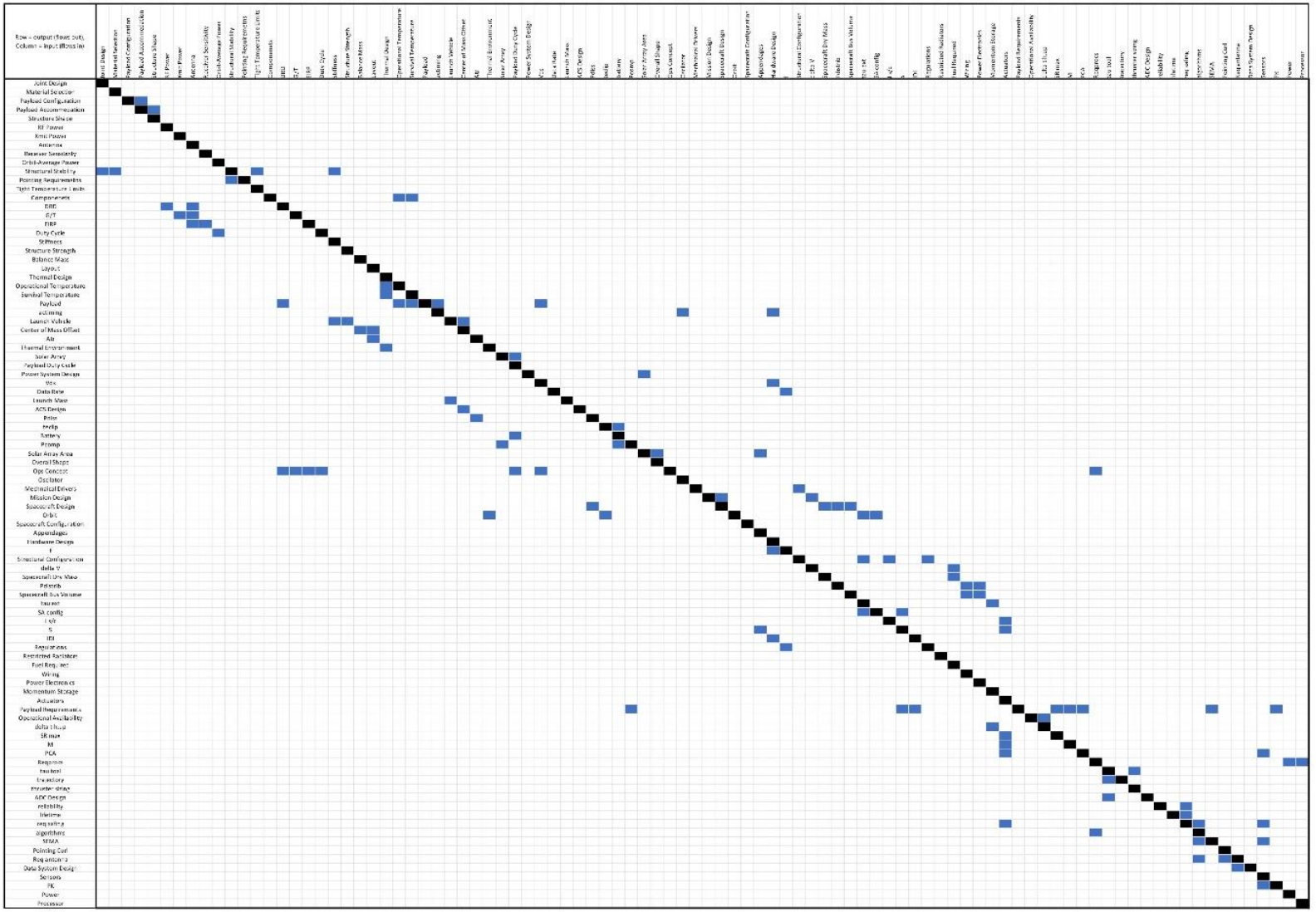

Figure 2.2 – Design Structure Matrix created based on the Drivers and Factors presented in *Space Mission Engineering*

As discussed in Chapter 1, FireSat II was chosen as the case study by which a system model was developed because the details of all the subsystems are readily available, as well as the potential for genuine scientific merit regarding wildland fires in the United States. The primary and secondary mission objectives are presented in Table 2.1 below.

Table 2.1 - FireSat II Mission Objectives [31]

Primary Mission Objective
To detect, identify, and monitor forest fires throughout the United Sates, including Alaska and Hawaii, in near real time and at a low cost
Secondary Mission Objectives
To demonstrate to the public that positive action is underway to contain forest fires
To collect statistical data on the outbreak and growth of forest fires
To monitor forest fires for other countries
To collect other forest management data

The options hypothesized in [50] as possible solutions are presented in Table 2.2 below.

Table 2.2 - The 2 Principal Options for FireSat II [50]

Element	**FireSat II**	
	Option A	**Option B**
Mission Concept	Automated fire detection on board the spacecraft with direct downlink	Manual fire detection at the ground station with results relayed via FireSat II
Subject	Heat from forest fire	
Payload	Small-aperture IR	Large-aperture IR
Spacecraft Bus	Small, 3-axis, Earth-pointing	Mid-large size, 3-axis, Earth-pointing
Launch System	Small launch vehicle	Large launch Vehicle
Orbit	LEO, 2 satellites, 55 degrees	GEO, 1 satellite centered over the west coast of the U.S.
Ground System	Single, dedicated ground station	
Communications Architecture	TDRS data downlink; commercial links to users	Direct to station; results relayed to users via FireSat II
Mission Operations	Continuous during fire season, partial otherwise	

This research aims to expound upon Option A by constructing feasibility and trade studies to determine whether or not a collection of disaggregated CubeSat sized modules could achieve comparable or improved functionality. Option B was not explored further because of the orbit and payload differences. The average altitude of CubeSat range between 200 and 1,000 km [51] and when considering the orbits of Option A and Option B, Option A occurs in low earth orbits

(LEO) which are defined as orbits that are less than 3,000 km [52] while Options B posits geosynchronous (GEO) orbits which occur at 35,856 km [52]. From this, the average CubeSat orbit more closely aligns with LEO orbits. Additionally, small-aperture IR cameras can be purchased as commercial off the shelf products [53] while large-aperture IR cameras are customized. Using this subsystem breakdown as a framework, each of the following sections explains the principal drivers and factors of the given subsystem and simplifies the subsystem with the modeling assumptions made. Each section also contains visual representations of the drivers, factors, and interactions, where drivers are represented by solid color blocks and factors are white boxes.

2.1 Propulsion Design Drivers and Factors

The three main drivers presented for the propulsion subsystem are: "Delta V" (ΔV), "Spacecraft Dry Mass" ($M_{s/c,dry}$), and "Thrust for Maneuvers and Control" (T_{total}). "Delta V" is defined as the total change in velocity required throughout the mission lifespan. [54] "Spacecraft Dry Mass" is the mass of the spacecraft before loading any propellants [55], and "Thrust for Maneuvers and Controls" is the total amount of thrust need through the mission lifespan to properly maneuver and control the spacecraft. These three drivers are initially related to six factors: "Mission Design," "Spacecraft Design," "Trajectory," "ADC (Attitude Determination and Control) Design," "Fuel Required," and "Thruster Sizing." The relationships between the subsystem factors and drivers are illustrated in Figure 2.3 below.

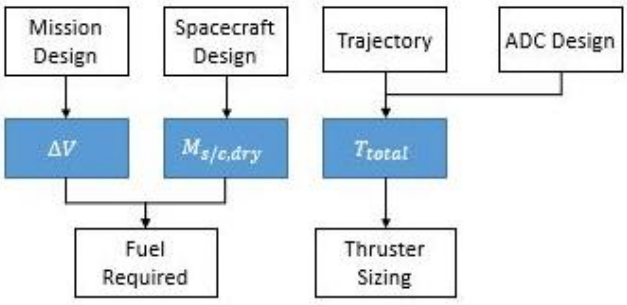

Figure 2.3 - Propulsion Subsystem Drivers

One of the simplifications made to the entire mission architecture was the elimination of station keeping. When including propulsion systems in CubeSats, it introduces further system safety checks and limits the number of launches where the satellite could be a secondary payload. For this mission (FireSat II), a collection of spin-stabilized CubeSats will tumble through LEO collecting data as they de-orbit. Adding a propulsion system to a CubeSat

increases the regulations and restricts the number of launches in which the system is an eligible secondary payload. [28] Despite the decision to forgo the inclusion of any propellant in the design of this mission, the Propulsion Subsystem remains a subsystem because of the potential for the addition of a propulsion system in other CubeSat missions. Considering these regulations and restrictions, the map for the propulsion subsystem can be simplified to Figure 2.4.

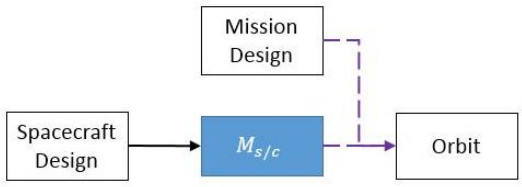

Figure 2.4 – Simplified Propulsion Subsystem Drivers

In performing initial simplifications the "Thrust for Maneuvers and Control" and "Delta V" drivers of the system were eliminated. Also, the three factors associated solely with these drivers – "Fuel Required", "Thruster Sizing", and "Attitude Determination and Control (ADC) Design" – do not need to be considered in this subsystem map. Additionally, the "Trajectory" factor was combined with the "Orbit" factor to streamline vocabulary as orbit, not trajectory, is the vernacular used with satellites.[56] Another change was the addition of a connection between the "Mission Design" factor and the "Orbit" factor because this mission is un-propelled and therefore the mission design has a direct input on the orbit and resulting lifespan of the CubeSats. In a similar vein, the "Dry Mass of the Spacecraft" driver has been converted to the "Total Mass of the Spacecraft ($M_{s/c}$)," since the spacecraft will not be losing mass due to the expulsion of propellant. Likewise launch mass is incorporated into the "Total Mass of the Spacecraft" driver. A connection has been added between the "Orbit" factor and the "Total Mass of the Spacecraft" driver as "Total Mass of the Spacecraft," too, has a bearing on the orbit of the spacecraft over time. Through the rest of this thesis, these added connections are noted by dashed purple arrows. After the initial simplification, the remaining factors and drivers were explored further do determine their importance in the system model and the creation of the mathematical model.

In the context of this work, "Spacecraft Design" was taken to mean the overall system design of the spacecraft required to complete the specified mission. When considering the "Spacecraft Design" driver under this explanation, the inclusion of this driver in the subsystem map was redundant.

The "Mission Design" factor contains the overarching goals and objectives of the mission. In the subsystem driver map this impacts the "Orbit" and "Payload" factors. When developing the model, the mission objectives for FireSat II were extracted from [31]; originally presented in Table 2.1, they are reiterated below.

Primary Mission Objective
To detect, identify, and monitor forest fires throughout the United Sates, including Alaska and Hawaii, in near real time and at a low cost
Secondary Mission Objectives
To demonstrate to the public that positive action is underway to contain forest fires
To collect statistical data on the outbreak and growth of forest fires
To monitor forest fires for other countries
To collect other forest management data

These mission objectives are broken down even further into Level 1 mission requirements which can be seen in Appendix 7.1. Eight mission requirements have been identified as main components to the "Mission Design" factor. They are presented in Table 2.3 below. The numbers in parenthesis correspond to the requirement number in the requirements document, see Appendix 7.1.

Table 2.3 - Targeted Mission Requirements [28,31]

Payload Requirements	
Ground Sample Distance (R1.03)	The mission shall be able to detect forest fires at up to 50m in resolution
Geolocation (R1.04)	The mission shall be able to determine forest fire locations within 1km geolocation accuracy
Coverage (R1.05)	The mission shall be able to cover specified forest areas within the US at least twice daily
Lifespan (R1.08)	The mission will last a minimum of 8 years
Cost (R1.14)	The mission will have a recurring cost of less than $3M/year
Ground Stations (R1.19)	The mission will be interoperable through NOAA ground stations
Sensitivity (R1.25)	The mission must be able to monitor changes in the mean forest temperature to +/- 2°C
Size Constraint (R1.33)	The mission will fit within a Standard CubeSat Size

Another driver that remained in Figure 2.4 after the initial simplifications was "Total Mass of the Spacecraft." This driver, along with the "Overall Shape," "Appendage," and "Structure Size" have been combined and reclassified as the "CubeSat Size" driver. This amalgamation of multiple factors and drivers originally identified in [31] is valid because of the size and space restrictions placed on the CubeSat Architecture and subsequent deployment devices. The

overall shape of the spacecraft will be dictated by the size of the CubeSat structure and whether or not there are deployable solar arrays. CubeSats come in a variety of sizes measured in U's – where each U is approximately 10 cm x 10 cm x 10 cm and no more than 1.33kg. Different CubeSat dimensions and masses are presented in the Table 2.4 below. Note that the mass presented in Table 2.4 is the mass of the CubeSat at launch but since the spacecraft is not losing mass due to propulsion this mass is the mass throughout the entire mission.

Table 2.4 – CubeSat Sizes and Corresponding Dimensions [28]

CubeSat Dimension Specifications				
Size	*Length (mm)*	*Width (mm)*	*Height (mm)*	*Mass (kg)*
1U	100	100	100	1.33
1.5U	100	100	156	2.00
2U	100	100	220	2.66
3U	100	100	327	4.00

The final selection for the size of the CubeSats will be dependent on the volume of the components. The cost of the outer CubeSat structure will be approximated based on available busses. Table 2.5 below has a sample of commercially available bus sizes and shapes pulled from CubeSat Shop [57–59]. Though there are guidelines in place from the CubeSat Design Standard, some commercially available busses deviate from those guidelines and come in sizes larger than 3U. Costs are presented in both Euros and United States Dollars (USDs) in the table below because the original price was in Euros and the prices were converted for consistency on April 15, 2017 when the exchange rate was 1.06 USDs to the Euro.

Table 2.5 – Commercially available CubeSat Structures [57,58]

Commercial Off the Shelf CubeSat Structures						
Name	*Brand*	*Cost*	*Structure Mass (g)*	*Length (mm)*	*Width (mm)*	*Height (mm)*
1-Unit CubeSat Structure	ISIS	$2,650 (€2,500)	107.7	100	100	113.5
1.5-Unit CubeSat Structure		$3,339 (€3,150)	184.5			170.3
2-Unit CubeSat Structure		$3,339 (€3,150)	206			227
2-Unit Long Stack CubeSat Structure		$3,339 (€3,150)	197.9			
3-Unit CubeSat Structure		$4,134 (€3,900)	304.3			340.5
6-Unit CubeSat Structure		$8,321 (€7,850)	1100		226.3	
8-Unit CubeSat Structure		$10,070 (€9,500)	1871	226.3		227

An orbit is defined as the "path of a spacecraft or natural body through space."[52] The orbits of the spacecraft analyzed in this thesis were defined and examined using Keplerian techniques. To approximate orbits as Keplerian, the following conditions must be met: 1) the central body is spherically symmetric, 2) the central body mass is much greater than that of the orbiting body, and 3) the central body and the orbiting body are the only two bodies in the system. [52] When working with a satellite in LEO, the central body is Earth, a celestial body which has a flattening of 0.0033528 [60] or 0.3% - this is close enough to zero that the first condition is satisfied. The Earth has a mass of 5.97237×10^{24} kg and a CubeSat mass ranges from 1.33 kg to 4.00 kg – the Earth is 24 orders of magnitude larger than the proposed CubeSats and thus the second condition is satisfied. Thirdly, since the mass of the earth is so much larger than the average mass of spacecraft in LEO [61] the primary gravitational force impacting the motion of the satellite is the earth and the system satisfies the third condition required to use Keplerian orbit approximations. Keplerian orbits can be defined by the following six elements:

1. Eccentricity (e) – "the ratio of the minor to major dimensions of an orbit." [62]
2. Semimajor Axis (a) – "one half of the major axis dimension.," [62] for circular orbits this is equivalent to the radius.
3. Inclination (i) – "the angle between the orbit plane and the reference plane or the angle between the normal to the two planes" [62]
4. Argument of the Periapsis (ω) – "the angle from the ascending node to the periapsis, measured in the orbital plane in the direction of spacecraft motion." [62]
5. Longitude of the Ascending Node (Ω) – "the angle between the vernal equinox vector and the ascending node measured in the reference plane in a counterclockwise direction as viewed from the northern hemisphere." [62]
6. True Anomaly (θ) – "the sixth element locates the spacecraft position on the orbit" [62]

"Orbit" as a design factor is effected by the "Mission Design" factor and regulations placed on space systems. Regulations are not included in the subsystem map because there are regulations affecting almost every design driver and factor and will be considered on a case by case basis when applicable. In this subsystem, the "Orbit" factor is only effected by the "Mission Design" factor and as the system has no means for propulsion, the initial altitude of the mission is the driving aspect that dictates the orbit. Lower and upper limits for the lifetime of the mission are dictated by "Mission Design" and the United Nations regulation helping to limit space debris, respectively. In using FireSat II as a case study, the mission must last eight years (see Table 2.3) and the primary regulation affecting the orbit of the spacecraft is, all un-propelled satellites must be in orbits that "avoid the long term-presence" in LEO [63].

From these explorations and implications, the following map, Figure 2.5, of the Propulsion Subsystem was created. It is important to note that four more design drivers were added to this map because it was important to maintain driver and factor relationships through the combination of the "CubeSat Size" driver. These additional drivers – "Center of Mass Offset," "Stability," "Solar Array Area," and "Payload Accommodation" – are a part of the Mechanical Subsystem and will be addressed in Section 2.6.

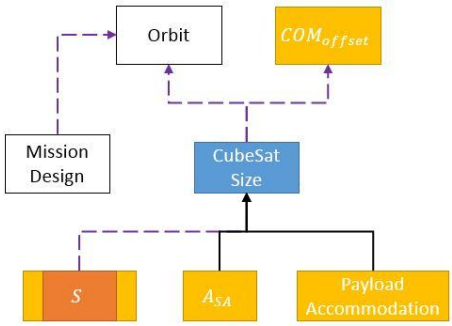

Figure 2.5 –Final Map of Propulsion Subsystem Drivers

2.2 Attitude Determination and Control (ADC) Design Drivers

The primary purpose of the Attitude Determination and Control Subsystem (ADC) is to monitor and modify the spacecraft attitude and trajectory. Attitude refers to the three dimensional orientation of the spacecraft in the specified reference frame [64]. One of the most complex satellite subsystems, the ADC subsystem is presented as having twelve primary design drivers. Their names, abbreviations, and definitions are presented in Table 2.6 below.

Table 2.6 – ADC Design Drivers

ADC Design Drivers		
Name	*Abbreviation*	*Definition/Explanation*
Pointing Control Accuracy	PCA	"How accurately the spacecraft must point will impact the accuracy of the sensors and the precisions of the actuators" [54]
Pointing Knowledge	PK	"The on-board knowledge is typically better than the pointing because of the errors introduced by the actuators. The ground knowledge of pointing is generally better than the on-board solution."[54]
Stability	S	"The stability of the payload pointing will be affected by imbalance of reaction wheels and motion of spacecraft appendages as well as structural stiffness and stability over temperature, both for the payload mounting and the ADC sensor and actuator mounting."[54]
Maneuvers	M	Use of the propellant/propulsion system to make changes to the orbit of the spacecraft.
Max Slew Rate	SR_{max}	Slew rate is the rate at which the position of an antenna is changed [65]
Spacecraft Moment of Inertia	$J_{s/c}$	"a tensor that determines the torque needed for a desired angular acceleration about a rotational axis. It depends on the body's mass distribution and the axis chosen, with larger moments requiring more torque to change the body's rotation."[66]

Table 2.6 – ADC Design Drivers Continued

Name	*Abbreviation*	*Definition/Explanation*
External Torques	τ_{ext}	There are four environmental factors that create external toques on the spacecraft which the ADC subsystem need to mitigate: gravity-gradient effects, magnetic fields torques on a magnetized vehicle, impingement by solar-radiation, and aerodynamic torques for LEO satellites. [64]
Time between momentum unloads	$\Delta t_{h,un}$	Momentum is created by reaction wheels and stored until the spacecraft dumps the excess momentum using thrusters or electromagnets. Dumping momentum adds instability to the system so the longer between momentum unloads the better. [54]
Sun, Earth, Moon Avoidance	$SEMA$	Depending on the payload requirements, the CubeSat may need to avoid exposing a particular side to direct sunlight, or something like that. This is dependent on the payload and impacts the sensor choice and the algorithms used to control ADC.
Safing Requirements	Req_{safing}	Designing a system to fail safe requires the following three things: 1) "Power Positive – more power being generated by the solar arrays than being consumed by the system, so that the battery recharges. If the battery becomes fully discharged, there is no longer any way to communicate with the spacecraft y, and the attitude control system will no longer function, preventing a change in attitude that would allow recharging of the battery. In other words, a spacecraft with a dead battery is dead. 2) Thermally Benign – all temperatures must stay within survival limits 3) Commandable – the orientation of antennas and the configuration to the receiver must be such that the ground can send commands in order to correct problems. The transmitter is frequently off in safe mode to save power, but the mode must support output of housekeeping telemetry when the ground commands transmit, to enable troubleshooting"[54]
Solar Array Configuration	SA_{config}	ADC systems control the pointing of solar arrays to maximize the amount of power generated. Depending on whether or not the CubeSat is designed with deployable solar arrays can impact this.

Antenna pointing requirements	$Req_{antenna}$	Similarly, ADC systems need to be aware of the location of earth so that they can adequately orient the antenna for ground communications.

These design drivers and the factors that influence them are illustrated in Figure 2.6.

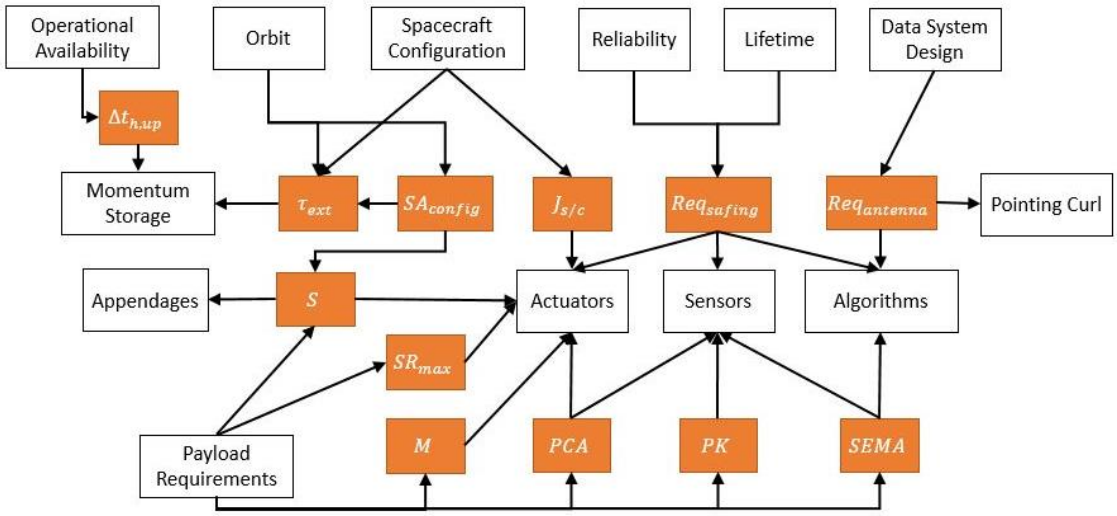

Figure 2.6 – ADC Design Drivers

Figure 2.6 is simplified to Figure 2.7 after making the following changes. "Maneuvers" is eliminated as a design driver as there is no propulsion system planned for this spacecraft. "Safing Requirements" driver has also been removed since CubeSats are cheap to produce. This also allowed for the removal of "reliability" and "lifetime" as factors. And, connections (noted as purple dashed arrows) have been added between "Pointing Control Accuracy" and "Pointing Knowledge" to "Stability" as the accuracy and control of the spacecraft pointing will have an impact on the stability of the CubeSat.

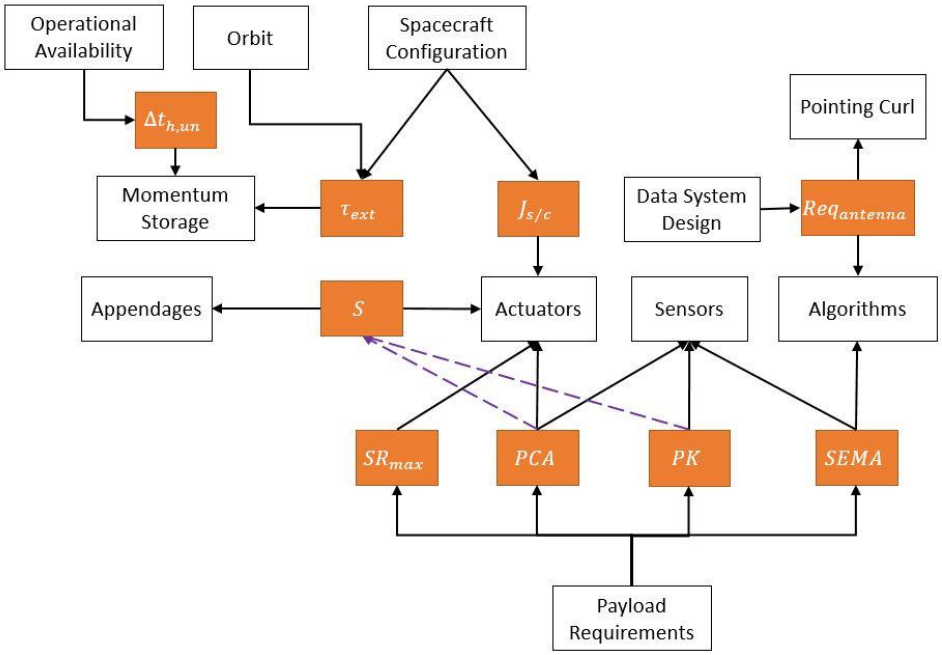

Figure 2.7 – Simplified ADC Subsystem Drivers

After the initial simplification, the remaining factors and drivers were explored further do determine their importance in the system model and the creation of the mathematical model.

As stated in Table 2.6, there are four environmental factors that create external toques on the spacecraft: gravity-gradient effects, magnetic fields torques on a magnetized vehicle, impingement by solar-radiation, and aerodynamic torques for LEO satellites. [64] Gravity-Gradient effects are caused when the center of gravity and center of mass of a spacecraft are not aligned with respect to the local vertical. [64] The center of gravity of a spacecraft is dependent on the attitude of the spacecraft relative to the body it is orbiting – in this case earth. The gravity-gradient torque increases as the angle between the local vertical and the minimum principal axis of the spacecraft as the gravity-gradient effect is creating a torque to align the two. Gravity-Gradient torque can be calculated simply using the following equation.

$$\tau_g = \frac{3\mu}{2R}\left|I_z - I_y\right| \sin 2\theta \quad (1)$$

Where μ is Earth's gravitational constant, R is the distance from the spacecraft to the center of the earth in meters, θ is the angle between the local vertical and the principal Z axis, and I_y and I_z are the moments of inertia about the Y and Z axes in kg*m².

Magnetic torque occurs when a spacecraft's residual magnetic field does not align with earth's magnetic field and can be calculated simply by multiplying the spacecraft's residual dipole moment, D, in A*m² by the magnetic field strength, B, in tesla.

$$\tau_m = DB \tag{2}$$

The magnetic field strength, B, can be calculated in the following equation.

$$B = \frac{M}{R^3}\lambda \tag{3}$$

Where M is the magnetic moment of the Earth multiplied by the magnetic constant, R is the distance from the spacecraft to the center of the earth in meters, and λ is a "unitless function of the magnetic latitude that ranges from 1 at the magnetic equator to 2 at the magnetic poles" [64].

Atmospheric drag torques occur when the center of atmospheric pressure is not aligned with the center of mass.[64] It can be estimated using the following equation.

$$\tau_a = \frac{1}{2}\rho C_d A_r V^2 (cp_a - cm) \tag{4}$$

Where the ρ is the atmospheric density in kg/m^3, C_d is the drag coefficient – usually between 2.0 and 2.5 for spacecraft [64], A_r is the cross-sectional area in the ram direction – direction perpendicular to the movement of the spacecraft, V is the orbital velocity of the spacecraft in m/s, and cp_a and cm are the centers of aerodynamic pressure and center of mass, respectively, in meters.

Because of the momentum of sunlight, when it reflects on or is absorbed by objects it transfers that energy to the object. In space, the magnitude of these effects is much closer to the magnitude of other physical effects and can impact the movement of the spacecraft. The following equation can be used as a "good starting estimate" for the torques generated by solar radiation pressure by assuming "a uniform reflectance" of the spacecraft [64].

$$\tau_s = \frac{\Phi}{c} A_s (1 + q)(cp_s - cm) \cos\varphi \tag{5}$$

Where Φ is the solar constant adjusted for the actual distance from the sun, c is the speed of light, A_s is the surface area the sunlight is impacting in m^2, q is the unitless reflectance factor – ranging from 0 for perfect absorption to 1 for perfect reflection, φ is the sun incidence angle, and cp_s and cm are the centers of solar radiation pressure and center of mass, respectively, in meters.

From Figure 2.7, "Orbit" only impacts "External Torques" in the ADC Subsystem. Of the variables in the previous 5 equations – Equations (1), (2), (3), (4), and (5) – only ρ, V, R, D, B, and λ are a function of the orbit of the spacecraft. The other variables are either constants or dependent on the structure of the spacecraft. Further development of the mathematical model and the relationship between equations is presented in Chapter 3.

There are two main types of actuators: momentum-exchange devices and external torque actuators. Momentum-exchange devices conserve the angular momentum of the spacecraft for future use, while external torque actuators, when activated, change the angular momentum of the spacecraft. [64] Reaction and momentum wheels, control moment gyros (CMG), and magnetic torquers all fall under the momentum-exchange category while thrusters are external torque actuators. As this system is comprised of CubeSats, thrusters are removed as a possible type of actuator. A quick inventory of CubeSatShop [67–72] provides options for attitude actuators, summaries are presented in Table 2.7 and Table 2.8 below. Costs are presented in both Euros and United States Dollars (USDs) in the table below because the original price was in Euros and the prices were converted for consistency on April 15, 2017 when the exchange rate was 1.06 USDs to the Euro.

Table 2.7 – Possible Reaction Wheels [67,69]

CubeSatShop Reaction Wheels					
Name	*Brand*	*Cost*	*Mass (g)*	*Torque (mNms)*	*Power (W)*
Cubewheel Small	CubeSpace	$4,558 (€4, 300)	60	1.7	0.12
Cubewheel Medium		$5,724 (€5,400)	140	10	0.24
Cubewheel Large		$6,890 (€6,500)	220	30	0.27
MAI – 400	Maryland Aerospace	$7,100	110	0.635	0.85

Table 2.8 – Possible Magnetic Torquers [68,70,71]

CubeSatShop Magnetic Torquers					
Name	*Brand*	*Cost*	*Mass (g)*	*Moment (+/- Am²)*	*Power (W)*
Cubetorquer	CubeSpace	$1.696 (€1,600)	28	0.24	--
Cubecoil			46	0.13	--
iMTQ	ISIS	$8,480 (€8,000)	196	0.2	1.2
MT01 Compact Magnetorquer	EXA	$848 (€800)	75	0.19	0.75

When determining the momentum capacity necessary for each spacecraft, cyclic and secular disturbances in the spacecraft's movement need to be distinguished. [64] Reaction wheels must be able to store the full cyclic component without the need for frequent momentum dumping,

the average disturbance torque for ¼ to ½ of an orbit determines the minimum capacity of the wheels. [64] Since these actuators are used to store excess momentum in addition to attitude control, the "Momentum Storage" factor was incorporated into the "Actuator" driver.

Additionally, as the spacecraft moves though the orbital environment, momentum is generated by reaction wheels in an attempt to stabilize the system and is stored until the spacecraft has the opportunity to dump the excess momentum using thrusters or electromagnets. Typically, dumping momentum adds instability to the system so a longer time between momentum unloads is preferred. [54] However, the "Time between momentum unloads" driver has been eliminated because of the lack of additional momentum storage.

Moment of Inertia

The "Moment of Inertia" of an entire spacecraft is calculated by taking the sum of the mass moments of inertia for the varying components about a particular axis. In preliminary calculations each component used in the spacecraft is approximated as a point mass. The approximation equation is presented below.

$$I = \sum_i m_i r_i^2 \tag{6}$$

Where m is the mass of the particular component and r is the distance from that component's center of mass to the axis around which the moment of inertia is being taken.

The "Antenna Requirements" driver was combined with the "Antenna" factor to create a new "Antenna" Driver. "Antennas are used to launch an electromagnetic wave into space or receive an electromagnetic wave, and to amplify the transmitted or received signals that travel in particular directions relative to the antenna."[73] From CubeSatShop [74–76], there were two distinct options: the L-Band deployable antenna from HCT and the product family of UHF/VHF frequency deployable antennas from ISIS. These deployable antennas from ISIS came with the following options: supply voltage – either 3.3 V or 5V, frequency type – either UHF or VHF, or type of antenna – turnstile, dipole, monopole, or combined. These ISIS combinations ranged from $4,770 (€4,500) to $5,830 (€5,500) while the HCT antenna was $11,000. The ISIS antennas also take up about 1/5th of the volume that the HCT antenna does. Costs are presented in both Euros and United States Dollars (USDs) in the table below because the original price was in Euros and the prices were converted for consistency on April 15, 2017 when the exchange rate was 1.06 USDs to the Euro.

Table 2.9 – Possible Antennas [74,75]

CubeSat Shop Antennas					
Name	*Brand*	*Cost*	*Supply Voltage (V)*	*Frequency Type*	*Antenna Variety*
Helios Deployable Antenna	HCT	$11,00	8	L-Band	Helix
Deployable Turnstile Antenna System	ISIS	$5,830 (€5,500)	3.3	UHF	Turnstile
Deployable Turnstile Antenna System	ISIS	$5,830 (€5,500)	5	UHF	Turnstile
Deployable Turnstile Antenna System	ISIS	$5,830 (€5,500)	3.3	VHF	Turnstile
Deployable Turnstile Antenna System	ISIS	$5,830 (€5,500)	5	VHF	Turnstile
Deployable Dipole Antenna System	ISIS	$4,770 (€4,500)	3.3	UHF	Dipole
Deployable Dipole Antenna System	ISIS	$5,565 (€5,250)	5	UHF	Dipole
Deployable Dipole Antenna System	ISIS	$4,770 (€4,500)	3.3	VHF	Dipole
Deployable Dipole Antenna System	ISIS	$5,565 (€5,250)	5	VHF	Dipole
Deployable Monopole Antenna System	ISIS	$4,770 (€4,500)	3.3	UHF	Monopole

Table 2.9 – Possible Antennas [74,75] **Continued**

Name	*Brand*	*Cost*	*Supply Voltage (V)*	*Frequency Type*	*Antenna Variety*
Deployable Monopole Antenna System	ISIS	$4,770 (€4,500)	3.3	VHF	Monopole
Deployable Monopole Antenna System	ISIS	$5,300 (€5,000)	5	UHF	Monopole
Deployable Monopole Antenna System	ISIS	$5,300 (€5,000)	5	VHF	Monopole
Deployable Combined Antenna System	ISIS	$5,035 (€4,750)	3.3	UHF	Combined
Deployable Combined Antenna System	ISIS	$5,035 (€4,750)	3.3	VHF	Combined
Deployable Combined Antenna System	ISIS	$5,300 (€5,000)	5	UHF	Combined
Deployable Combined Antenna System	ISIS	$5,300 (€5,000)	5	VHF	Combined

Additionally, the ADC Subsystem design drivers "Pointing Control Accuracy" and "Pointing Knowledge" have been incorporated into the Antenna driver. "Pointing accuracy typically drives sensor accuracy. For pointing requirements on the order of several degrees, a set of coarse sun sensors and a magnetometer can provide sufficient pointing accuracy. Horizon sensors and fine sun sensors provide accuracies around half a degree or so. Below a half a degree down to tens of arcseconds, a star tracker combined with an inertial measurement unit (gyro) with sufficient knowledge." [54] The ADC subsystem design factor "Pointing Curl" was also incorporated into this driver. Pointing curl is related to the pointing capabilities, and error in those capabilities, of an antenna. As the design of a new antenna is outside the scope of this work, "Pointing Curl"

was not considered as an individual design elements and was combined into the "Antenna" driver.

Ideally for imaging missions, the spacecraft needs to be stable in its orbit to receive high quality data, and adequately transmit the data back to the ground stations. There are many things that impact the stability of the system – many of which are geometric and depended on the layout, structure, and size of the satellite. Though there is no formula to determine 'stability' of the system – this design driver dictates the sizing of the actuators in the system and will be considered accounted for if the actuators selected can mitigate the external torques on the system which lead to instability in the spacecraft.

The maximum slew rate for a given satellite can be calculated using the following equations:

$$\dot{\theta_{max}} = \frac{V_{sat}}{D_{min}} = \frac{2\pi(R_E + H)}{P D_{min}}$$

$$D_{min} = R_E \left(\frac{\sin \lambda_{min}}{\sin \eta_{min}}\right)$$

Where R_E is the radius of the earth, H is the altitude of the spacecraft, P is the period, D_{min} is the minimum slant range to the viewing target, λ_{min} is the minimum earth central angle, and η_{min} is the minimum angle from nadir. [77]

Operational availability is considered if the system has failure mitigation methods as "availability can be thought of as the proportion of total time that the vehicle is operational." [78] If the spacecraft is able to recover from system failures operational availability is important, however, most CubeSats do not have enough redundant systems due to size and mass constraints. This factor was eliminated from consideration in this work.

Upon recombination of the final subsystem driver map, "Spacecraft Configuration" was changed to "Layout" to match terminology and convention in other subsystems.

According to [31] there are five main types of attitude sensors: gyroscopes, sun sensors, star sensors, horizon sensors, and magnetometers. Sun Sensors and Horizon Sensors are the most commonly used sensors in CubeSats, as summarized in the tables below. Costs are presented in both Euros and United States Dollars (USDs) in the table below because the original price was in Euros and the prices were converted for consistency on April 15, 2017 when the exchange rate was 1.06 USDs to the Euro.

Table 2.10 – CubeSat Sun Sensor Options

CubeSat Shop Sun Sensor			
Name	*Brand*	*Cost*	*On Axis FOV (+/- deg)*
BiSon64	Lens R&D	$4,378.86 (€4,131)	55
BiSon64-B		$5,341.34 (€5,039)	55
NANO-SSOC-A60 analog sun sensor	Solar MEMS	$2,332 (€2,200)	60
NanoSSOC-D60 digital sun sensor		$3,816 (€3,600)	60
SSOC-A60 2-Axis analog sun sensor		$7,632 (€7,200)	60
SSOC-D60 2 -Axis digital sun sensor		$12,932 (€12,200)	60
NSS CubeSat Sun Sensor	New Space	$3,300	114
NSS Fine Sun Sensor		$12,000	140

Table 2.11 – Sample CubeSat Horizon Sensors

CubeSat Shop Infrared Horizon Sensors					
Name	*Brand*	*Cost*	*Central Wavelength (10e-6 m)*	*Height (mm)*	*Diameter (mm)*
Infrared Band-Pass Filter 18 Type	HEAD	$32,939.50 (€31,075)	15.1	1.5	18
Infrared Band-Pass Filter 18 Type				1.5	25
Infrared Band-Pass Filter 18 Type				2	
Infrared Band-Pass Filter 18 Type				1.8	30

This factor has been incorporated into a new "On Board Computer" design driver for the Command and Data Handling Subsystem.

From these explorations and implications, the simplified map of the ADC design drivers is shown in Figure 2.8 below. An additional eight drivers were incorporated into the following figure as they impact the ADC subsystem drivers after combinations and simplifications. The "CubeSat Size" driver is a part of the Propulsion Subsystem and has already been discussed in Section 2.1. "On Board Computer" is a part of the Command and Data Handling (CDH) subsystem and will be discussed in the next section. "Center of Mass Offset," and "Solar Array Area" are a part of the Mechanical subsystem and will be discussed in Section 2.6. "Layout" and "Temperature Range" are in Section 2.7 – the Thermal subsystem, and "Ground Station" and "Data Rate and Distance" are in the Telemetry Tracking and Command subsystem presented in Section 2.4.

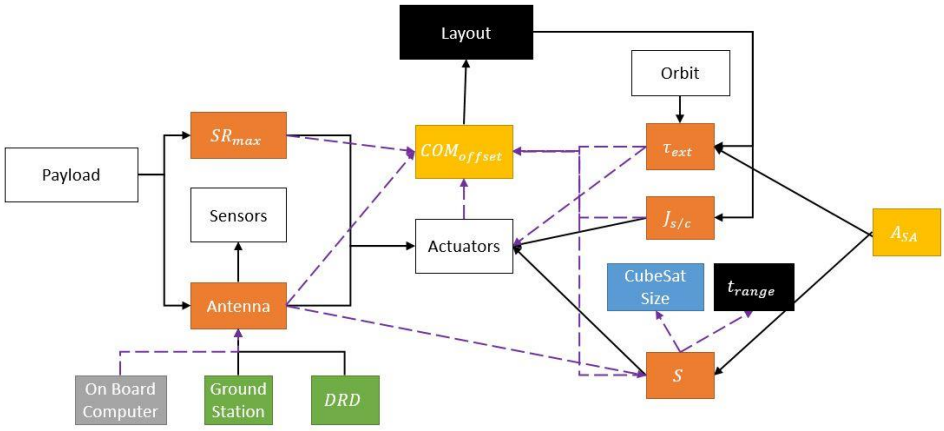

Figure 2.8 – Final Map of ADC Subsystem Drivers

2.3 Command and Data Handling (CDH) Design Drivers

Figure 2.9 is the direct representation of the isolated CDH Subsystem design drivers and factors from Figure 2.1. As a subsystem CDH is responsible for receiving, validating, decoding, and distributing commands as well as collecting and processing spacecraft housekeeping and mission data for downlink or use by onboard computer. There are four primary design drivers that impact the CDH subsystem [79]: "Instrument Data Interface" (IDI), "Processing Requirements" (Req_{procs}), "Data Storage Volume" (V_{ds}), and "Timing Accuracy" (ac_{timing}).

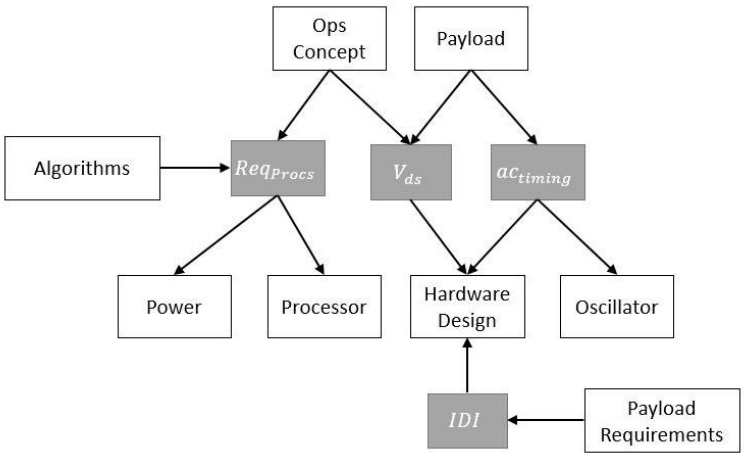

Figure 2.9 – CDH Design Drivers

"Instrument Data Interface" involves the "hardware and software interfaces for commanding the payloads and reading the data impact the complexity of the C&DH."[54] The "Processing Requirements" "define the speed of the processor, the dynamic memory (typically Random Access Memory or RAM), and the non-volatile memory (usually Programmable Read Only Memory, PROM, or Electrically Erasable Programmable Read Only Memory, EEPROM)." [54] The "Data Storage Volume" is the amount of memory needed to store the data collected by the payload. This is dictated by the amount of data generated by the payload and the ability of the spacecraft to downlink the collected data. "Timing Accuracy", is the accuracy with which the spacecraft needs to keep time – by using an oscillator as a reference, the spacecraft is able to keep time by keeping track of the number of cycles performed since powering up the system. [54]

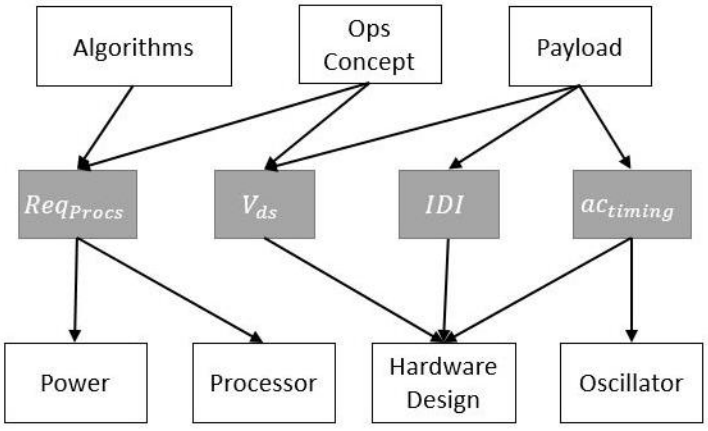

Figure 2.10 – Simplified CDH Design Drivers

Figure 2.10 represents the simplifications made to the CDH subsystem map when considering a CubeSat architecture. The primary change was the combination of the "Payload" and "Payload Requirement" factors. After the initial simplification, the remaining factors and drivers were explored further do determine their importance in the system model and the creation of the mathematical model.

"Processing Requirements" "define the speed of the processor, the dynamic memory (typically Random Access Memory or RAM), and the non-volatile memory (usually Programmable Read Only Memory, PROM, or Electrically Erasable Programmable Read Only Memory, EEPROM)." [54] "Data Storage Volume" is the amount of memory needed to store the data collected by the payload. This is dictated by the amount of data generated by the payload and the ability of the spacecraft to downlink the collected data. "Instrument Data Interface" involves the "hardware and software interfaces for commanding the payloads and reading the data impact the complexity of the C&DH."[54] "Timing Accuracy", is the accuracy with which the spacecraft needs to keep time – by using an oscillator as a reference, the spacecraft is able to keep time by keeping track of the number of cycles performed since powering up the system. [54] Additionally, the "Algorithms" factor has also been incorporated into the new "On Board Computer" driver and the "Processor" factor itself is also included here.

An operations concept – also known as a mission concept or concept of operations – is a "broad statement of how the mission will work in practice." [49] It is the plan by which the designed system will execute tasks to achieve the desired mission objectives. Typically for missions that need to relay information to the earth, there are four main elements in the operations concept: 1) data delivery, 2) tasking, scheduling, and control, 3) communications architecture, and 4) program timeline. [79] These aspects of the operations concept are developed by asking questions – like "How is imagery collected?" "Which forested areas are receiving attention this month?" and "What is the schedule for satellite replenishment?" – and by performing trade studies [79].

Oscillators on satellites are used as precision instruments essential to navigation systems, experiments, communications, and altimetry. [80] However, in CubeSats these oscillators are already incorporated.

After exploring the design drivers and factors remaining in Figure 2.10 and the resulting combinations and eliminations, Figure 2.11 was generated. Due to the combination of "Processing Requirements," "Data Storage Volume," "Instrument Data Interface," "Processor,"

"Algorithms," and "Timing Accuracy" into the unified "On Board Computer" driver, two additional driver blocks were added to this system map: the "Power Consumption" and "Antenna" drivers. The "Power Consumption" driver is a part of the Power Subsystem and was added in place of the "Power" factor as the "On Board Computer" needs a certain amount of power in order to function. This new driver is addressed in Section 2.5 and the "Antenna" driver was addressed in the previous section on the Attitude Determination and Control Subsystem (Section 2.2).

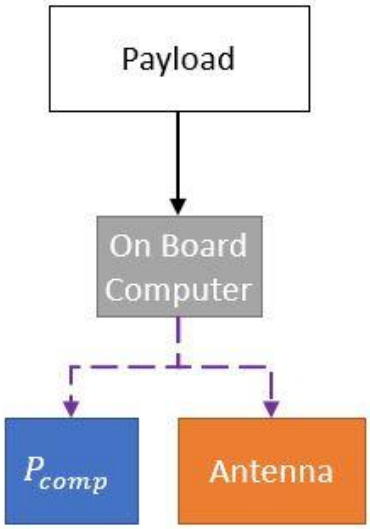

Figure 2.11 – Final Map of the CDH Subsystem

2.4 Telemetry, Tracking and Command (TTC) Design Drivers

The Telemetry, Tracking, and Command (TTC) subsystem generates and manages the link between the spacecraft and the ground stations through radio waves. Not only does it provide the communication avenue, but also determines the spacecraft's distance and velocity over time. [54] The TTC subsystem is defined by five drivers. These drivers and their associated factors are isolated from Figure 2.1 and are illustrated in Figure 2.12 below.

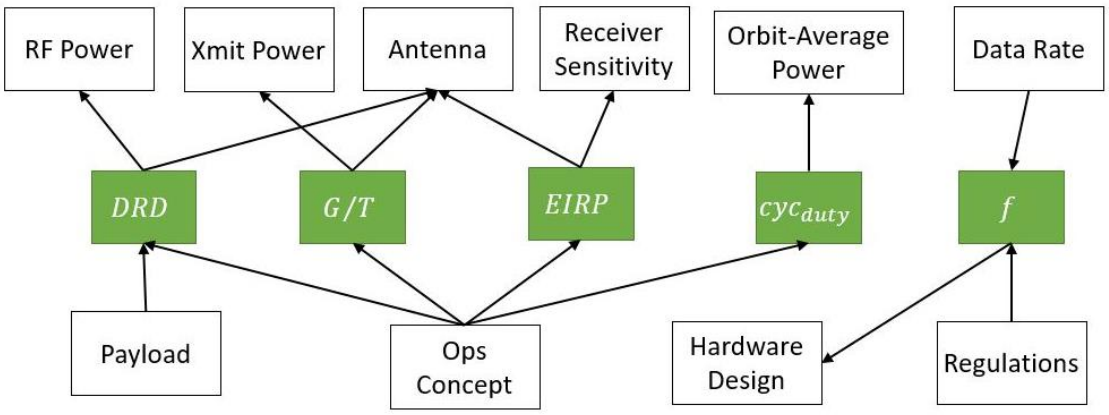

Figure 2.12 – TTC Design Drivers

"Data Rate & Distance" (DRD) is rate at which data is communicated to the ground stations and the distance the data must go to reach the ground station. "Frequency" (f), refers to the radio frequency on which the CubeSat is allowed to broadcast. "Ground Station Effective Isotropic Radiated Power" (EIRP), is a ground station parameter which is the combination of the transmitter power, antenna gain, and the ground station G/T ratio. [54] "Ground Station G/T ratio" (G/T), is the antenna gain divided by the noise temperature of the receiver. [54] "Duty Cycle" (cyc_{duty}), is the fraction of one period in which a signal or system is active. [81] This subsystem did not immediately simplify based on CubeSat design requirements, in fact, as seen in Figure 2.13, a connection was added between "Ground Station G/T Ratio" and "Ground Station Effective Isotropic Radiated Power."

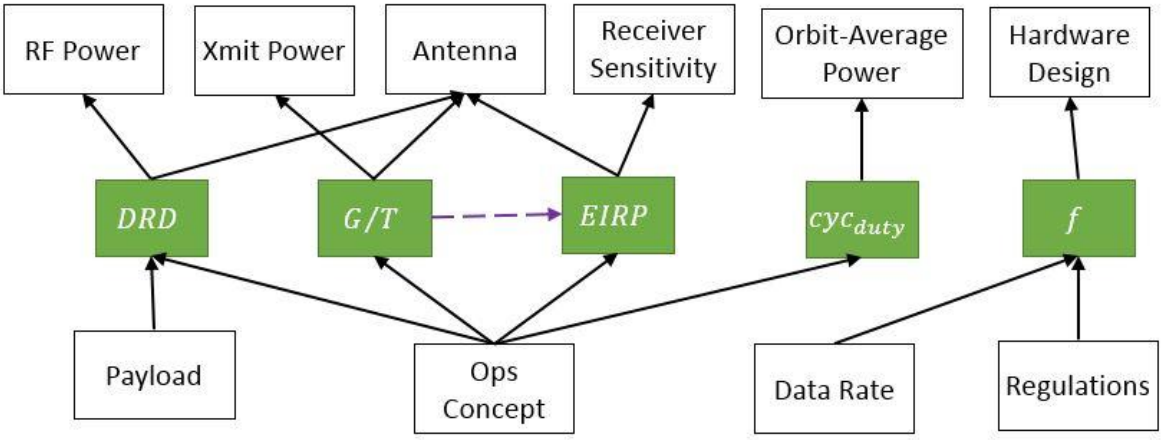

Figure 2.13 – Simplified TTC Design Drivers

After the initial simplification, the remaining factors and drivers were explored further do determine their importance in the system model and the creation of the mathematical model.

Since "Ground Station Effective Isotropic Radiated Power" and "Ground Station G/T Ratio" are things that are typically not selected independently for a CubeSat mission, they have been combined into one driver "Ground Station." A sample of ground stations available for purchase are in Table 2.12. Each of these ground stations comes with: 1) and instrumentation rack containing the receiver, a PC with Local Ground Station Software, a rotator controller, and cavity filters to suppress UMTS interferences, 2) a steerable antenna system with lightning protection, 3) standard software with satellite tracking software pre-installed, and 4) the ability to operate remotely through the internet. Costs are presented in both Euros and United States Dollars (USDs) in the table below because the original price was in Euros and the prices were converted for consistency on April 15, 2017 when the exchange rate was 1.06 USDs to the Euro.

Table 2.12 – ISIS Full Ground Station Packages for Purchase [82]

Ground Stations	
Frequency Band	*Cost*
S-Band	$49,290 (€46,500)
VHF/UHF	$43,990 (€41,500)
VHF/UHF/S-Band	$59,890 (€56,500)

If the mission requires more continuous access to the spacecraft than a couple purchased ground stations can supply, then the other option is to purchase time on a previously established network. One of these networks is Spaceflight – through them you can purchase a radio (communications system) and data plans either per minute or per month with costs depending on the frequency used [83]. Other similar services are currently in development like BridgeSat, Leafspace, Atlas Ground, and Kongsberg Satellite Services [84–87], to name a few. Most of these companies do not publicly disclose their prices. But BridgeSat cost $1.95/minute for UHF versus $19.95/minute for S/X Band on the pay per minute plan and $3,000/month for UHF versus $50,000/month for S/X band on the pay per month plan.

The "Frequency" driver has also been incorporated into this section. "Frequency, f," refers to the radio frequency on which the CubeSat is allowed to broadcast.

"Duty Cycle" is the fraction of one period in which a signal or system is active. [81] In Figure 2.1 there are two design drivers with duty cycle in their titles, one for the payload and one for the rest of the system. The "Payload Duty Cycle" driver was identified as a design driver for the

Power Subsystem and "Duty Cycle" was a driver for the TTC subsystem. In this work these two drivers have been combined into a single "Duty Cycle" driver.

"Data Rate and Distance" is the rate at which data is communicated to the ground stations and the distance the data must go to reach the ground station. As seen in Figure 2.13 there is also a "Data Rate" factor in addition to the "Data Rate and Distance" design driver. These two have been combined into a unified "Data Rate and Distance" driver. Though the data rate part of the "Data Rate and Distance" will be determined by the antenna specifications, the distance aspect is dependent on the network of ground stations and the orbit of the spacecraft. This will be explored further in the generation of the mathematical model in Chapter 3.

The quantity and type of battery selected will determine how much energy the system is able to store. A battery pack is comprised of individual cells connected in series and parallel. The number of cells required is determined by the bus voltage requirements, power consumed by the system, and the length of time the system will not be generating power. [88] It is important that the batteries of the spacecraft are able to store enough energy for the system to remain operational during eclipse periods. The following table include some details of batteries considered for use in the CubeSats generated by this study.

Table 2.13 – A sample of batteries found on CubeSatShop [89–91]

Batteries				
Name	*Brand*	*Power System Included*	*Max Voltage (V)*	*Watt Hours (Wh)*
BP4 2P-2S	GomSpace	N	8.4	38.5
BP4 1P-4S		N	16.8	38.5
BPX 2S-4P		N	8.4	77
BPX 4S-2P		N	16.8	77
BPX 8S-1P		N	33.6	77
BM 1 2S2P	Pumpkin	N	8.25	40
EPS 1	EnduroSat	Y	4.2	10.4
EPS 1 Plus		Y	4.2	20.8
EPS 2		Y	12.6	20.7
EPS 2 Plus		Y	16.8	41.4

The "Orbit Average Power" factor has two parts – the average power generated over an orbit, and the average power consumed by the system during an orbit. The average power generated over an orbit can be calculated based on the type of solar panel and the amount of time the

system is not in eclipse. The power consumed by the system will be the sum of the power consumed by the individual components.

Since the commercial off the shelf antennas have predetermined transmitters and receivers, "RF Transmit Power," "Xmit Power," and "Receiver Sensitivity" have all been combined into the "Antenna" driver.

Following the exploration of the design drivers and factors presented in Figure 2.13, the subsystem map of the Telemetry, Tracking and Command subsystem was reduced to Figure 2.14.

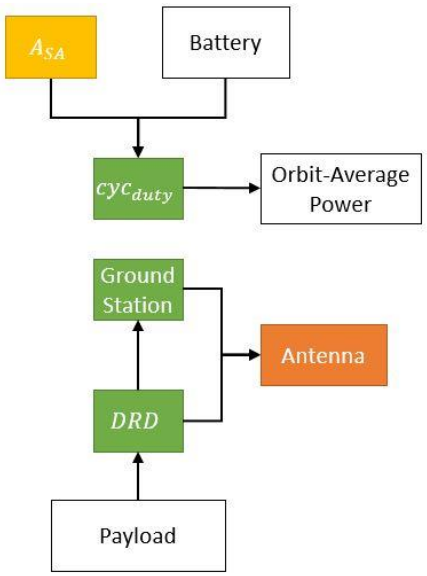

Figure 2.14 – Final Map of the TTC Subsystem

As seen in Figure 2.14 above, the number of drivers for the TTC subsystem has reduced from five design drivers to three. There are however two new design drivers – primarily associated with other subsystems – that have been included in this new system map: the "Antenna" and the "Solar Array Area" drivers. The "Antenna" driver is a part of the ADC subsystem and was discussed in Section 2.2. "Solar Array Area" is a part of the Mechanical Subsystem and will be discussed in Section 2.6.

2.5 Power Design Drivers

The Power subsystem is responsible for generating, storing, and distributing the electricity required by the spacecraft. In this work, this subsystem will be considered as a means to ensure that the payload can function on the smaller satellite architecture. The primary consideration when designing the power subsystem is the payload – as the purpose of the production, launch,

and maintenance of the satellite, the payload is the reason for the mission, and therefore takes precedence when designing the power subsystem. However, there are other drivers and factors that have been isolated from Figure 2.1 and are presented in Figure 2.15 below.

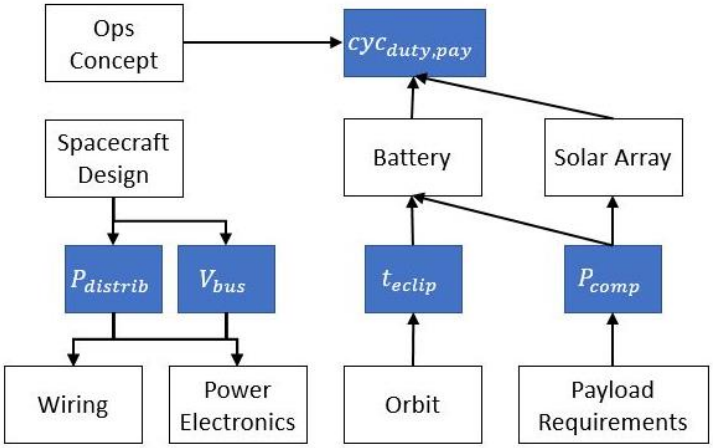

Figure 2.15 – Power Design Drivers

The initial map of this subsystem has five design drivers and eight factors. The "Power Consumption" (P_{comp}) driver is the amount of power consumed by all of the components in the satellite, for each component this can be calculated using the standard voltage times current equation, $P = V \times I$. The "Power Distribution" ($P_{distrib}$) driver is the distribution and layout of components that use power. The "Eclipse duration" (t_{eclip}) driver is the amount of time when the satellite is not generating energy; when designing for this it is crucial that the power storage of the system can support the necessary electronics during the eclipse period. The "Bus Voltage" (V_{bus}) driver is system regulated voltage which flows through the satellite. And the "Payload Duty Cycle" ($cyc_{duty,pay}$) driver is the fraction of time in which the payload needs to be operational. Initial simplification are made to the system map by considering the satellite system from the perspective of CubeSat architecture. The new simplified design driver map is presented in Figure 2.16.

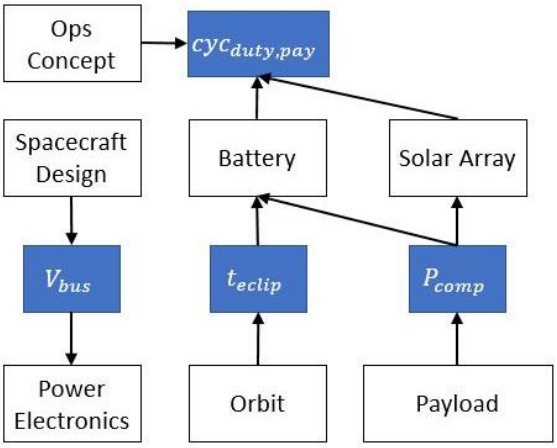

Figure 2.16 – Simplified Power Design Drivers

The primary difference was the removal of "Power Distribution" as a driver because of size and interconnectedness of CubeSat electronics. As a result of this decision the "Wiring" factor was also removed. Additionally, "Payload Requirements" was changed to "Payload" in order to streamline the terminology used throughout this work. After the initial simplification, the remaining factors and drivers were explored further do determine their importance in the system model and the creation of the mathematical model.

First, the "Payload Duty Cycle" driver was removed from this subsystem as it was combined with the TTC design driver "Duty Cycle."

Bus voltages are typically 5V or 3.3V, though other common voltages include 3V,-5V, and 6V. [92] These voltages typically correspond to the supply voltages required by many of the sensors, actuators and payloads. If any of the components need a different supply voltage then additional equipment is necessary to either step up or down the voltage to ensure optimum functionality.

A satellite is considered to be in an eclipse when it enters the umbra of the central body. The umbra is defined as the conical region experiencing total shadow where the intensity of solar radiation is zero. This region is projected from the earth on the side opposite to the sun. [93] When sliced by the CubeSat orbit plane this results in an elliptical shadowed region dependent on the inclination of the sun to the orbital plane. To calculate the amount of time the CubeSat experiences in total shadow, the intersections between the satellite orbit and ellipse representing the umbra needs to be calculated. In polar coordinates, this can be done using the following equation [93].

$$cos\theta_G = \pm\sqrt{\frac{1-\left(\frac{R_E}{R}\right)^2}{\cos i_S}} \tag{7}$$

Where R_E is the radius of the Earth, R is the radius of the cubesat from the center of the earth, and i_S is the inclination angle of the sun onto the orbital plan of the satellite. This value, θ_G, is the Geocentric angle. To calculate the total angle in which the satellite passes through the umbra the following equation is used [93].

$$\theta_E = 2(180 - \theta_G) \tag{8}$$

And then the amount of time spent in the umbra can be calculated using [93]:

$$t_{SH} = \frac{\theta_E}{360} P \tag{9}$$

Where P is the orbital period of the satellite dependent on the altitude of the satellite. From these formulae and using a variety of solar incidence angles, a satellite in a LEO orbit like a CubeSat could expect to experience 20%-43% of each period in the shadows, or anywhere from 25 – 37 minutes in shadows. Figure 2.17 below illustrates the percentage of time the satellite would be in shadow as a function of altitude and solar incidence angle.

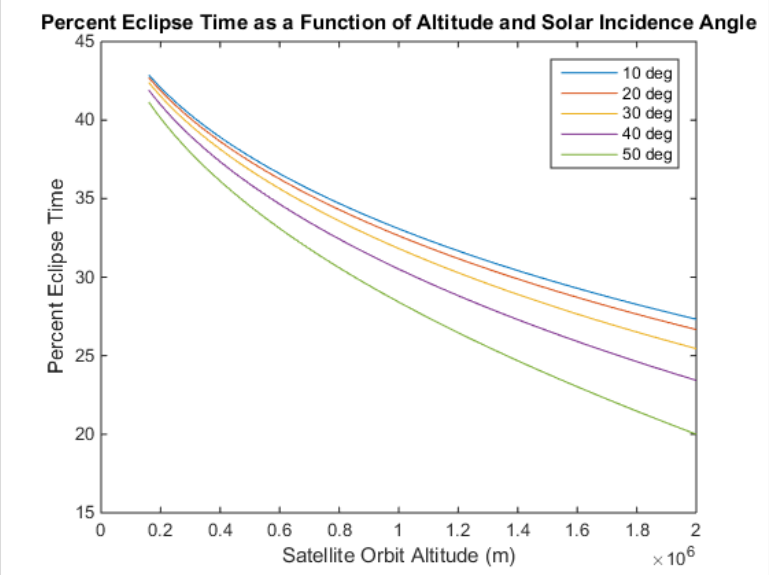

Figure 2.17 – Percent of orbital period when a LEO satellite would be in Earth's Shadow

"Power Consumption" is the amount of power consumed by all of the components in the satellite, for each component this can be calculated using the standard voltage times current equation, $P = V \times I$. This driver will be considered in as a constraint in the design process as the satellite must be able to produce greater than or equal to the amount of power consumed

by the system. This section, in conjunction with "Duty Cycle" can be used to determine the amount of power needed and the size and shape of the solar array needed to properly power the spacecraft.

Figure 2.16 contains "Solar Array" as a design factor in the power subsystem, however as seen in Figure 2.1 there is also a design driver called "Solar Array Area." For the purposes of this work, the two have been combined into the Mechanical Subsystem driver "Solar Array Area."

To control the distribution of power in the spacecraft, the system needs "Power Electronics." Power electronics control the charging of the battery, and the switching of power to the spacecraft loads. [54] In performing a search of commercial off the shelf parts for a CubeSat architecture, it was found that the "Power Electronics" are included in the computers aboard the spacecraft. Thus, this factor has been incorporated into the "On Board Computer" driver from the CDH subsystem.

The four design drivers became three with the incorporation of "Payload Duty Cycle" into "Duty Cycle" in the TTC Subsystem, and the seven design factors became four. Additionally, the "On Board Computer" design driver of the CDH subsystem was added and the "Solar Array Area" driver of the Mechanical subsystem as also added. This design driver will be discussed in Section 2.6.

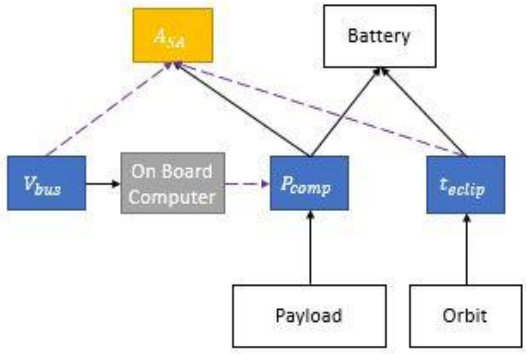

Figure 2.18 – Final Map of the Power Subsystem

2.6 Mechanical Design Drivers

The Mechanical subsystem is responsible for supporting the components of the spacecraft and providing the structure that defines the system. The six primary Mechanical Subsystem design drivers isolated from Figure 2.1 can be seen in Figure 2.19 below. These drivers are associated with 15 factors and an additional driver from the thermal subsystems.

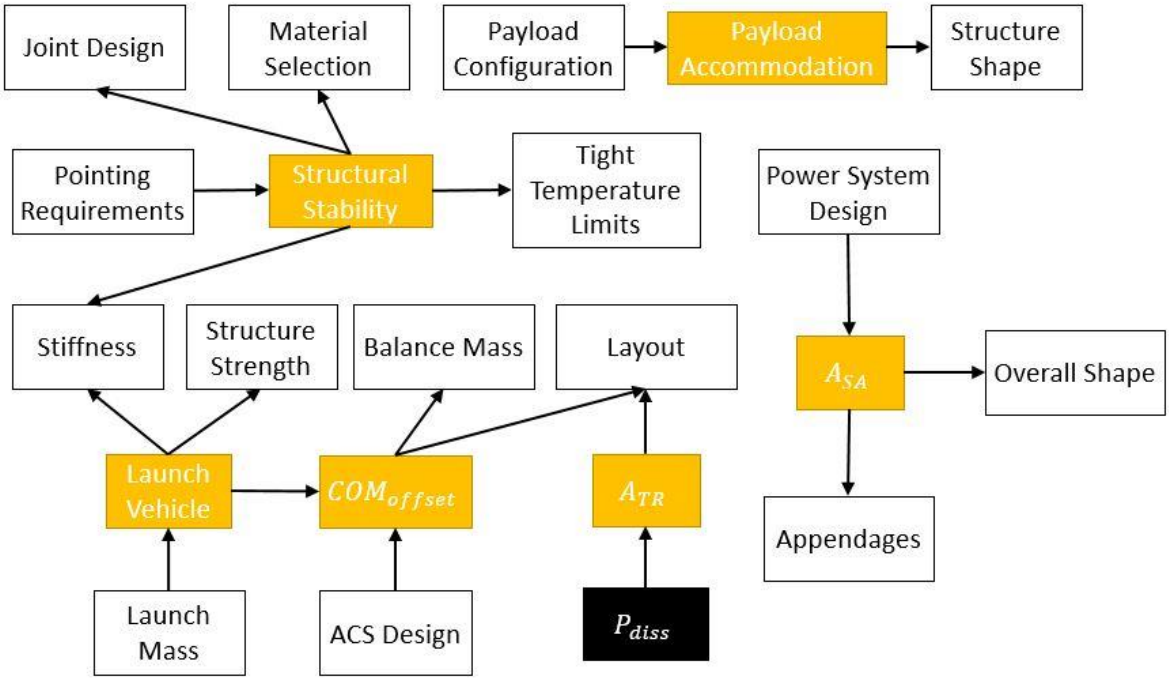

Figure 2.19 – Mechanical Design Drivers

"Launch Vehicle" is defined as a driver for the mechanical subsystem however most CubeSats do not get to select their ride to space and are launched using P-PODs which are fitted to a variety of launch vehicles, as such there already structure strength and stiffness requirements placed on the system. Therefore, "Launch Vehicle," "Structure Strength," and "Stiffness" can be eliminated as the factors impacting this subsystem. The "Payload Accommodation" driver is of importance because it is dependent on the primary objective of the mission, if the payload requires high-precision pointing, the movement of the overall structure due to temperature changes and other environmental conditions does not impact the payload's ability to perform the primary mission. The "Solar Array Area" (A_{SA}) driver is defined as the size of the solar array necessary to power the satellite – as driven by the "Power Subsystem," – this driver dictates the necessity of any "Appendages" and the "Structure Shape," and "Overall Shape" of the CubeSat. "Structural Stability" is the ability of the structure to remain stable in orbit as dictated by "pointing requirements," these requirements are covered in the ADC design drivers and have been combined. "Center of Mass Offset" (COM_{offset}) is the degree or quantity to which the center of mass of the spacecraft is offset from the specified point. As the center of mass offset can have large impacts on flight dynamics of the launch vehicle and of the spacecraft itself. However, this is another structural element that is constrained by the CubeSat Standard to be

no more than 2 cm from the geometric center in both the X and Y directions and no more than 2, 3, 4.5, or 7 cm from the geometric center in the Z direction for a 1U, 1.5U, 2U, or 3U CubeSat respectively. [28] "Thermal Radiator Area" (A_{TR}) is the area of thermal radiator necessitated by the amount of power the power subsystem needs to dissipate.

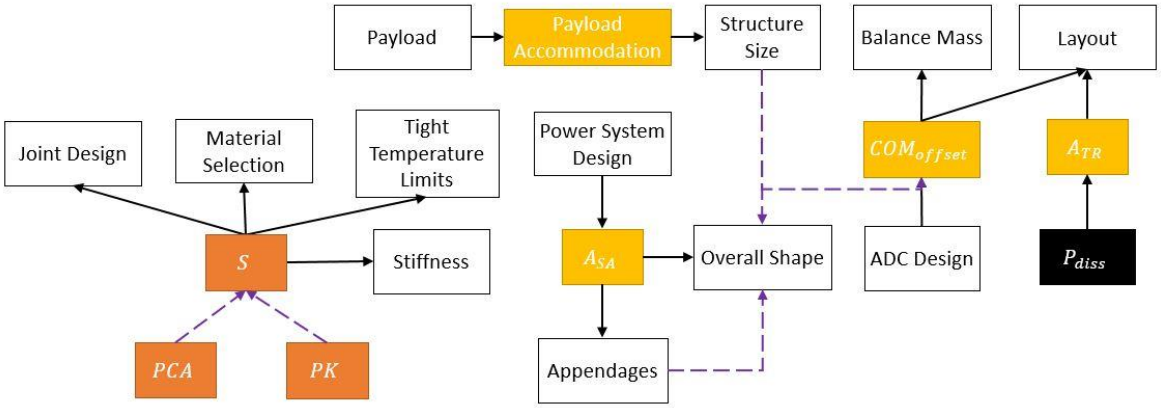

Figure 2.20 – Simplified Mechanical Subsystem Design Drivers

"Launch Vehicle" was deleted as a design driver because it is not something CubeSats get to control. "Launch mass" was also deleted, this is something specified in the CubeSat design standard and is constrained by the size of the CubeSat. "Structure strength" was also deleted because it was something that is defined by the CubeSat Standard and P-POD launch requirements but no longer connects to any of the Mechanical Subsystem design drivers. The "Payload Configuration" factor was changed to "Payload" in order to better group connected factors for later mathematical modeling. The "Structure Shape" factor was changed to "Structure Size" as discussed previously. Arrows were added from "Appendages" and "Structure Size" to "Overall Shape" as those two combined with the area of the solar array will dictate the overall shape of the CubeSat once deployed. The "ACS Design" factor was changed to "ADC Design" as that is the acronym used throughout the rest of the paper for streamlining purposes. And an arrow was added from "Structure Size" to "COM_{offset}" since it is directly specified as a factor of the size of the CubeSat from the CubeSat standard. The "Stability" design driver block has been changed to both a driving design factor in the mechanical subsystem and the ADC subsystem, and "Pointing Requirements" was substituted out for the two point factors in the ADC subsystem: "Pointing Control Accuracy, PCA", and "Pointing Knowledge, PK." After the initial simplification, the remaining factors and drivers were explored further do determine their importance in the system model and the creation of the mathematical model.

"Appendages," "Overall Shape," and "Structure Size" have been combined into the "CubeSat Size" driver. And thus, they were replaced in the final system map by "CubeSat Size" and were eliminated from further examination. After these simplifications, the remaining subsystem drivers and factors are explored for further potential changes.

If the payload requires high-precision pointing, the movement of the overall structure due to temperature changes and other environmental conditions does not impact the payload's ability to perform the primary mission.

Not all of the power generated by a system is used, this results in the dissipation of power in a system often times in the form of heat. In order to maintain the proper thermal environment in a satellite, thermal radiators are used to distribute the dissipated power throughout the system to maintain the required temperature range. In a CubeSat the volume of the spacecraft is dictated by external size constraints [28] and the size of the thermal radiators is dependent on excess space in the system.

The center of mass of the system is another driver of the mechanical subsystem that is dictated by external regulations. As seen in Table 2.14 below, depending on the size of the CubeSat selected, there are constraints placed on the location of the center of mass of the system.

Table 2.14 – Center of Mass Requirements [28]

Center of Gravity Requirements	
2.CS.24	The CubeSat center of gravity shall be located within 2 cm from its geometric center in the X and Y directions
2.CS.25	The 1U CubeSat center of gravity shall be located within 2 cm from its geometric center in the Z Direction
2.CS.26	The 1.5U CubeSat center of gravity shall be located within 3 cm from its geometric center in the Z Direction
2.CS.27	The 2U CubeSat center of gravity shall be located within 4.5 cm from its geometric center in the Z Direction
2.CS.28	3U and 3U+ CubeSats' center of gravity shall be located within 7 cm from its geometric center in the Z

Solar array area will be dictated by the amount of power the spacecraft needs to generate over the course of an orbit as well as the physical space the solar cells can occupy on the spacecraft. This driver has been combined with the "Solar Array" factor. Solar panels are typically around 29% efficient and can generate about 2.3W per 100cm^2. Table 2.15 below lists potential solar panels which have been specifically designed for CubeSat use.

Table 2.15 – Solar Panels available for CubeSat Use [94–96]

Solar Panels					
Name	*Brand*	*Magnetorquer Included*	*Size*	*Power Generation (W)*	*Mass (g)*
Solar Panel X/Y	EnduroSat	N	1U	2.4	44
Solar Panel X/Y		Y	1U	2.4	53
Solar Panel Z		N	1U	2.4	48
Solar Panel Z		Y	1U	2.4	57.5
SPC-CS10	DHV Technology	Y	1U	2.42	39
SPC-CS30		Y	3U	8.48	132
P110A	GomSpace	N	1U	2.3	26
P110UA		Y	1U	2.3	57
P110B		N	1U	2.3	26
P110UB		Y	1U	2.3	57
P110C		N	1U	2.3	29
P110UC		Y	1U	2.3	65
End Solar	Clyde Space	--	1U	2	49
1U deployable		--	1U	4.1	89
2U Single deployed long edge		--	2U	10.2	148
2U single deployed short edge		--	2U	10.2	143
3U Single deployed long edge		--	3U	14.3	303
3U Body Panel		--	3U	7.1	159

Balance Masses in a satellite are often pieces of an incredibly dense material – like lead – used to manipulate the center of mass into a desired location.

After further exploration and simplifications Figure 2.20 has been updated to Figure 2.21. The five mechanical subsystem design drivers remain however, the 12 factors have been changed to match the rest of the system and four factors remain while 11 drivers from other subsystems have been added.

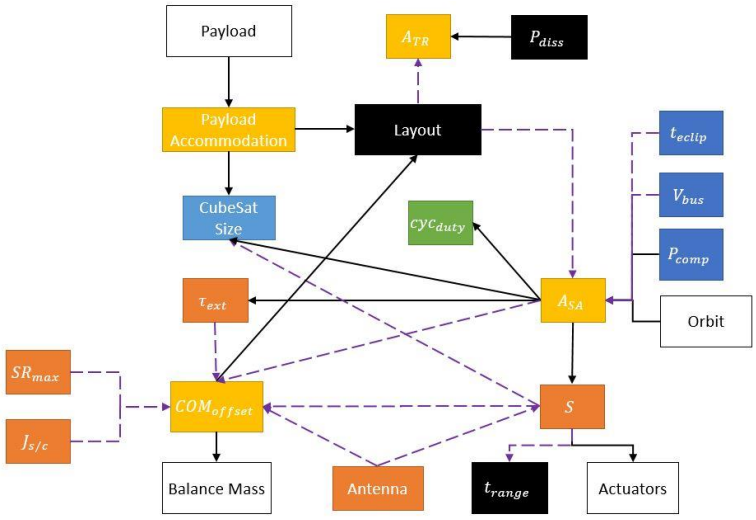

Figure 2.21 – Final Map of the Mechanical Subsystem

In comparing Figure 2.20 and Figure 2.21, the "Power System Design" factor has been replaced with the design drivers of the Power System. The "Joint Design" factor has been eliminated as they are only of consideration if there are deployable solar panels used with the system and even then, when using commercial off the shelf components – these joints have already been designed. "Material Selection" is another aspect of the system which has been dictated by CubeSat regulations [28] and was removed as a factor. "Tight Temperature Limits" has been incorporated in the "Temperature Range" design driver of the Thermal Subsystem. Other added drivers include "Power Dissipation" and "Layout".

2.7 Thermal Design Drivers

The Thermal Subsystem is responsible for disturbing thermal energy throughout the spacecraft to maintain an appropriate operating environment. From Figure 2.1, the six primary design drivers for the Thermal Subsystem are identified below, along with their seven corresponding factors (and single non-Thermal Subsystem driver) that influence them.

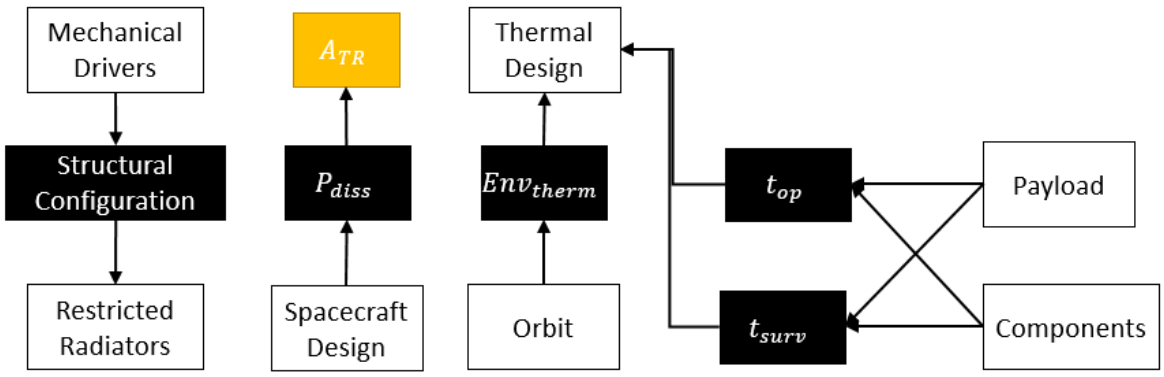

Figure 2.22 – Thermal Subsystem Design Drivers

The "Thermal Environment" (Env_{Therm}) driver is comprised of the thermal considerations at any given point during the orbit of the spacecraft. The system must both "conduct internally-generated heat to the outside of the spacecraft where it can be radiated to space," [54] and distribute externally generated head as necessary. The "Power Dissipation" (P_{diss}) driver is the amount of power dissipated by the entire system – this value can be calculated using the following equation: $P_{diss} = I^2 \times R$, where I is the current and R is the resistance. While the thermal environment and the power dissipation are the primary drivers, the thermal design can be complicated by the "Operating Temperature" (t_{op}) and the "Survival Temperature" (t_{surv}) drivers. These two temperatures dictate the range in which the system can operate successfully, and survive during downtime or in the case of temporary system failure. These values are dictated by the components and the payload on the spacecraft. The final driver, "Structural Configuration," is the overall structure of the spacecraft and how it is laid out. This can have an impact on the size of the thermal radiators available to dissipate heat. By considering the phrases used in other subsections as well as the limits placed on the CubeSat architecture, Figure 2.22 has been reorganized into Figure 2.23 below.

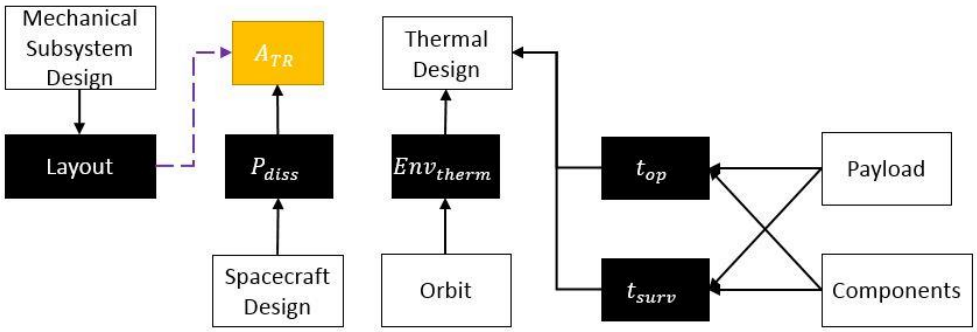

Figure 2.23 – Simplified Thermal Subsystem Drivers

The primary change between Figure 2.22 and Figure 2.23 was renaming the "Mechanical Drivers" factor to be "Mechanical Subsystem Design" to better capture the meaning of this block. Additionally, the "Structural Configuration" driver was changed to "Layout," to match the convention used in all the other subsystems. Also, the "Restricted Radiators" factor was deleted because size restrictions imposed by the layout of the spacecraft could be adequately considered when determining the area of the thermal radiators, A_{TR}. In deleting the "Restricted Radiators" factor a new connection was drawn between "Layout" and "A_{TR}". After the initial simplification, the remaining factors and drivers were explored further do determine their importance in the system model and the creation of the mathematical model.

"Spacecraft Design" was eliminated and the "Components" factor was split into all of the other factor blocks that represent the primary components of the system: "Sensors," "Actuators," "Battery," and "On Board Computer."

The "Layout" of the system is defined as the orientation and location of the components involved in the system.

"Power Dissipation" is the amount of power released by the components in the system.

The "Thermal Environment" is the impact of the orbit on the thermal properties and distribution in the system. As space is a vacuum, heat does not transfer easily and often the side of the satellite facing the sun will be much warmer than the sides facing away.

The "Operating Temperature" and "Survival Temperature" drivers were combined into the new "Temperature Range" driver. This driver is operating temperature range for the constituent parts in the system. Determined simply by the limits placed on the individual components, this range is taken from the highest minimum temperature and the lowest maximum temperature.

The "Thermal Design" driver dictates the means to distribute the residual heat through the system.

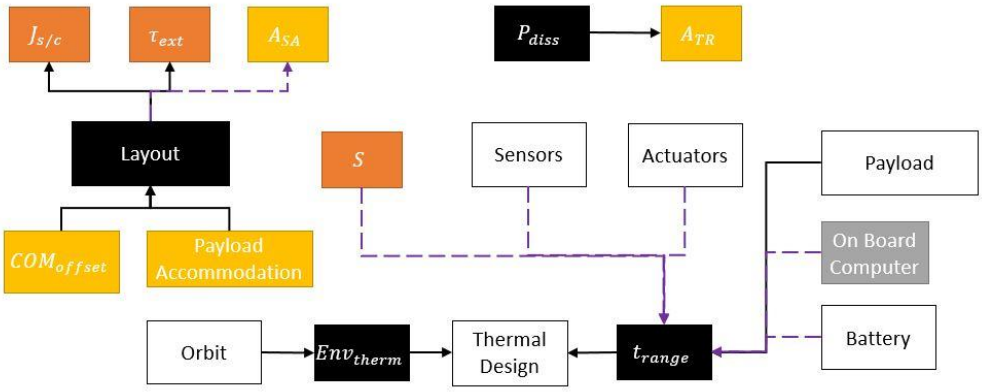

Figure 2.24 – Final Subsystem Map for the Thermal Subsystem

The primary change from Figure 2.23 to Figure 2.24 was the combination of "Operating Temperature" and "Survival Temperature" into the "Temperature Range" driver. Additionally, "Mechanical Subsystem Design" was replaced by the important drivers from the Mechanical Subsystem and "Components" was broken into "Sensors," "Actuators," "Battery," and "On Board Computer" to match with the convention in the previous subsystem maps.

2.8 Total System Map Recombination

Upon combining all of final driver maps from the seven subsystems – see Figure 2.5, Figure 2.8, Figure 2.11, Figure 2.14, Figure 2.18, Figure 2.21, and Figure 2.24 – the DSM in Figure 2.25 was generated. A DSM was chosen to visually represent the final system breakdown because so many of the components were too closely coupled to form a subsystem map like those seen in previous sections.

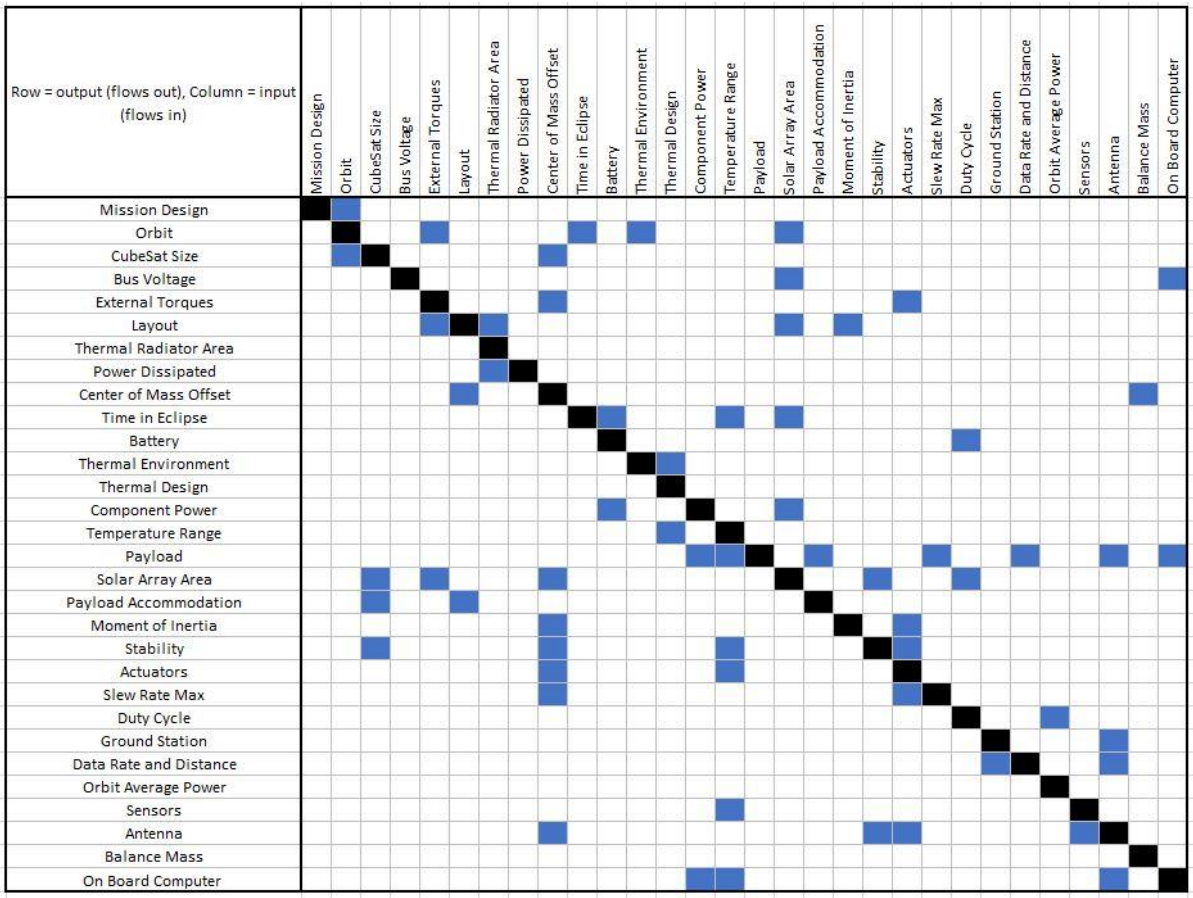

Figure 2.25 – DSM of Final Driver and Factor Breakdown

Using the knowledge gained from exploring the individual factors and drivers for each subsystems as well as the interactions between them, the next step is to build a mathematical model of the system. Moving forward, these subsystem maps and DSMs will be used as guides to facilitate understanding and direct the mathematical model.

2.9 System Decomposition Conclusion

Using DSMs and system maps generated from the identified subsystem drivers and factors, the number of influential drivers and factors when looking at a CubeSat architecture was reduced from 87 to 30 as drivers and factors were combined and eliminated. These simplifications were made for a variety of reasons from streamlining the terminology used, to combining drivers based on commercial off the shelf available CubeSat products, to elimination of factors which had no bearing on this particular system. In performing these simplifications the system itself became less modular as more of the components are interconnected with each other. However, since the proposed mission involves a collection of CubeSats used to complete the specified

mission requirements, each of the CubeSats can be seen as modules in the system that can be interchanged to meet changing needs and requirements.

3 CREATING A MATHEMATICAL MODEL OF A CUBESAT

In the previous section, the subsystem maps and interactions for a CubeSat architecture were created to mimic the monolithic FireSat II. This section aims to create an understanding of each of these factors and variables and the impact they have on the creation of a mathematical system model. Driving requirements for the mission design of FireSat II were chosen as metrics to guide the creation of a mathematical model.

Table 3.1 – FireSat II Mission Objectives [31]

Primary Mission Objective
To detect, identify, and monitor forest fires throughout the United Sates, including Alaska and Hawaii, in near real time and at a low cost
Secondary Mission Objectives
To demonstrate to the public that positive action is underway to contain forest fires
To collect statistical data on the outbreak and growth of forest fires
To monitor forest fires for other countries
To collect other forest management data

These mission requirements are broken down even further into a collection of Level 1 Mission requirements that can be seen in Appendix 7.1. Eight of these mission requirements were chosen as guiding requirements for the creation of the mathematical model. Each of these requirements can be tied to the cost of the mission by whether or not it is able to achieve the primary mission objective: "To detect, identify, and monitor forest fires throughout the United Sates, including Alaska and Hawaii, in near real time and at a low cost." [31] These guiding requirements are presented in Table 3.2 below.

Table 3.2 – FireSat II Mission Requirements Driving the creation of the Mathematical Model

Model Driving Requirements		
ID	*Requirements*	*Branches*
R1.03	The mission shall be able to detect forest fires at up to 50 m in resolution	Scientific Mission
R1.04	The mission shall be able to determine forest fire locations within 1km geolocation accuracy	Scientific Mission
R1.05	The mission shall be able to cover specified forest areas within the US at least twice daily	Coverage and Location
R1.08	The mission will last a minimum of 8 years	Coverage and Location
R1.14	The mission will have a recurring cost of less than $3M/year	Satellite Design
R1.19	The mission will be interoperable through NOAA ground stations	Coverage and Location
R1.25	The mission must be able to monitor changes in the mean forest temperature to +/- 2C	Scientific Mission
R1.33	The mission will fit within a Standard CubeSat Size	Satellite Design

These requirements are then broken down into three branches – scientific mission requirements, satellite design requirements, and coverage and location requirements. Requirements 1.03, 1.04 and 1.25 are classified as driving requirements for the scientific mission, requirements 1.14 and 1.33 are drivers for satellite design, and 1.05 and 1.19 are drivers for coverage and location. These requirements, and their impact on the creation of the mathematical model are discussed in the following sections.

3.1 System Models Used

In order to model and accommodate the 8 driving mission requirements, two types of models were created. The first were categorized as "Physical Models" that dealt with specifications and relationships between system design variables, and the second were categorized as "Interaction Models" that developed the relationships between designed systems and the earth. In the Physical Models, there are two models: The Ground Sample Distance Model, and The Camera Size Model. In the Interaction Model category, there are three models: The Orbit Model, the Ground Track Model, and the Swath Width Model. Each of these models are explained in more depth in the following sections.

3.1.1 Physical Models

The two models included in this section are used to size the payload necessary for the mission to meet the specified mission requirements, and to size the CubeSat based on the payload. These two models tie back to the Scientific Mission requirements presented in Table 3.2. The first model discussed – the ground sample distance model – focuses on the resolution of the payload, while the second – the Camera Size Model – determines the size of the camera to facilitate CubeSat size selection.

3.1.1.1 Ground Sample Distance Model

For the first of the three target requirements to be met, the camera must be able to have at minimum 50m² ground sample distance. The ground sample distance (GSD) is defined in Equation (10).

$$GSD = IFOV * H \tag{10}$$

Where IFOV is the instantaneous field of view and H is the altitude of the camera. The instantaneous field of view can be calculated as seen in Equation (11) below.

$$IFOV = {}^{p}/_{L} \tag{11}$$

In this equation, p is the pixel pitch of the sensor array and L is the focal length [97]. Effective focal length can be defined as the lens diameter multiplied by the f/N number. This is seen in Equation (12) below.

$$L = (d)(f/N) \tag{12}$$

These three equations – (10), (11), and (12) – can be combined to form the overall equation used to calculate GSD. This equation is presented in Equation (13) below.

$$GSD = \frac{(p)(H)}{(d)(f/N)} \tag{13}$$

As seen in Equation (13), the ground sample distance is not only a function of camera design variables but also of the altitude of the spacecraft. Since the CubeSats will be un-propelled, this is not a constant value and is time dependent. The model used to determine the altitude as a function of time is discussed in Section 3.1.2.1.

To test the feasibility of using commercial off the shelf IR cameras. A sample of available cameras were collected from FLIR; these cameras can be seen in Appendix 0. Since the goal is to achieve the same level of functionality as the FireSat using the CubeSat platform, these sampled commercial off-the-shelf cameras were tested to determine their GSDs as a function

of altitude. However, when using the ranges specified in Table 3.6, none of the commercial off-the-shelf cameras can achieve the desired resolution at the altitudes required to achieve the minimum 8-year lifespan required using only one CubeSat. As seen in Figure 3.1, the greater the altitude the fewer number of sampled cameras can achieve the required resolution.

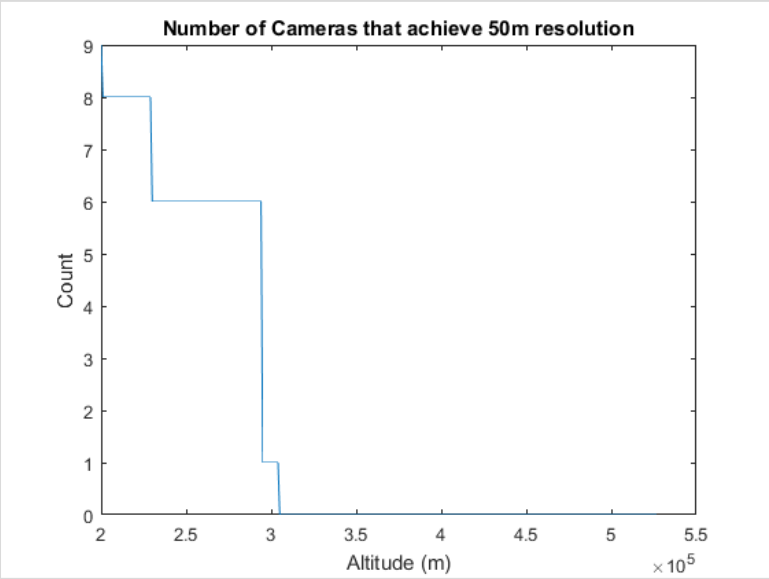

Figure 3.1 – Number of Cameras which can achieve the desired GSD at a given altitude

From Figure 3.1, it can be seen that no sampled cameras work above 304km – putting the functional lifespan of the Cubesat at 65 days for a 1U CubeSat, 71 days for a 1.5U, 72 days for a 2U CubeSat, and 77 days for a 3U CubeSat (as seen in Figure 3.2).

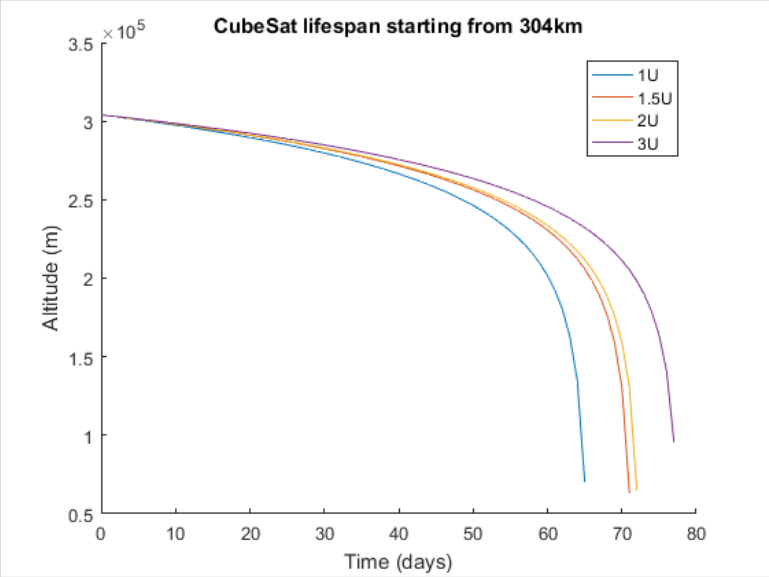

Figure 3.2 – Length of functional time based on CubeSat Size

However, 304 km was not placed as an upper limit for CubeSat launches because this is not long enough to cover a single fire season (160 days). Additionally, if the ranges for pixel pitch, lens diameter, and f/N number are examined individually and combined the required ground sample distance can be generated at higher altitudes. From the sampled cameras FLIR cameras, there are 3 different pixel pitches 12 µm, 17 µm, and 25 µm, and 29 different focal lengths ranging from 2.3mm to 16cm. From these, the potential ground sampling distances are calculated using Equation (10) and the altitude ranges from the Karman Line (100km) to 527km. They can be seen in Figure 3.3.

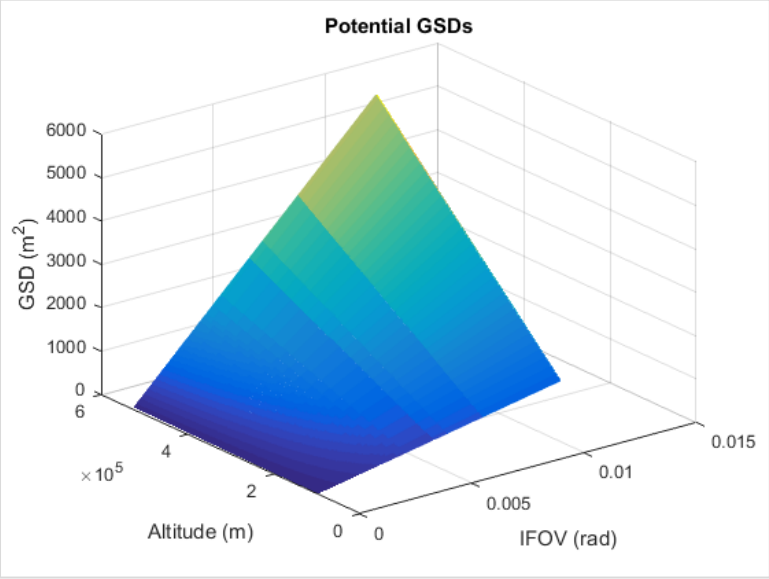

Figure 3.3 – Possible Ground Sampling Distances

As seen in Figure 3.3, a wide range of ground sampling distances are possible, but the requirement states that the GSD must be 50m² or less. The section of Figure 3.3 which represents GSDs that meet the requirement is shown below in Figure 3.4.

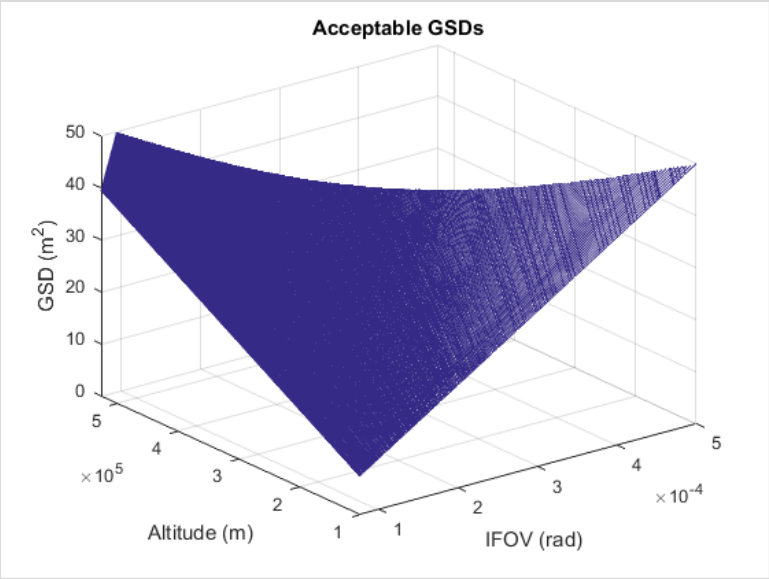

Figure 3.4 – Potential GSDs below 50m²

If a lens could be built to any specifications within the sampled range, and by using known pixel pitches and f/N numbers, it is possible to achieve cameras that are able to meet the 50m² GSD requirement all the way up to the maximum altitude of 527km as seen in Figure 3.5 below.

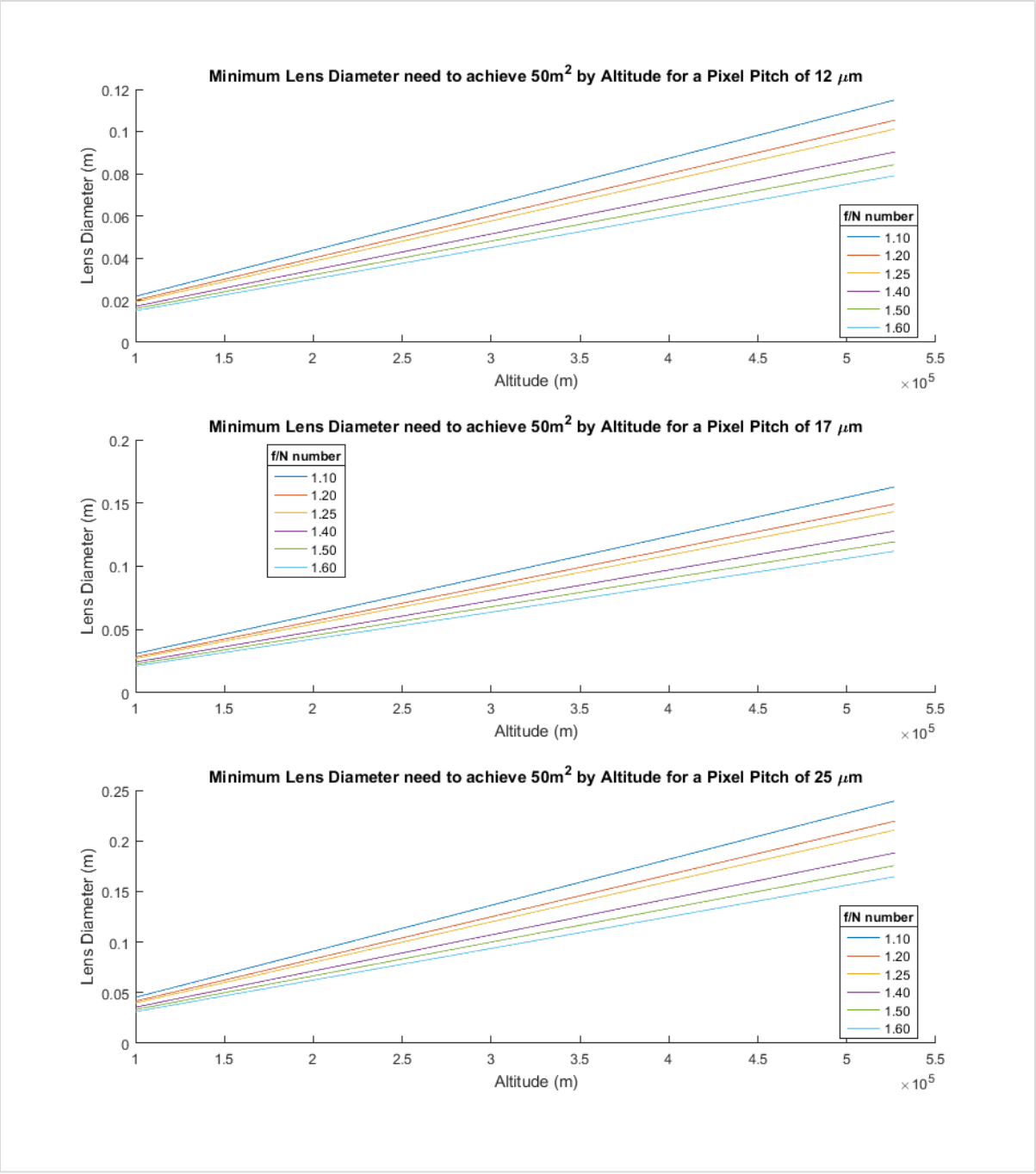

Figure 3.5 – Lens Diameters required to meet 50m² for a given altitude

However, due to geometric constraints of the CubeSat architecture, the diameter of the lens is limited to 10 cm. Moving forward with the mathematical model the pixel pitch, lens diameter, and f/N will be constrained to the following ranges:

Table 3.3 - Variables and their Ranges relating to the Ground Sample Distance Model

Variable	Range	Integer or Discrete
Pixel Pitch	[12 μm, 17 μm, 25 μm]	Integer
Lens Diameter	7.5 mm to 10 cm	Positive Real – rounded to three significant figures
f/N number	[1.1, 1.2, 1.25, 1.4, 1.5, 1.6]	Integer

When combining all of the information together into one, succinct, mathematical model, Equation (13), reiterated below, will be used to calculate the GSD at any given altitude based on the pixel pitch, lens diameter, and f/N number form the camera, and altitude from the orbit model.

$$GSD = \frac{(p)(H)}{(d)(f/N)}$$

Of the sampled cameras (see Appendix 0), the Tau 2 from FLIR was chosen as the model camera type for the rest of the investigation because its product family captured 2 of the 3 possible pixel pitches and it has the capability to be paired with a wide range of lenses. System information taken from the Tau 2 product family data sheet helped create the cost model for the payload as presented in Section 3.3.1.1.

3.1.1.2 Camera Size Model

Using the FLIR Tau 2 as the model camera – because it has interchangeable lenses – the physical space needed for the camera is modeled as the housing and the lens.

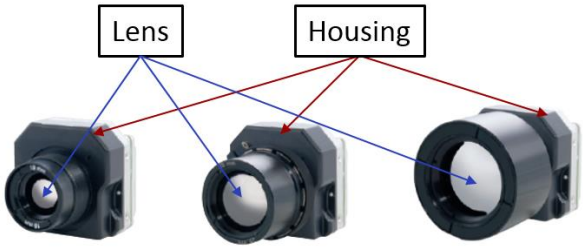

The housing of the Tau 2 model is 4.44 cm x 4.44 cm x 2.99 cm (1.75 in x 1.75 in x 1.18 in)[53] and the lenses range in diameter and length. The mass of the lens and camera for the Tau 2 product family is given and an approximate model for weight as a function of lens diameter is generated.

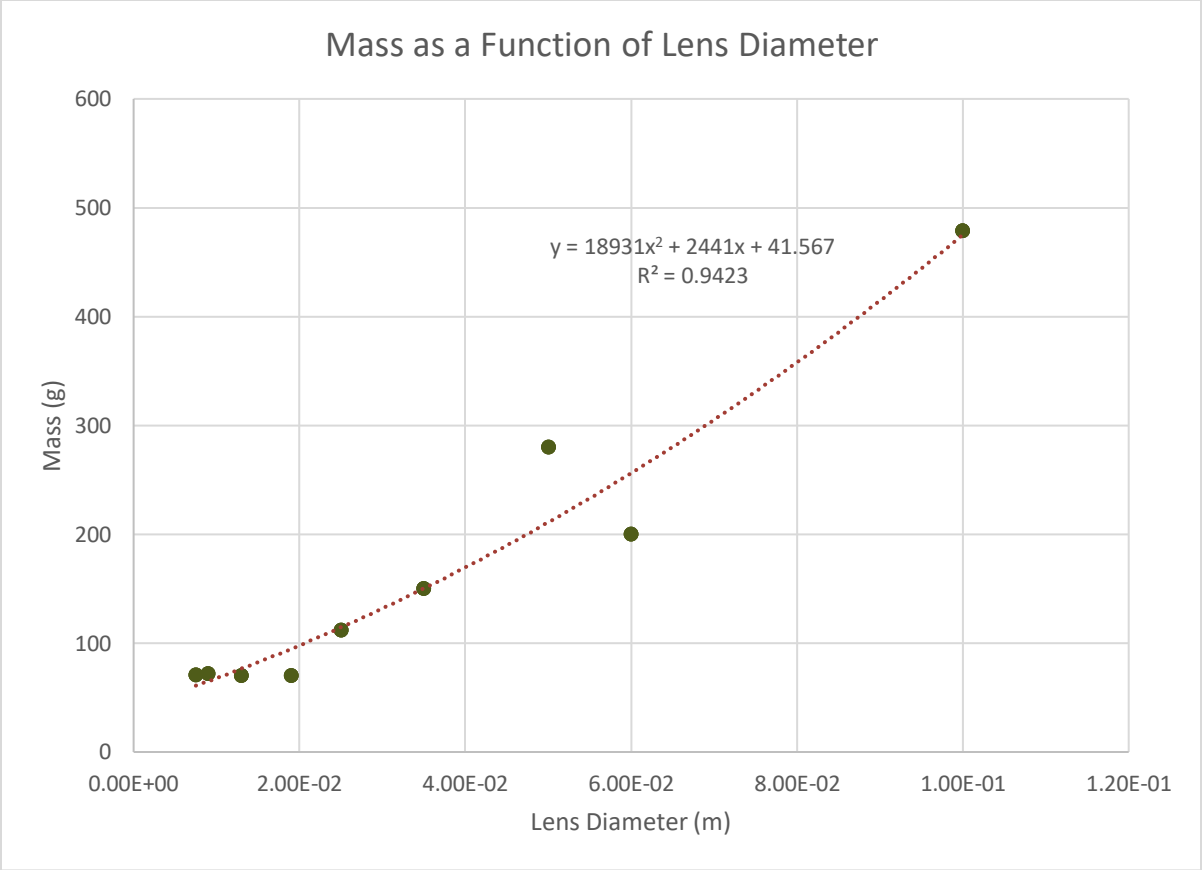

Figure 3.6 – Mass of the Total Camera Assembly as a Function of Lens Diameter

As seen in Figure 3.6, the 2nd order polynomial trend line represented the data with a good R^2 value. The following equation will be used moving forward to represent the mass of the camera as a function of the lens diameter.

$$m_{camera} = 18931d^2 + 2441d + 41.567 \quad (14)$$

A similar linear regression was done for the length of the camera as a function of the lens diameter.

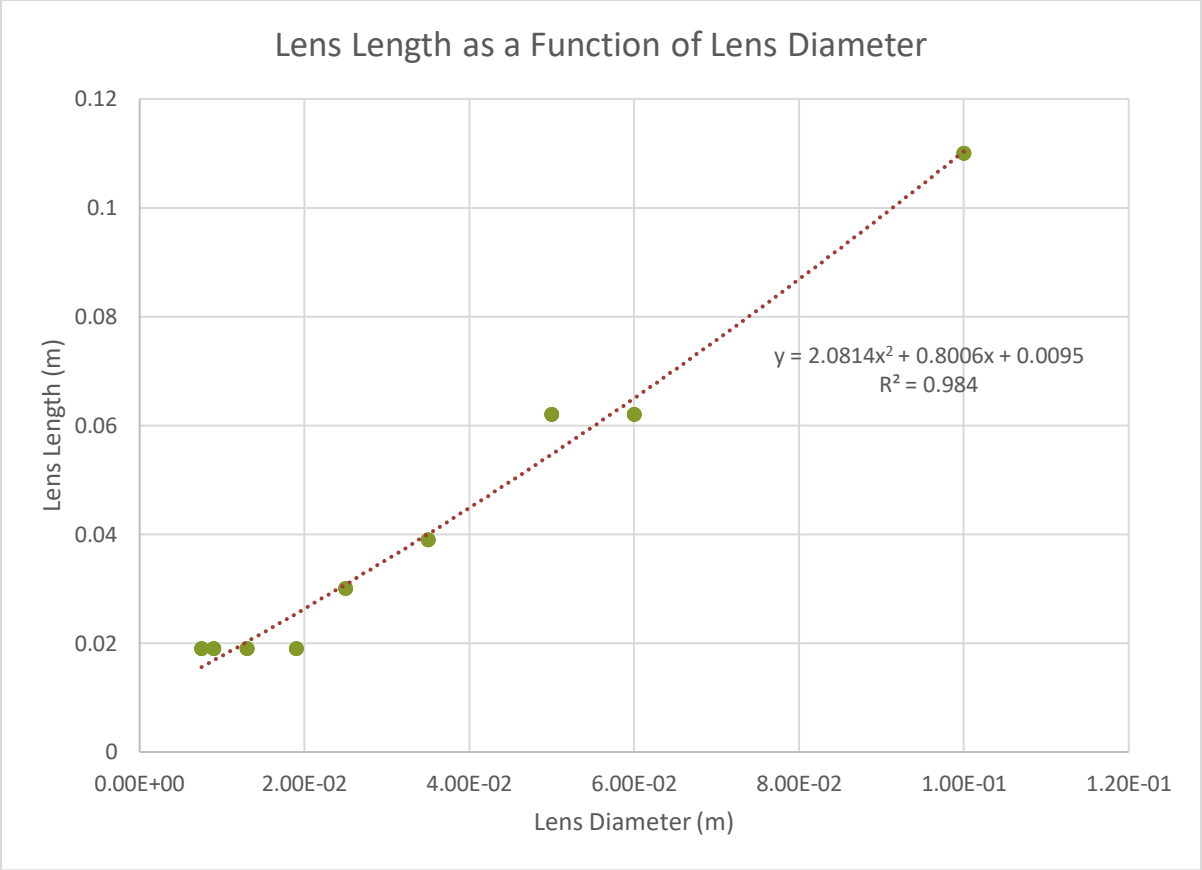

Figure 3.7 – Lens Length as a Function of Lens Diameter

As seen in Figure 3.7, the 2nd order polynomial trend line matches the data with a strong R^2 value. The following equation will be used moving forward to represent the volume of the camera as a function of the lens diameter.

$$V_{camera} = d^2(2.0814d^2 + 0.8006d + 0.0095) + 5.89x10^{-5} \quad (15)$$

Therefore, the final size of the hypothetical camera can be modeled in two parts: the mass of the system and the volumetric envelope it must occupy. Moving forward with the mathematical model, Table 3.4 contains the variables and ranges used to set limits.

Table 3.4 – Variables and their Ranges relating to the Camera Size Model

Variable	Range	Integer or Discrete
Lens Diameter	7.5 mm to 10 cm	Positive Real – rounded to three significant figures

This Camera Size model will be used to determine the size of the CubeSat needed to fit a particular payload. This model in conjunction with the Ground Sample Distance model comprise the physical models used to characterize the CubeSat in this thesis. These models

focus primarily on the payload, one of the assumptions in this work is that the remaining parts to create a viable CubeSat mission can be purchased as commercial off the shelf parts. The purpose of this thesis was not to fully design a CubeSat version of the FireSat II mission but to explore the potential performance gains from using the CubeSat architecture.

3.1.2 Interaction Models

Once launched, it is important to know how the CubeSat as a system interacts with the body it is observing – Earth. The models explored in this section primarily relate to the Coverage and Location requirements (presented in Table 3.2). There are three models in this section: 1) the Orbit Model, 2) the Ground Track Model, and 3) the Swath Width Model. The Orbit Model tracks the altitude as a function of time for a de-orbiting spacecraft, the Ground Track Model identifies the physical location on Earth that the satellite orbit corresponds with over time, and the Swath Width Model determines the size of the area examined by the spacecraft at any given point in time. These models and their driving variables are discussed in the following sections.

3.1.2.1 Orbit Model

In general, satellites require some amount of station keeping to maintain the desired/required orbit. However, since the proposed system is un-propelled, as soon as the CubeSat is deployed from the launch vehicle it will begin de-orbiting. In order to meet the requirements set forth by the mission and the UN regulation regarding orbit lifetime, a de-orbit model was required to determine the lifespan of the CubeSat. There are three major environmental factors that impact the rate at which a satellite will de-orbit: 1) solar radiation pressure, 2) atmospheric drag, and 3) gravity. Solar radiation pressure is the pressure generated on the spacecraft by impact from light waves – both through reflection and absorption, but is primarily dependent on the distance from the light source (the sun)[98]. Solar radiation pressure is essentially constant at all altitudes and only becomes an important disturbance when the satellite is far from planets and moons. [64]

Since the satellite will remain in LEO, the overall distance from the sun changes insignificantly throughout its orbit and the solar radiation pressure can be assumed as a constant. Atmospheric drag is the force generated on the spacecraft due to friction caused by the atmospheric particles, unlike solar radiation pressure, this is dependent on the altitude of the spacecraft and is considered in the de-orbit model. Gravity, like solar radiation pressure, is held constant through the work. The simple program presented in the fourth section of [99]

was used to generate the de-orbit model – this program assumes a constant solar radio flux and geomagnetic index, thus using atmospheric drag as the primary deorbiting factor. Equation (4), reiterated below, is the expression for atmospheric torque; where the ρ is the atmospheric density, C_d is the drag coefficient, A_r is the cross-sectional area, V is the orbital velocity of the spacecraft, and cp_a and cm are the centers of aerodynamic pressure and center of mass, respectively, in meters.

$$\tau_a = \frac{1}{2}\rho C_d A_r V^2 (cp_a - cm)$$

The atmospheric torque is simply the atmospheric drag multiplied by the difference between the center of aerodynamic pressure and the center of mass. Removing these terms, the atmospheric drag force can be calculated by the following equation.

$$F_a = \frac{1}{2}\rho C_d A_r V^2 \tag{16}$$

Where the velocity of the spacecraft is dependent on the mass of the spacecraft and its distance from the central body as seen in the following equation.

$$V = \sqrt{\frac{m_{s/c} G}{R_e + H}} \tag{17}$$

Where $m_{s/c}$ is the mass of the spacecraft, G is the gravitiaonal constant for the central body, and R_e is the radius of the central body, and H is the height above the central body. Therefore, Equations (16) and (17) can be combined into the following equation for atmospheric drag.

$$F_a = \frac{1}{2}\rho C_d A_r \frac{m_{s/c} G}{R_e + H} \tag{18}$$

Atmospheric density, the drag coefficient, the gravitational constant of the earth, and the radius of the earth are consistent across all proposed satellites and the influencing variables for the orbit model for each satellite are the initial altitude, the mass of the satellite and the cross-sectional area. Based on this information, Figure 3.8 illustrates the inputs and outputs of the orbit model.

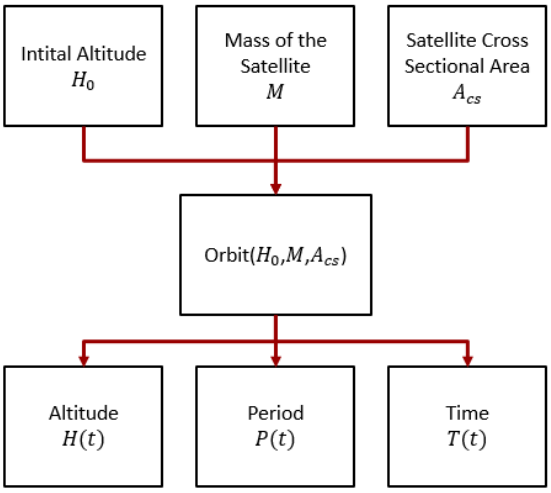

Figure 3.8 – Visual representation of the Orbit Model

From this the range of allowed altitudes can be calculated to both test the validity of the model and provide design variable limits for in the complete mathematical model. According to Table 3.5 below, orbit lifespans become too long to abide by space debris regulations at 600km. This value was used as the upper limit of initial altitudes to determine the range of altitudes which generated the specified lifespan for a given CubeSat size.

Table 3.5 – Satellite Lifespan Estimates [51]

Satellite Lifespan Estimates	
Altitude	*Orbit Lifespan*
<200 km	Hours to days
300 km	Months
500-600 km	25 years or less
800 km	Hundreds of years

The altitudes used in this test ranged from the Karman Line – the beginning of outer space, defined at 100km – to 600km. Using these initial altitudes, the lifespan of 1U, 1.5U, 2U, and 3U CubeSat orbital lifespans were calculated using the model generated in the previous section. Figure 3.9, shows the time spent in orbit of a CubeSat based on its initial altitude and size characteristics. In this initial approximation of orbital lifespan, the cross-sectional area was represented as a weighted average of the 6 primary faces of regulation CubeSat sizes (presented in Table 2.5), if deployable systems are used then the lifespan will change.

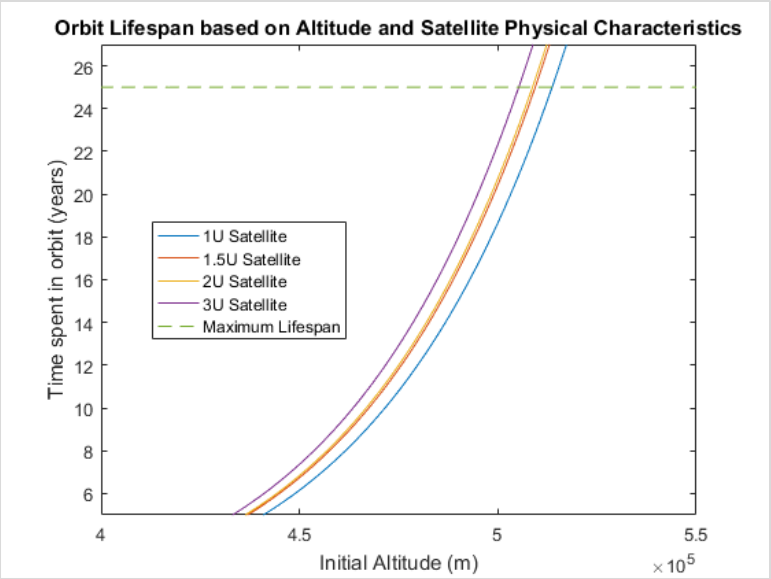

Figure 3.9 – Maximum Lifespans as a function of initial altitude and CubeSat size, highlighting the intersection of the lifespans and maximum altitude

The maximum lifespan was chosen to be 25 years to comply with orbital debris regulations. Though it is highly unlikely that a CubeSat would function for anywhere close to 25 years, from the initial ground sample distance calculations in Section 3.1.1.1m it is possible to achieve the desired ground sample distance up to these altitudes. Therefore, this upper limit was selected so to prevent a long term presence in space for the 'dead' spacecraft. The minimum lifespan was chosen to be 162 days – the length of one fire season. These are presented in Figure 3.10 below.

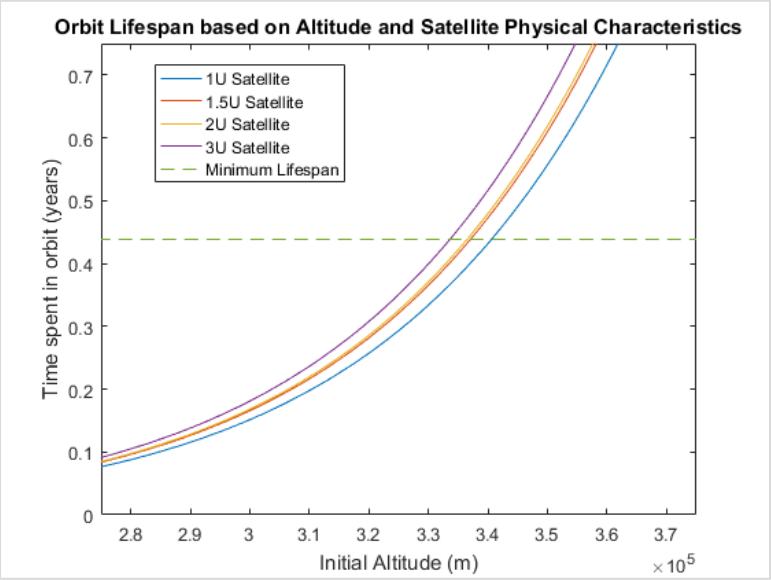

Figure 3.10 – Minimum Lifespans as a function of initial altitude and CubeSat size, highlighting the intersection of the lifespans and minimum altitude

Both the minimum lifespan and the maximum lifespan are included on theses graphs as dashed lines for reference. The intersection of the minimum and maximum lifespan with each of the CubeSat sizes is included in the Table 3.6.

Table 3.6 – Calculated Altitude Ranges

CubeSat Altitude Ranges	
Size	*Range*
1U	341 – 513 km
1.5U	338 – 509 km
2U	337 – 508 km
3U	334 – 505 km

From this, the initial altitudes of the spacecraft were limited to 350km and 450 km, so that the orbital lifespan of the satellite fell well within the desired range (presented in Table 3.7 below).

Table 3.7 – Lifespan Ranges

CubeSat Lifespan Ranges	
Size	*Range*
1U	203 days – 6.14 years
1.5U	222 days – 6.73 years
2U	226 days – 6.83 years
3U	243 days – 7.35 years

These calculations were initially performed with a time step of 1 day, however since the model is iterative, it is important to check that the model holds true with even smaller times steps. In further calculations it will be important to know the location of the satellite for more than once a day, as LEO orbits take around 90 minutes to complete. To appropriately approximate the ground track of the satellite, the time step needs to be small enough to hit the target location, however, since both orbit model and the ground track model are iterative approximations of the path experienced by the satellite, there is question on accuracy of the model. To test this, the orbit model was run with each of the four Standard CubeSat sizes and nine time steps ranging from 1 day to 1 min – generating 36 trials. The final data points – length of time in orbit – are presented in Table 3.8 below. These trials began with an initial altitude of 400km.

Table 3.8 – Orbital Lifespan as a Function of CubeSat Size and Time Step

Time Step (day)	Time Step (min)	Cube Sat Size			
		1 U	*1.5 U*	*2 U*	*3 U*
1	1440	702 days	791 days	842 days	904 days
0.5	720	700 days	789 days	840 days	902 days
0.25	360	699 days	788 days	838 days	901 days
0.125	180	698 days	787 days	838 days	900 days
0.041667	60	698 days	787 days	837 days	899 days
0.020833	30	698 days	787 days	837 days	899 days
0.010417	15	698 days	787 days	837 days	899 days
0.005208	7.5	698 days	787 days	837 days	899 days
0.000694	1	698 days	787 days	837 days	899 days

The range in lifespan for a 1U CubeSat is 3.911 days, 1.5U is 3.682 days, 2U is 4.29 days, and 3U is 4.209 days. This amounts to 0.5% on average, proving that changing the timestep of the de-orbit modle does not dramtically effect the orbit lifespan. Moving forward with the mathematical model, Table 3.9 contains the variables applicable to the orbit model and ranges used to set limits. Satellite size can be used to calculate the mass and the cross-sectional area of the CubeSat as these are standard features of the CubeSat architecture.

Table 3.9 – Variables and their Ranges relating to the Orbit Model

Variable	Range	Integer or Discrete
Satellite Size	[1,1.5,2,3]	Integer – represented as 1-4 to the corresponding sizes
Launch Altitude	350 km to 450 km	Integer

3.1.2.2 Ground Track Model

In conjunction with the GSD of each satellite, the location with respect to earth is important in formulating penalty function 2. Requirement 1.05 states that "The mission shall be able to cover specified forest areas within the US at least twice daily." This requirement was broken into two parts for modeling: 1) modeling the ground track of the satellite and 2) determining the swath width of the payload.

The ground track of a satellite is influenced by two things: orbit and time. This model must have higher fidelity than the de-orbit calculations due to the increase in spatial knowledge need for ground tracks. Modeling the ground track requires a more precise definition of the orbit of the spacecraft – using all six Keplerian elements and time to determine the latitude and longitude of the spacecraft as functions of time. This is illustrated below in Figure 3.11.

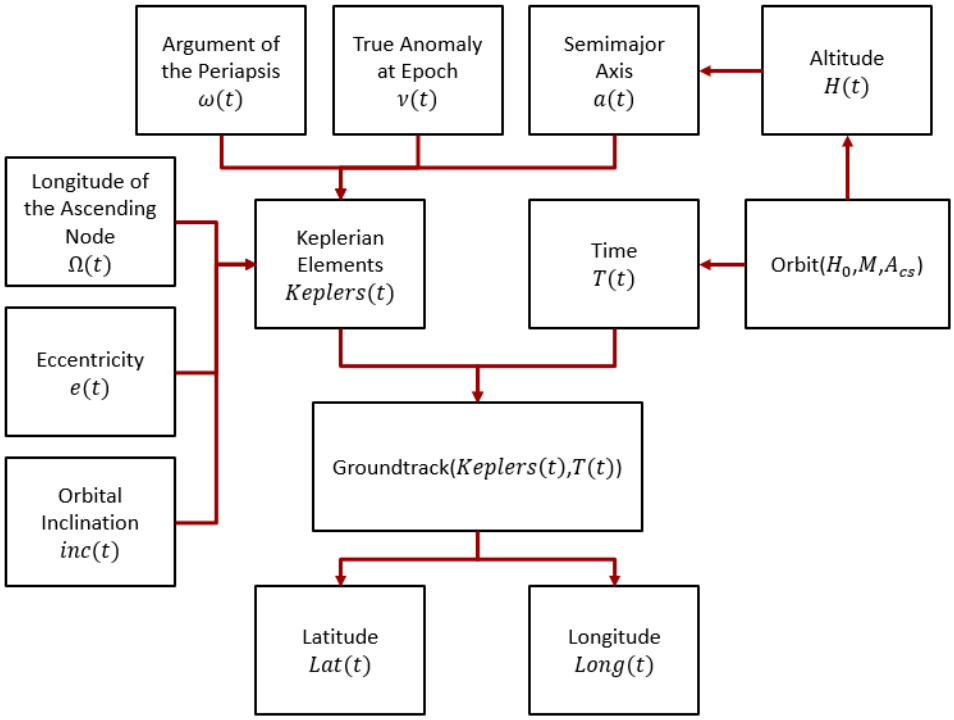

Figure 3.11 – Visual representation of the ground track model used

Since the orbits are being modeled as circular, eccentricity is zero and the altitude as a function of time generated from the deorbit model is used to represent the semimajor axis as a function of time. Argument of the Periapsis, True Anomaly at Epoch, and Longitude of the Ascending Node were all set to range from 0-360. When considering the initial parameters in a launch it is important to know where the satellite has been launched from. The United States has 4 primary launch locations capable of orbital flight. They are presented in Table 3.10, these inclinations form the range of possible inclinations in orbit calculations.

Table 3.10 – United States Launch Locations and Resulting Inclinations

United States Launch Sites				
Location	*Latitude*	*Longitude*	*Minimum Inclination (degrees)*	*Maximum Inclination (degrees)*
Kodiak Launch Complex, Alaska [100]	57.43533°N	152.33931°W	59.6	110.2
Vandenberg Air Force Base, California	34.77204°N	120.60124°W	51.0	145.0
Kennedy Space Center, Florida	28.6082°N	80.6040°W	28.0	62.0
Wallops Flight Facility, Virginia [101]	37.9401°N	75.4663°W	38.0	60.0

Orbital inclination was determined based on the values in Table 3.10. This range was identified to be continuous from 28.0° to 145.0°, as all inclinations in this range can be accounted for by one of the four US launch sites. Similar to the orbit model, the ground track model is iterative and dependent on the size of the time steps. Because the altitude is derived from the orbit model, in looking at this requirement, a higher fidelity time step is needed to be able to map the orbit of a LEO satellite along its ground track with any degree of accuracy. Figure 3.12 below shows the differences in ground track paths calculated based on the time step input into the system.

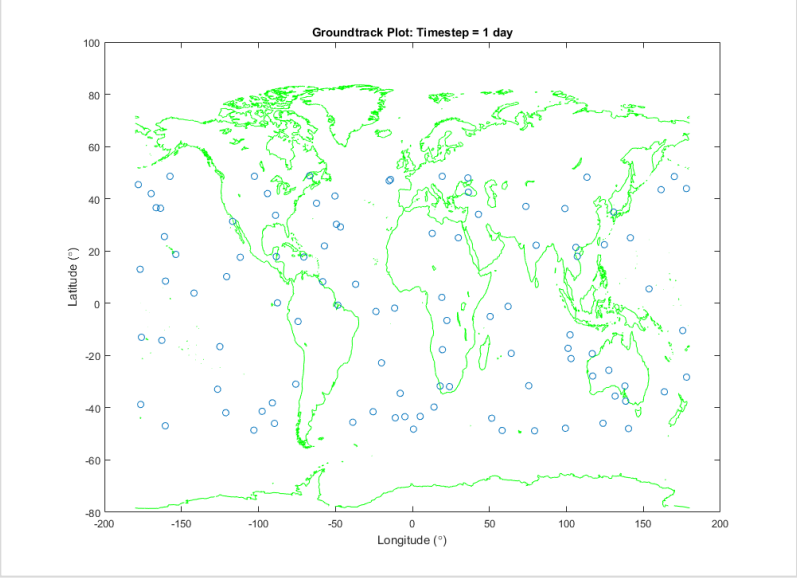

(a) Latitude and Longitude calculated once per day

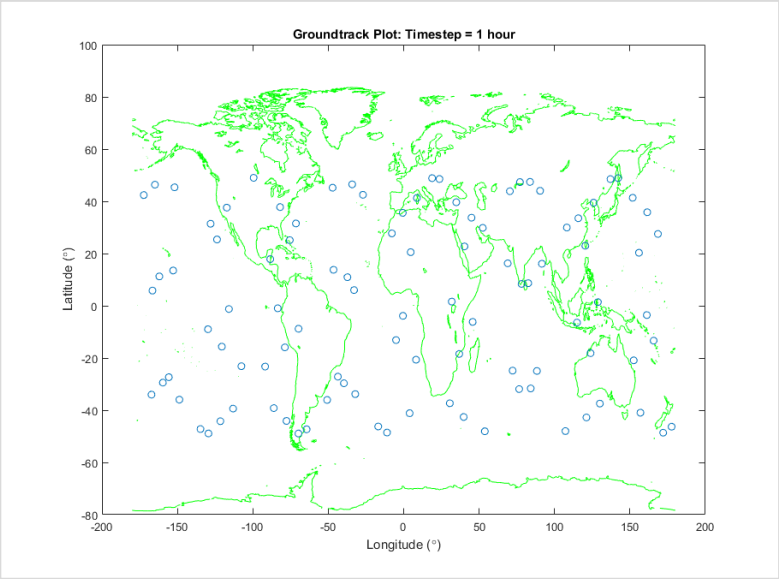

(b) Latitude and Longitude calculated once per hour

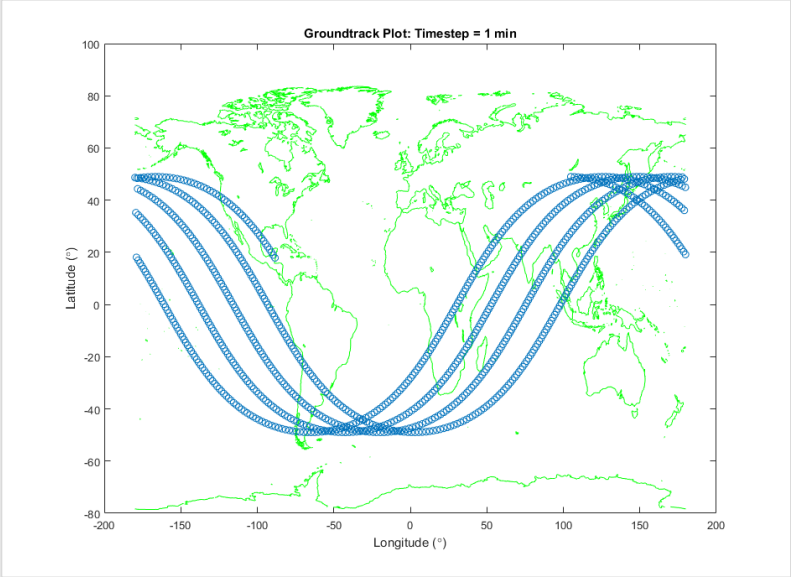

I Latitude and Longitude calculated once per minute

Figure 3.12 – Differences in Fidelity of the Ground Track Model based on Time Step

Based on other satellites in Low Earth Orbit, such as the ISS, and the periods generated by the orbit model the period is approximatly 90 minutes. The goal is to use the largest timpstep possible for processing ease. As there are 360 degrees in an orbit, with approximately 90 minutes to orbit, the satellite can be expected to move about 4deg/min – give or take a few degrees depending on the actual orbital period. In order to minimize the number of data points required yet still capture all the necessary information, for each satellite profile evaluated, the time step

will be determined based on the swath width of the payload in order to create a clear picture of the captured ground track – this will be modeled in the followng section. Moving forward with the mathematical model, Table 3.11 contains the variables applicable to the ground track model and ranges used to set limits.

Table 3.11 – Variables and their Ranges relating to the Ground Track Model

Variable	Range	Integer or Discrete
Eccentricity	0 (left in the design string for future work)	Integer
Inclination	28-145 degrees	Integer
Longitude of the Ascending Node	0 – 360 degrees	Integer
Argument of the Periapsis	0 – 360 degrees	Integer
True Anomaly	0 – 360 degrees	Integer
Launch Altitude	350 km to 450 km	Integer

3.1.2.3 Swath Width Model

The swath width can be described as the arc on the surface of the earth which runs from horizon to horizon. [62] It creates a circle centered on the ground track of which the spacecraft can "see." (This is demonstrated visually in Figure 3.13)

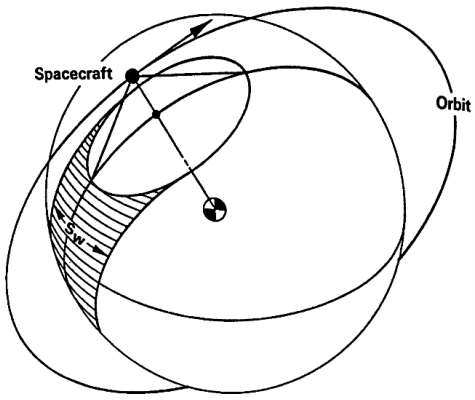

Figure 3.13 – Swath Width [62]

There is both a swath width for the spacecraft and a swath width for onboard instruments. In this portion of the model – the swath width for the camera is the important feature. Swath width for the instrument (in this case the camera) is dependent on the field of view and altitude. A visual representation of the variables and their impact on instrument swath width can be seen in Figure 3.14 below.

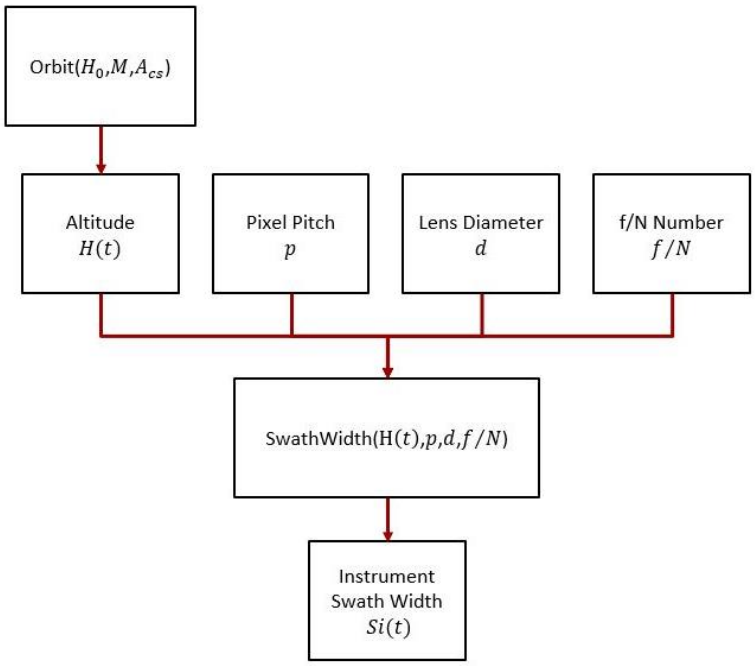

Figure 3.14 – Visual Representation of the Instrument Swath Width Model Used

These swath width calculations are important as they allow the determination of the maximum size of the time step based on each camera. These times steps were generated from the following equation.

$$\Delta T = \frac{360(2Si)}{P} \tag{19}$$

Where Si is the average swath width over the lifespan and P is the average period in minutes. Typically, the period ranges by about 5 minutes and the swath width by about 6 degrees. The standard deviation for swath width is around 0.69 degrees and the standard deviation of period is around 45 seconds. This means that a majority of the data is included in the 1.38 degree range around the mean of the swath width and the 90 seconds around the mean of the period. Thus this approximation does not introduce large errors. Moving forward with the mathematical model, Table 3.12 contains the variables applicable to the swath width model and ranges used to set limits.

Table 3.12 – Variables and their Ranges relating to the Swath Width Model

Variable	Range	Integer or Discrete
Satellite Size	[1,1.5,2,3]	Integer – represented as 1-4 to the corresponding sizes
Launch Altitude	350 km to 450 km	Integer
Pixel Pitch	[12 μm, 17 μm, 25 μm]	Integer
Lens Diameter	7.5 mm to 10 cm	Positive Real – rounded to three significant figures
f/N number	[1.1, 1.2, 1.25, 1.4, 1.5, 1.6]	Integer

3.1.3 Summary of Models

These five models form the mathematical model by which the system will be analyzed. With all the variables included, the overall system model is organized in the following manner presented in Figure 3.15 below.

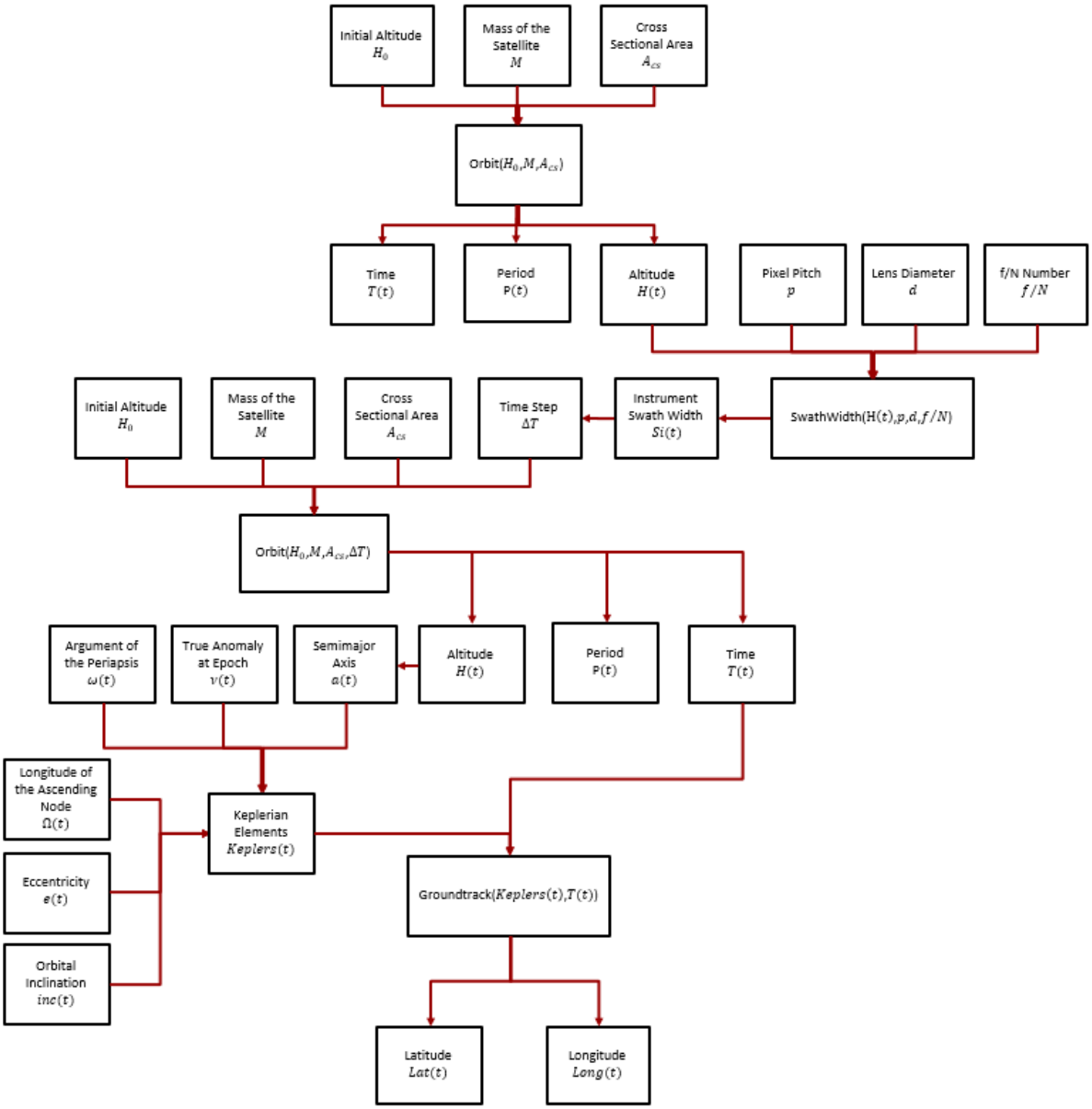

Figure 3.15 – Overall System Model

The variables used in this model and their ranges are presented in the Table 3.13 below.

Table 3.13 – Variables and their ranges used in the System Model

Variable	Range	Integer or Discrete
Pixel Pitch	[12 μm, 17 μm, 25 μm]	Integer
Lens Diameter	7.5 mm to 10 cm	Positive Real – rounded to three significant figures
f/N number	[1.1, 1.2, 1.25, 1.4, 1.5, 1.6]	Integer
Satellite Size	[1,1.5,2,3]	Integer – represented as 1-4 to the corresponding sizes
Launch Altitude	350 km to 450 km	Integer
Eccentricity	0 (left in the design string for future work)	Integer
Inclination	28-145 degrees	Integer
Longitude of the Ascending Node	0 – 360 degrees	Integer
Argument of the Periapsis	0 – 360 degrees	Integer
True Anomaly	0 – 360 degrees	Integer

From this information, the design string for the mathematical model can be created. These models will form the basis by which the requirements presented in Table 3.2 will be used to place limits on the system and employ a genetic algorithm to create viable mission profiles that meet the stated requirements.

3.2 Design String Formulation

In order to use a genetic algorithm, a design string of the important variables is needed. Looking at Table 3.13, there are 10 variables associated with the satellite design. These 10 variables will constitute the majority of the design string but since the overall system will be comprised of multiple satellites, two more variables are added: the number of satellites and the frequency at which they are launched. Together they form 12 design variables. These 12 design variables could either be an integer or a positive real number. Of these 12 variables, 2 of them are single values, and the other 10 are 1-by-MaxSat vectors that contain a variable for each of the possible satellites. MaxSat is a variable generated in the beginning of the optimization process, it is calculated in order to set a constant design string length and is based on four assumptions: 1) minimum launch frequency, 2) minimum launch altitude (and thus minimum time in orbit), 3) minimum CubeSat size, and 4) length of mission. These four things, coupled with the de-orbit model calculated the number of satellites required to meet the mission length requirements. The design string is formulated this way because each calculation is performed on the combination of satellites and their launch frequency; that is, each individual satellite

represented in the design string is not considered independently. The variables with their type and ranges are presented in Table 3.14 below.

Table 3.14 – Variables included in the Design String

Variable	Range	Integer or Discrete
Launch Frequency	6 – 36 months	Integer
Number of Satellites	1 – MaxSat (determined based on a six month launch frequency, launched at the lowest possible altitude for the duration of the mission)	Integer
Satellite Size	1-4 (representing the 4 CubeSat sizes)	Integer
Launch Altitude	350 km to 450 km	Integer
Eccentricity	0 (left in the design string for future work)	Integer
Inclination	28-145 degrees	Integer
Longitude of the Ascending Node	0 – 360 degrees	Integer
Argument of the Periapsis	0 – 360 degrees	Integer
True Anomaly	0 – 360 degrees	Integer
Pixel Pitch	1-3 (representing the three pixel pitches modeled)	Integer
Lens Diameter	7.5 mm to 10 cm	Positive Real – rounded to three significant figures
f/N number	1-6 (representing the 6 f/N number options modeled)	Integer

Figure 3.16 below illustrates the design string. For each candidate design (henceforth called a mission profile) the algorithm looks at the second location to determine the number of satellites launched in each design string and then collects that information from the appropriate location in each of the following design strings.

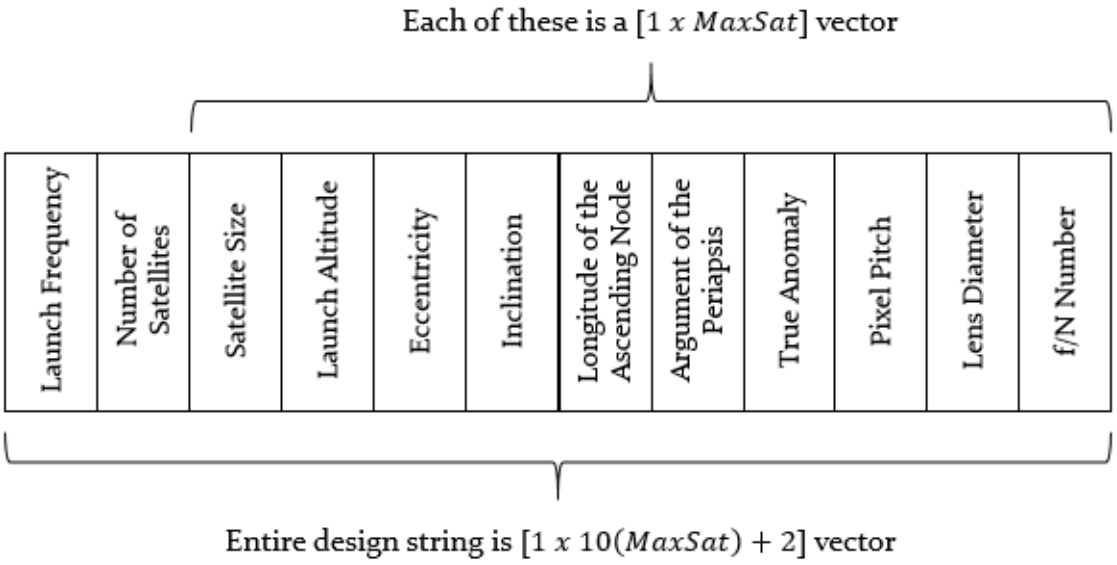

Figure 3.16 – Design String

Eccentricity, though constrained at zero in this thesis, was left in the model to allow for expansion of the orbit and ground track models in future work. The rest of the design variables are used in models presented in the previous section to mathematically model the proposed satellite architecture against the driving system requirements.

3.3 Cost Models

To determine if the proposed satellite architecture is comparable to the traditional FireSat II model, the driving requirements in Table 3.2 are related to penalty functions. By doing so, this provides a metric though which the performance can be measured in a quantifiable way. To do so, each of the requirements was related to a cost associated with fires missed and this penalty cost is compared with the cost of the satellites. This section discusses the development of the cost model of the satellite and the cost of the fires missed.

3.3.1 Satellite Cost Model Generation

One of the driving requirements for the system is that the entire system will have a reoccurring cost of less than $3 million a year. To check the validity of this, and provide a means for optimizing the system, a cube sat cost model was generated. This model was broken up into four phases: 1) Design and Development, 2) Construction, 3) Launch Preparation, and 4) Launch. Two of these phases (Phase 1 and Phase 4) are constant for each satellite and the other two are dependent on the size and components in each satellite. The total cost of the mission will be derived from the sum of the different phases for each satellite. Phase 1 (Design and

Development) costs were approximated to $5,000 dollars per satellite design, as the standardized nature of the CubeSat architecture eliminates the need for research and development costs. [102] Phase 1 costs are represented by Equation (20) below, where $nDesigns$ is equal to the number of unique satellite designs used, if the same satellite design is used throughout the mission, then $nDesigns$ is equal to one.

$$Phase1 = \$5000(nDesigns) \tag{20}$$

Phase 2 (Construction) is the most complex cost to develop. Each of the subsystems, and the payload, have individual costs which must be accounted for. ADC, CDH, TTC, and Thermal all have a set cost per satellite, which was approximated based on the parts database generated in Chapter 2. These values are presented in Table 3.15 below.

Table 3.15 – Subsystem Cost Approximations

CubeSat Subsystem Cost	
ADC	$2,120 (€2,000)
CDH	$9,010 (€8,500)
TTC	$3,180 (€3,000)
Thermal and Misc.	$6,646.2 (€6,270)

Power costs were approximated based on the cost of solar cells per U. From the parts database generated in Chapter 2, this is seen to be about $2,120 per U. This information, in conjunction with the payload costs (explained in the following section) make up the cost of the satellite. Equation (21) presented below is the structure for the cost of Phase 2, where $CameraCost$ is the total cost of the camera as explained in Section 3.3.1.1, and $SizeCost_i$ is the cost of the CubeSat structure as presented in Table 2.5 and reiterated below.

$$Phase2 = \$20{,}956.2(nSat) + \sum_{i=1}^{nSat} \$2{,}120(Size_i) + CameraCost_i + SizeCost_i \tag{21}$$

Commercial Off the Shelf CubeSat Structures	
Name	*Cost*
1U	$2,650 (€2,500)
1.5U	$3,339 (€3,150)
2U	$3,339 (€3,150)
2U Long	$3,339 (€3,150)
3U	$4,134 (€3,900)

Phase 3 (Launch Preparation) costs are broken down into two costs: the cost of the CubeSat deployer and the cost of transportation and installation. The standard CubeSat deployer launches 3Us, in whatever combinations generate a total of 3U. Assuming ride sharing, the cost of the deployer can be divided based on the percentage of the deployer the satellite occupies. Table 3.16 below highlights those costs. Costs are presented in both Euros and USDs in the table below because the original price was in Euros and the prices were converted to USD from Euros on April 15, 2017 when the exchange rate was 1.06 Euros to the USD for consistency.

Table 3.16 – Cost of CubeSat Deployers based on CubeSat Size

CubeSat Deployer Cost	
1U	$8,832.98 (€8,333)
1.5U	$13,250 (€12,500)
2U	$17,665.96 (€16,666)
3U	$26,500 (€25,000)

This information presented in Table 3.16, is combined with a standard $5,000 transport and installation cost to account for time and labor required perform safety checks on the CubeSat and to integrate the satellite into the deployer. This phase is represented in Equation (22) below.

$$Phase3 = \$5{,}000(nSat) + \sum_{i=1}^{nSat} \$26{,}500\left(\frac{Size_i}{3}\right) \quad (22)$$

Phase 4 (Launch) costs are dependent on the particular launch vehicle and the percentage increase in mass getting launched which is hard to estimate without flight manifests, however, as any cube sat generated by this model will be under 4 kg, this is such a miniscule percentage of the mass of the launch vehicle itself that the cost has been approximated to be $1000 per satellite. This is represented in Equation (23) below.

$$Phase4 = \$1000(nSat) \quad (23)$$

3.3.1.1 Payload (Camera) Cost Trends

The camera cost model is generated based on information from FLIR – presented in Table 3.17.

Table 3.17 – Cost Data Provided from FLIR Representative

Tau Part Number	Description	Unit Price
	Cores	
666400007H-FPNLX	Tau 2 640 x 480, 17 µm Pixel Pitch, 60 Hz, 7.5 mm f1.2 90° lens	$6,492
46336007H-FPNLX	Tau 2 336 x 240, 25 µm Pixel Pitch, 60 Hz, 7.5 mm f1.2 42° lens	$3,078
46324007H-FPNLX	Tau 2 324 x 240, 25 µm Pixel Pitch, 60 Hz, 7.5 mm f1.2 42° lens	$3,078
	Lenses	
322-023-02	6.8mm, f/1.3 Lens Cell for Tau2 336 & lower resolution	$200
322-0452-02	7.5mm, f/1.2 Lens Cell for all Tau2 Cameras	$300
322-0139-02	9mm, f/1.25 Lens Cell for Tau2 336,320,160 (WFOV)	$300
322-0198-02	9mm, f/1.4 Lens Cell for Tau2 640 WFOV	$375
322-0141-02	13 mm, f/1.25 Lens Cell for all WFOV Tau 2 Cameras	$230
322-0143-02	19mm, f/1.25 Lens Cell for all WFOV Tau 2 Cameras	$260
322-0160-02	25mm, f/1.1 Lens for all NFOV Tau2 Cameras	$785
322-0169-02	35 mm, f/1.2 Lens for all NFOV Tau2 Cameras	$965
322-0170-02	50mm, f/1.2 Lens for all NFOV Tau 2 Cameras	$1,300
322-0191-02	35mm, f/1.5 WFOV Lens Cell for Tau2 Cameras	$525
322-0133-02	60mm, f/1.25 Lens for NFOV Tau 2 Cameras	$1,585
322-0208-02	60mm, f/1.25 Lens, Atherm, HC, for NFOV Tau2 Cameras	$1,850
322-0118-02	100mm, f/1.6 Lens for all NFOV Tau2 Cameras	$1,950

From this information a cost model was generated based on the three optical factors: pixel pitch, lens diameter, and f/N number. In the Tau 2 camera, the pixel pitch is contained within the core and was modeled based on the cost of two cores – one with a 17 µm pixel pitch and the other with a 25 µm pixel pitch. Though there was not a 12µm core offered with the Tau 2 Camera,

FLIR does offer other cameras with a 12 µm core. To increase our camera options, this additional core was included and the cost was extrapolated from the two 17 and 25 µm cores. This trend was modeled linearly.

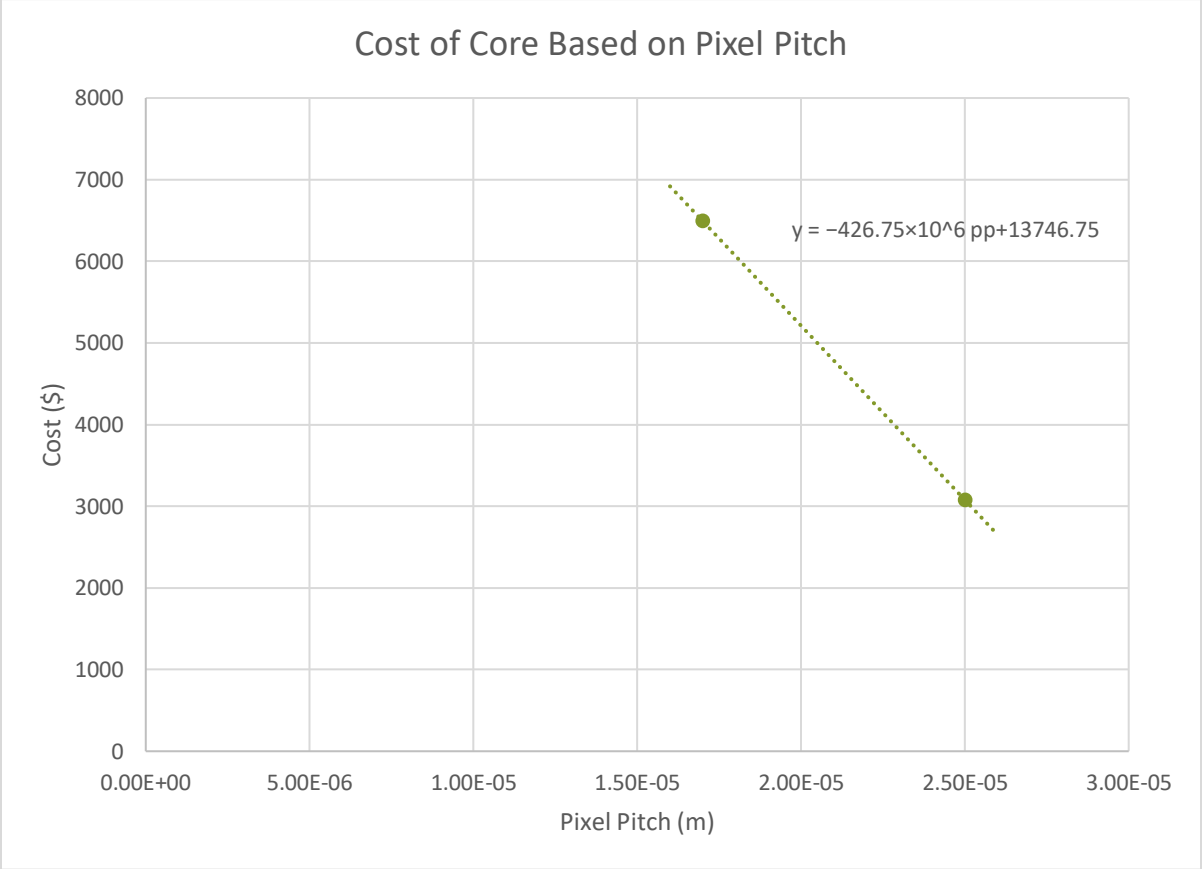

Figure 3.17 – Cost Model for Pixel Pitch

As seen in Figure 3.17, the cost decreases with an increase in pixel pitch. This was modeled linearly by Equation (24) presented below, where pp is the pixel pitch.

$$C_{pp} = -426.75 \times 10^6 pp + 13746.75 \quad (24)$$

From this, three discrete costs were generated and are presented in below.

Table 3.18 – Pixel Pitch Cost Model

Pixel Pitch (µm)	Cost of Core
12	$8625.75
17	$6492
25	$3078

In the data provided by FLIR, the lens diameter and the f/N numbers were coupled with the prices. As a result, the cost model generated was calculated based on the effective focal length

of the lens, which is the product of f/N number and lens diameter. Figure 3.18 below shows the relationships between cost and the effective focal length.

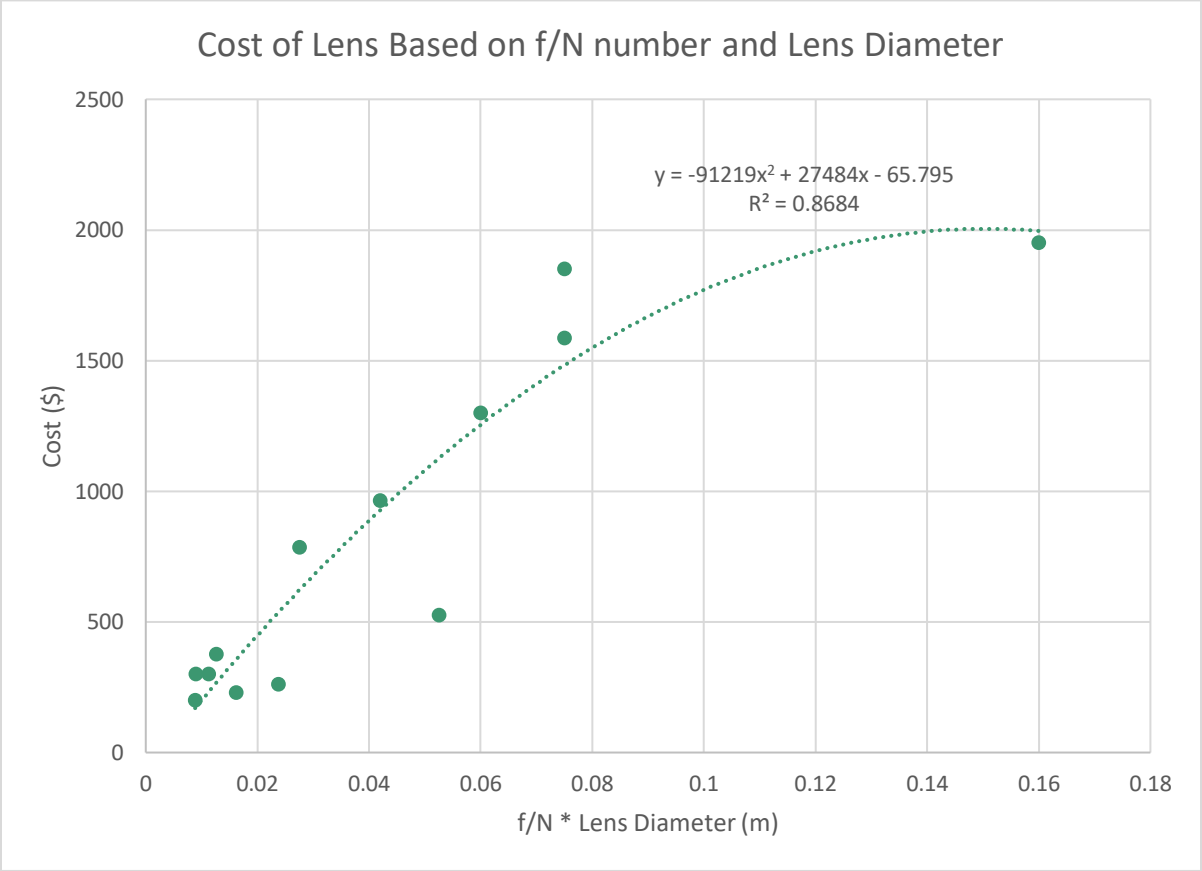

Figure 3.18 – Cost Model of Lens based on Effective Focal Length

As seen in Figure 3.18 above, a second order polynomial fit is best. Equation (25) below is the formula used to generate the cost of the lens though the rest of the model.

$$C_{lens} = -91219[(d)(f/N)]^2 + 27484[(d)(f/N)] - 65.795 \quad (25)$$

Combinations of different lenses and f/N numbers can yield the same lens cost, as seen in Equation (25) above. In fact, most costs have 6 possible combinations of lens diameter and f/N number as seen Figure 3.19 in below, if you were to draw a horizontal line it would intersect all the possible combinations. From $251 to $1845, there are 6 combinations that generate the same price.

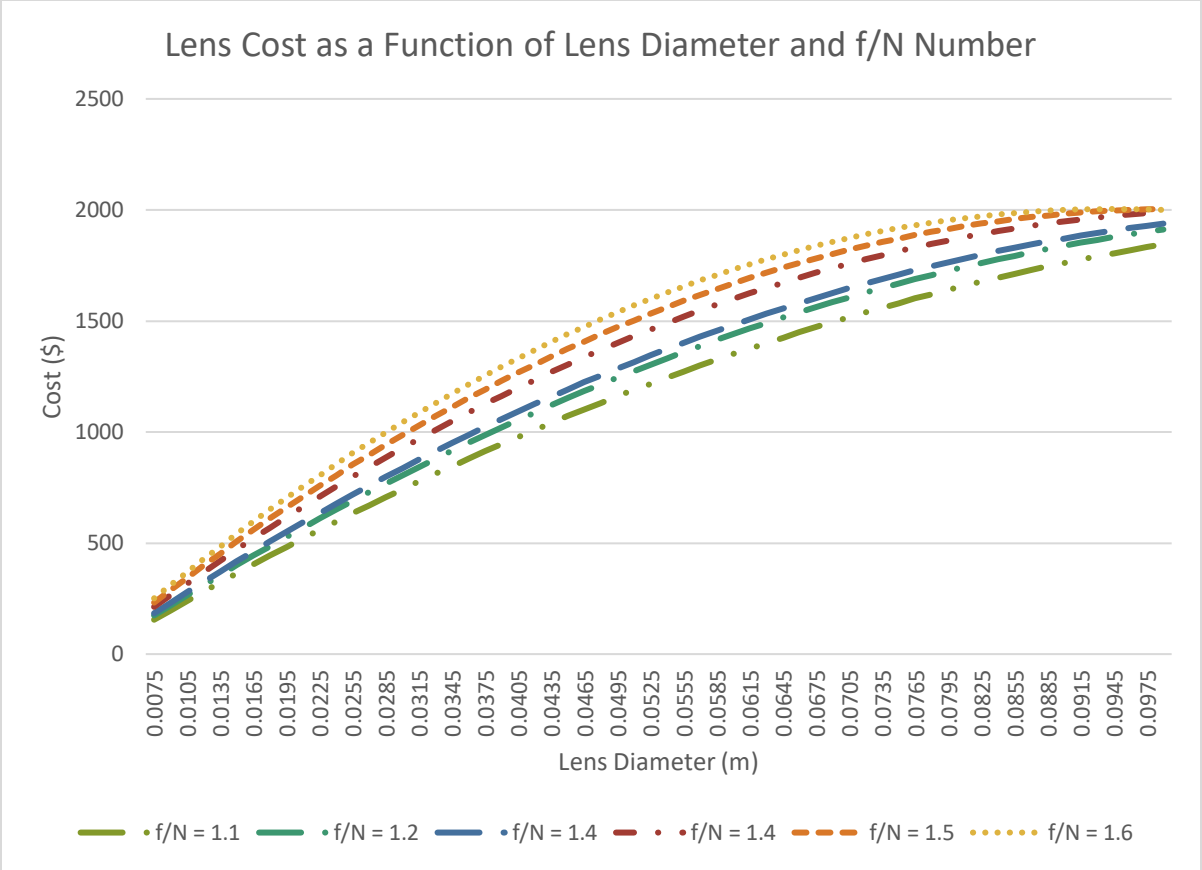

Figure 3.19 – Cost Combinations

From this, it should be considered that there are multiple camera solutions that will cost the same when considered in the mathematical model. This means that while solutions may appear different at first glance, it is possible for them to have converged at the same satellite cost. With this in mind, equation (24), the cost of the core, and equation (25), the cost of the lens, can be combined to form the cost model of the entire camera as presented in the equation below.

$$CameraCost = -426.75 \times 10^6 pp + 13681 - 91219[(d)(f/N)]^2 + 27484[(d)(f/N)] \quad (26)$$

The mission requirements state that the mission should last a minimum of eight years, and part of the proposed benefit of using the CubeSat architecture is the ability to introduce new, and better technologies as they progress. In this work, the technological development over time is only explored for the cameras. By looking 22 digital cameras over the past 30 years, it can be seen that the resolution increases over time and the cost decreases, shown in Figure 3.20 and Figure 3.21 below.

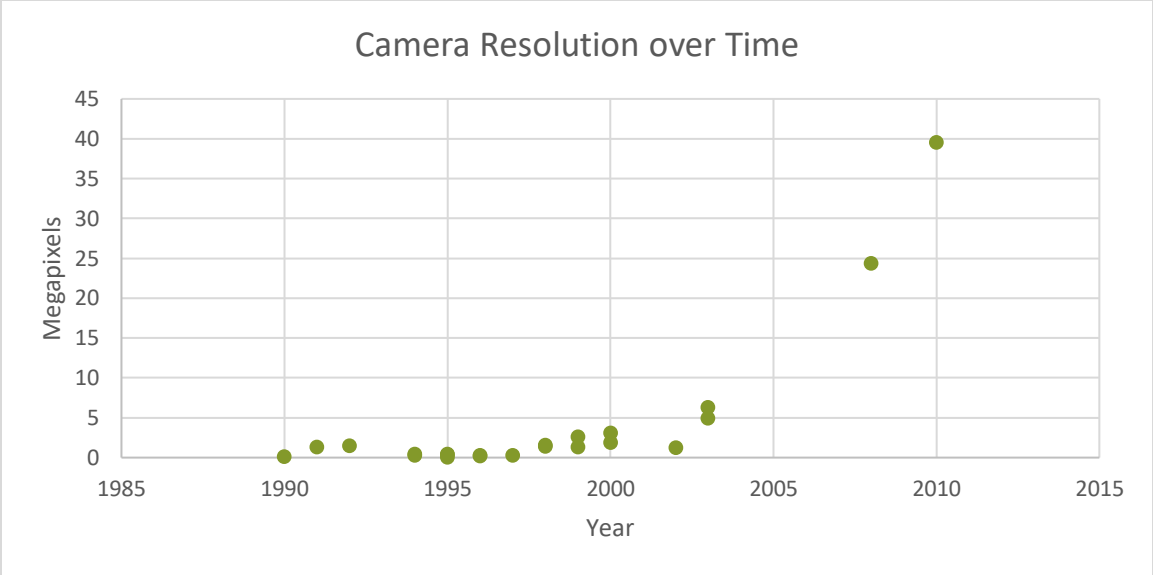

Figure 3.20 – Camera Resolution Trends over time

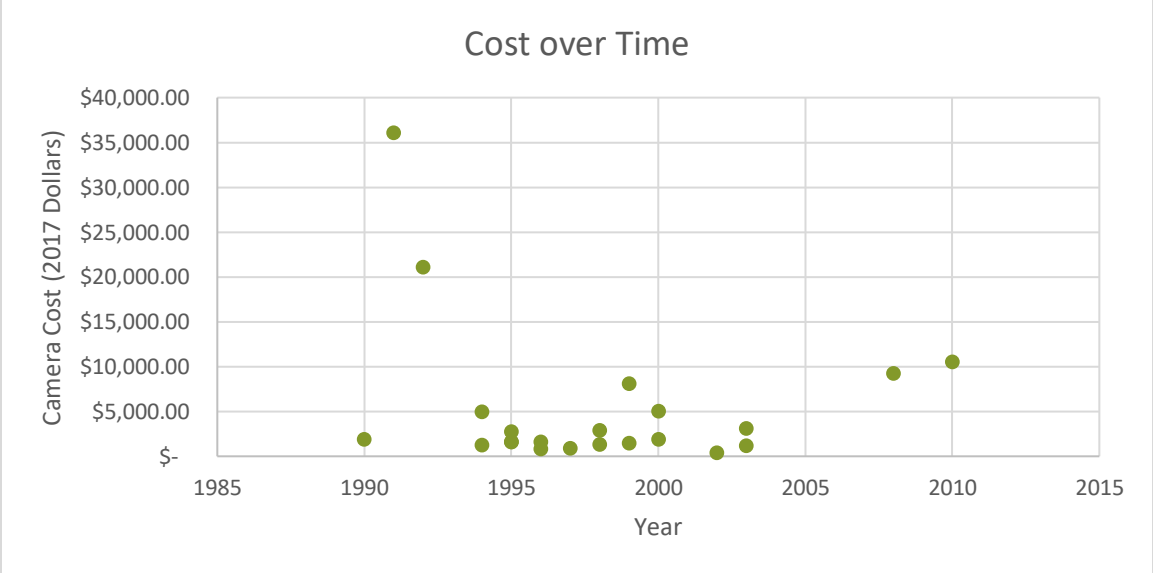

Figure 3.21 – Camera Cost over time

This is as expected, technologies steadily become better the longer they are on the market. However, cost only is not the best indicator for technology trends over time. According to Zhang and Berger, the most important indicator of technology performance is resolution per dollar, [103] or inversely, cost per megapixel of resolution. Figure 3.22 below illustrates the cost per megapixel.

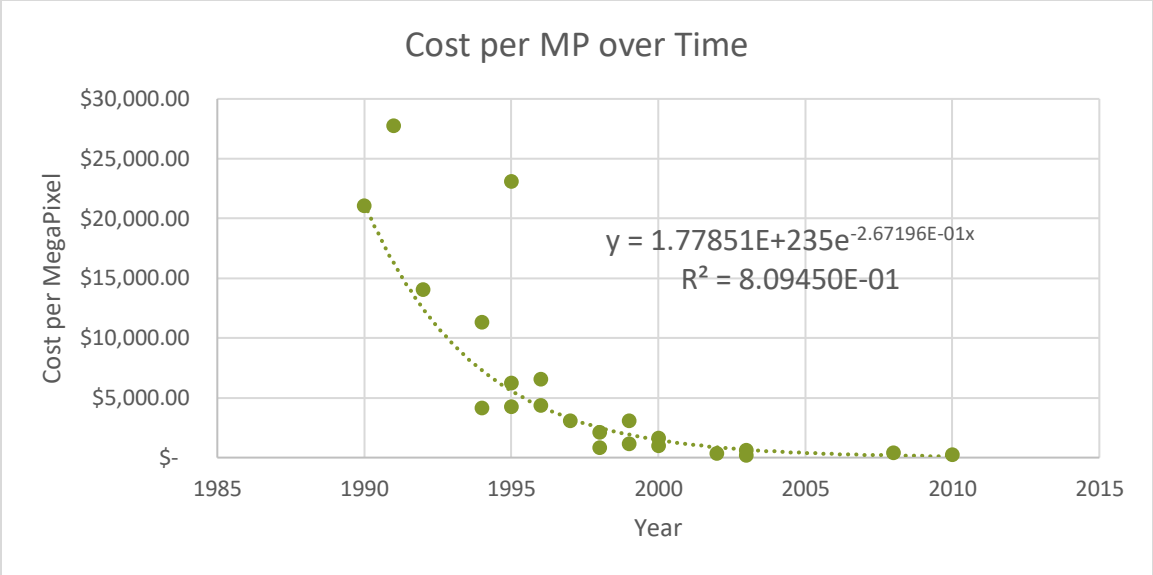

Figure 3.22 – Cost per Megapixel of Resolution in digital cameras over time

This relationship is modeled as exponential and the cost of the cameras decreases by 23.44% each year. This decrease in cost over time is built into the cost model of the satellite by using the time since the initial launch for each new satellite. Therefore, the total cost of the cameras over the course of the mission can be mathematically expressed in Equation (27) below.

$$TotalCameraCost = \sum_{i=1}^{nSat} 0.765523^{\frac{LaunchFrequency}{365}(i-1)} CameraCost_i \tag{27}$$

Substituting Equation (26) into Equation (27), the total cost of all the cameras used in the mission can be expressed as the following.

$$\begin{aligned} TotalCameraCost \\ = \sum_{i=1}^{nSat} 0.765523^{\frac{LaunchFrequency}{365}(i-1)} \{-426.75 \times 10^6 pp_i + 13681 \\ - 91219[(d_i)(f/N)_i]^2 + 27484[(d_i)(f/N)_i]\} \end{aligned} \tag{28}$$

From this, it can be seen that the final cost for Phase 2 is the combination of equation (22), the phase 2 equation prior to the inclusion of camera costs, and equation (26), camera costs. This is presented in Equation (29) below.

$$Phase2 = \$34{,}637.2(nSat) + \sum_{i=1}^{nSat} \left\{ \begin{array}{l} \$2{,}000(Size_i) \\ + 0.765523^{\frac{LaunchFrequency}{365}(i-1)} \{-\$426.75 \times 10^6 pp_i \\ - \$91219[(d_i)(f/N)_i]^2 + \$27484[(d_i)(f/N)_i]\} \end{array} \right\} \quad (29)$$

3.3.1.2 Satellite Cost Model Conclusions

Equation (30) is generated to represent the cost of each satellite launched.

$$TotalCost = Phase1 + Phase2 + Phase3 + Phase4 \quad (30)$$

Substituting in all the requisite equations creates the following satellite cost model. Equation (31) below is used to determine the cost of the mission based on each satellite and the number of designs, where $nSat$ is the number of satellites required to complete the mission and $nDesigns$ is the number of unique satellite designs used through the mission.

$$TotalCost = \$5{,}000(nDesigns) + \$40{,}637.2(nSat) + \sum_{i=1}^{nSat} \left\{ \begin{array}{l} \$10{,}833.3(Size_i) \\ + 0.765523^{\frac{LaunchFrequency}{365}(i-1)} \{-\$426.75 \times 10^6 pp_i \\ - \$91219[(d_i)(f/N)_i]^2 + \$27484[(d_i)(f/N)_i]\} + SizeCost_i \end{array} \right\} \quad (31)$$

3.3.2 Fire Cost Model Generation

In order to relate the requirements to the cost of the system in a quantifiable way, each penalty was related to the predicated cost of the fires missed. If the system does not meet the driving requirements then it did not successfully meet the overall goal of the mission and the wildland fires were not prevented. To properly relate these, a cost model of the missed fires was generated. The requirements in Table 3.2 do not specify a particular area in the United States where FireSat II would be monitoring for wildland fires, so an area in the western United States was selected as the target location. To determine the best location in the western United States, data was collected and examined from the National Interagency Fire Center on the number and type of fires experienced in each state over the course of a year. For the past 14 years, the National Interagency Fire Center presents historical year-end fire statistic by state. In these documents, fires are classified as either Wildland Fires or Prescribed Fires. Prescribed fires are important, controlled burns that help reduce the risk of larger, more catastrophic fires [104]. When selecting a location, a state that experienced a large number of fires that were mostly wildland fires was desirable. In 2016, 97% of the fires experienced in Nevada were wildland fires.

[105] At its base level, the fire cost model is simply the cost per acre multiplied by the number of acres burned – however, both number of acres burned and cost are variable. The general formula is presented in Equation (32) below.

$$FireCost = \sum_{i=1}^{nFires} CostPerAcre_i \times AcresBurned_i \tag{32}$$

Costs associated with wildland fires can be broken down into 5 categories: 1) Suppression, 2) Other Direct, 3) Rehabilitation, 4) Indirect, and 5) Additional. [106] These categories are further explained in Table 3.19 below.

Table 3.19 – Explanation of the types of Costs associated with Wildland Fires [106]

Suppression Costs	Other Direct Costs	Rehabilitation Costs	Indirect Costs	Additional Costs
• Aviation • Engines • Firefighting crews • Agency personal	• Private property losses • Damage to utility lines • Damage to recreation facilities • Loss of timber resources • Aid to evacuated residents	• Damaged watershed restoration • Post fire flooding • Prevention of erosion • Cost of combatting invasive species	• Lost tax revenues • Business revenue • Property value decrements as a result of the fires	• Loss of human life • Cost of resulting health problems • Loss of ecosystem services

Suppression costs typically account for about 20% of the total cost of fires [107]. Using data, Figure 3.23 was generated to show the distribution of cost per acre burned over the past 32 years. The number of bins and the bin sizes were determined based on the statistical convention of the rounded square root of the number of samples evenly distributed over the sample range.

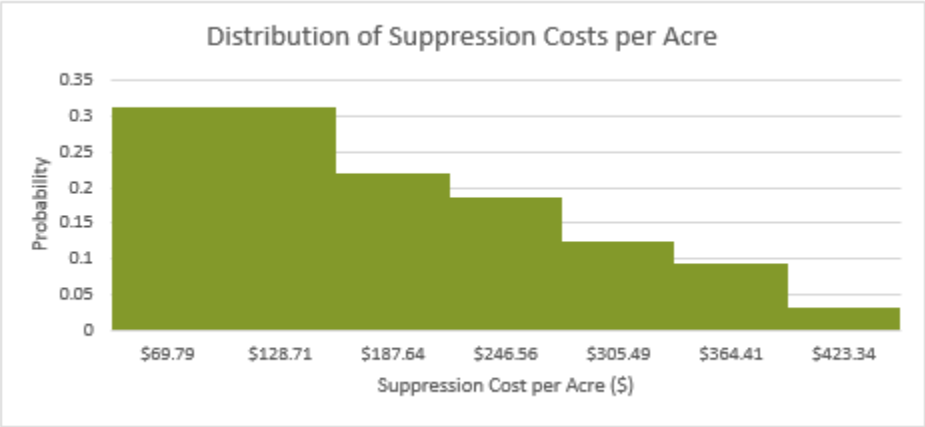

Figure 3.23 – Suppression Costs per Acre over the last 32 years [107]

As seen in Figure 3.23, the cost per acre of the fires burned will be determined by the probability of being in a particular bin, and then the cost is randomly distributed in each bin, based on the statistical information generated from the data presented in Figure 3.23. This number will then be scaled to get the total cost per acre based on the fact that suppression costs on average make up 20% of total fire costs. A $CostPerAcre$ will be calculated for each fire on a given day. This is then multiplied by the size of that fire generated from the distribution presented in Figure 3.24.

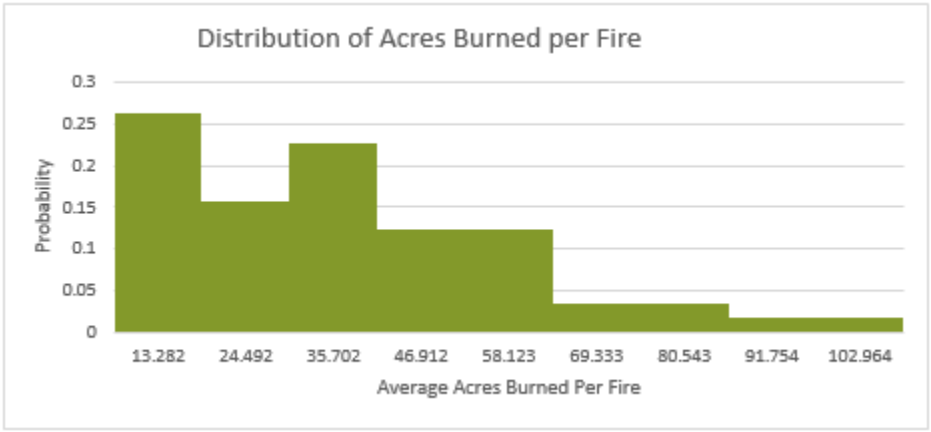

Figure 3.24 – Distribution of Acres Burned per Fire [107]

Both the Cost per Acre and the Number of Acres are calculated per fire for a given day within the fire season. On each of these days, there are an average number of fires that started. This information was calculated by dividing the number of fires in a year by the length of the fire season (taken to be 162 days [40]). There were only 15 data points for the number of fires in Nevada [93,97–110]. The number of fire starts per day were calculated based on these numbers and are presented in Figure 3.25 below.

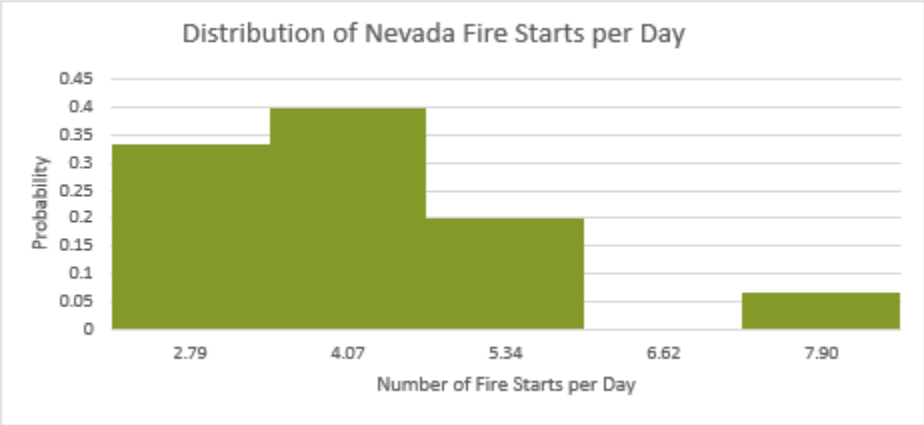

Figure 3.25 – Distribution of the number of Nevada Fire Starts per day in the last 15 years

Using these distributions seen in Figure 3.23, Figure 3.24, and Figure 3.25 – the cost per acre and the size of fire can be generated for each fire started on a given day in Nevada. These values are fed into equation (32), reiterated below, to generate the cost of the fires missed.

$$FireCost = \sum_{i=1}^{nFires} CostPerAcre_i \times AcresBurned_i$$

Based on this cost information, the requirements identified can be quantified as penalty functions based on the cost of the fires missed as a result of not meeting the requirements. Each of the penalty functions are addressed in the following sections.

3.4 Using System Requirements as Penalty Functions

To use the system requirements at penalty functions, the identified system requirements need to be related to the overall cost of the mission. As the goal of this mission is to identify wildland fires in the United States, the failure to meet the specified requirements can be related to the cost of damages from wildland fires. Of the 8 driving requirements identified in Table 3.2, 5 of these were translated into penalty functions and 3 were handled directly. The rest of this section will first discuss the requirements handled directly and then the penalty functions that derived from the remaining requirements.

3.4.1 Requirement 1.25 – Payload Sensitivity

Requirement 1.25 states that "The mission must be able to monitor changes in the mean forest temperature to +/- 2C." All of the cameras sampled (ass seen in Appendix 0) have a thermal

sensitivity of 0.05K to 0.06K, which easily meets the sensitivity requirement. Therefore, requirement was assumed to as met for all of the proposed mission profiles generated.

3.4.2 Requirement 1.19 – Communication Specification

Requirement 1.19 states that "The mission will be interoperable through NOAA ground stations." NOAA has 42 ground stations that are designed to interact with LEO satellites. These are seen in Figure 3.26 below.

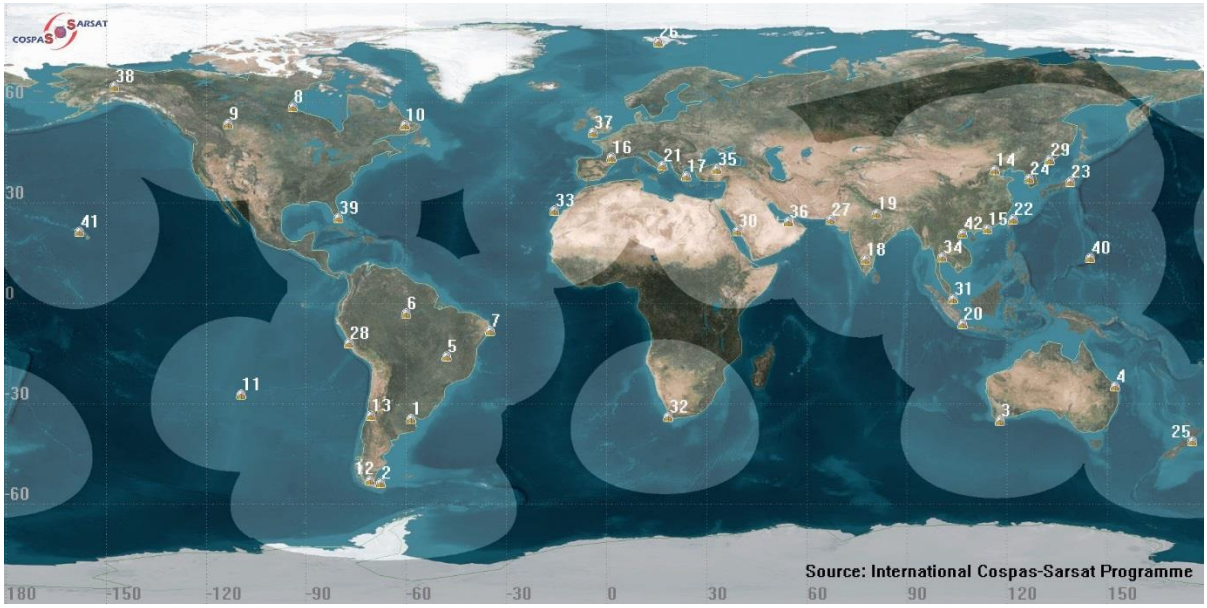

Figure 3.26 – NOAA LEO Ground Stations [122]

As seen in the figure above, much of the earth is accessible to at least one NOAA ground station, and thus it was concluded that for a majority of each orbit, each satellite will be in range of at least one NOAA ground station. These locations and their corresponding latitudes and longitudes are presented in Table 3.20 below.

Table 3.20 – Latitudes and Longitudes of NOAA Ground Stations

NOAA LEOLUT Ground Stations				
Number	*Location*	*Country*	*Latitude*	*Longitude*
1	El Palomar	Argentina	-34.6267	-58.5944
2	Rio Grande	Argentina	-53.7860	-67.7002
3	Albany	Australia	-35.0275	117.8840
4	Bundaberg	Australia	-24.8670	152.3510
5	Brasilia	Brazil	-15.7942	-47.825
6	Manaus	Brazil	-3.1190	-60.0217
7	Recife	Brazil	-8.0476	-34.8770
8	Churchill	Canada	58.7684	-94.1650
9	Edmonton	Canada	53.5444	-113.4909
10	Goose Bay	Canada	53.3017	-60.3261
11	Easter Island	Chile	-27.1130	-109.3496
12	Punta Arenas	Chile	-53.1638	-70.9171
13	Santiago	Chile	-33.4489	-70.6693
14	Beijing	China	39.9042	116.4074
15	Hong Kong	China	22.3964	114.1095
16	Toulouse	France	43.6047	1.4442
17	Penteli	Greece	38.0476	23.8696
18	Bangalore	India	12.9716	77.5946
19	Lucknow	India	26.8467	80.9462
20	Jakarta	Indonesia	-6.1745	106.8227
21	Bari	Italy	41.1171	16.8719
22	Keelung	Taiwan	25.1276	121.7392
23	Gunma	Japan	36.3907	139.0604
24	Sejong	Korea	36.5927	127.2938
25	Wellington	New Zealand	-41.2865	174.7762
26	Spitsbergen	Norway	77.8750	20.9752
27	Karachi	Pakistan	24.8615	67.0099
28	Callao	Peru	-12.0508	-77.1260
29	Nakhodka	Russia	42.8223	132.8834
30	Jeddah	Saudi Arabia	21.2854	39.2376
31	Singapore	Singapore	1.3521	103.8198
32	Cape Town	South Africa	-33.9249	18.4241
33	Maspalomas	Spain	27.7606	-15.5860
34	Bangkok	Thailand	13.7563	100.5018
35	Ankara	Turkey	39.9334	32.8597
36	Abu Dhabi	UAE	24.4539	54.3773
37	Combe Martin	UK	51.1995	-4.0243
38	Alaska	USA	64.2008	-149.4937
39	Florida	USA	27.6648	-81.5158
40	Guam	USA	13.4443	144.7937
41	Hawaii	USA	19.8968	-155.5828
42	Haiphong	Vietnam	20.8449	106.6881

3.4.3 Requirement 1.14 – Cost

Requirement 1.14 states that "The mission will have a recurring cost of less than $3M/year." Since the penalty functions have been related to the cost of the satellite, this requirement was not included as a penalty function as the cost of the mission profile and the resulting penalty functions are combined to form the metric by which the missions are evaluated. A final upper bound was placed on each of the resulting mission profiles and as long as the cost of the mission was below the stated value in the requirement, then the requirement was met. Additionally, the cost of the proposed system will be compared to this requirement to see if there are potential cost savings.

3.4.4 Mission Lifespan Penalty

Requirement 1.08 states that "The mission will last a minimum of 8 years." In order to satisfy this requirement, the primary model used was the Orbit Model. This model takes three inputs – the initial altitude, mass of the satellite, and cross-sectional area of the satellite – and generates three outputs – altitude as a function of time, period as function of time, and a time vector that accounts for the length of time the spacecraft is in orbit with the appropriate time steps.

If the mission is shorter than the desired mission length (in this case, 8 years) the number of missed fire season days are calculated and the associated cost of failing to detect those fires is the penalty. Figure 3.27 below illustrates the method used to determine the cost associated with the missed fires based on the mission life set forth in Requirement 1.08 and the length of fire seasons.

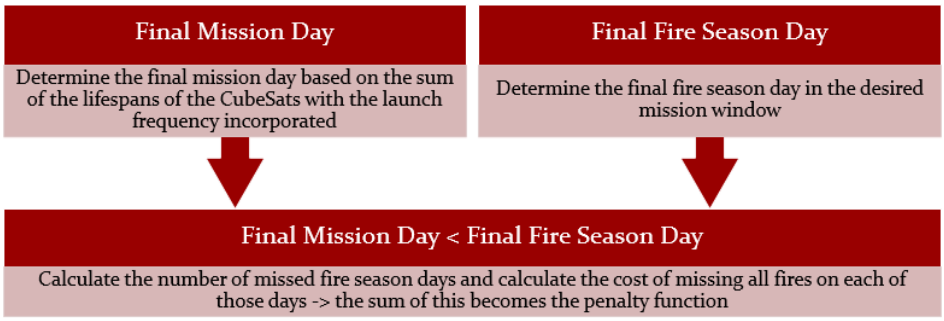

Figure 3.27 – Logic for Determining the Penalty Function for Mission Life

3.4.5 Coverage Penalty

The second penalty function considered is the penalty function associated with the resolution and location of the satellite. Requirement 1.03 states that "The mission shall be able to detect

forest fires at up to 50 m in resolution.," Requirement 1.04 states that "The mission shall be able to determine forest fire locations within 1km geolocation accuracy," and Requirement 1.05 states that "The mission shall be able to cover specified forest areas within the US at least twice daily." [31] Requirements 1.03 and 1.05 are the primary requirements are combined to form Penalty Function 2: Coverage.

For the mission to not be penalized based on this penalty function, the satellite must satisfy the two requirements identified for each day of the mission that falls within fire season. Therefore, for each and every fire season day over the desired mission length, the mission profile must have at least two passes over the specified location (Nevada) and these passes must have a GSD of $50m^2$ or less. To account for the geolocation accuracy (Requirement 1.04), a random chance was introduced that even if the satellites passes over the target location it is not capturing the correct information, this includes incorrect pointing, or error in satellite tracking. In order to determine this, both GSD and ground track location need to be determined as a function of time.

Combining the information generated by the GSD calculations and the ground track modeling, Penalty Function 2 can be generated. First, the number of times each of the CubeSats in the mission profile is in range of the target location for a given day is calculated. Then the GSD for each of the satellites is calculated for that day and then if on that given day there are 2 or more satellite passes and each of those passes have GSDs of less than $50m^2$ then all of the fires are "captured" and there is no penalty. If there is one pass on that day, then 50% of the fires started on that given day are captured. If the GSD of a satellite is greater than the requirement, then the percentage difference in the area is calculated and multiplied by the fire cost for that day. This is illustrated in the flow chart in Figure 3.28 below.

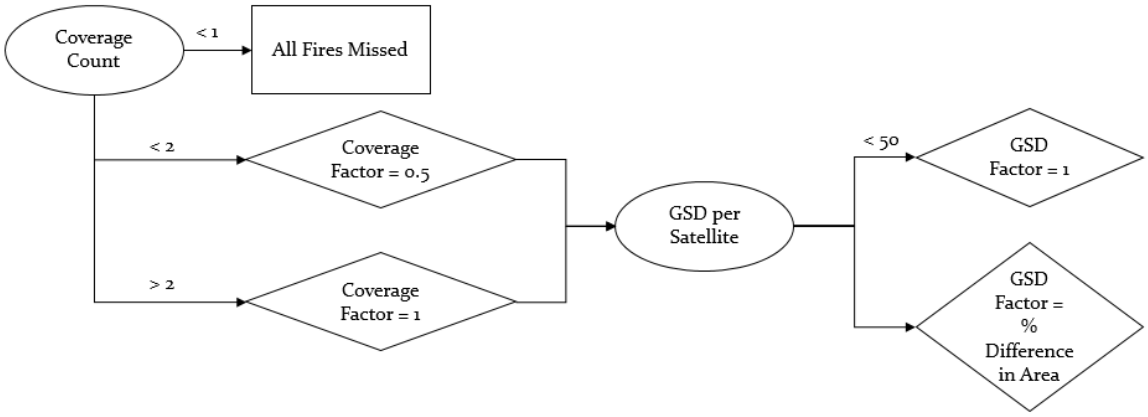

Figure 3.28 – Coverage Penalty Function Formulation

3.4.6 CubeSat Size Penalty

This penalty function is the only one not related to the cost of missed fires. It is instead related to the cost associated with going up a CubeSat size. If the mass and volume of the camera – as presented in Equations (14) and (15) – is greater 50% of the allowed total mass of the spacecraft and is greater than 50% of the internal volume, then the system is penalized. Figure 3.29 and Figure 3.30 below illustrate the limits place on the camera size based on the CubeSat size.

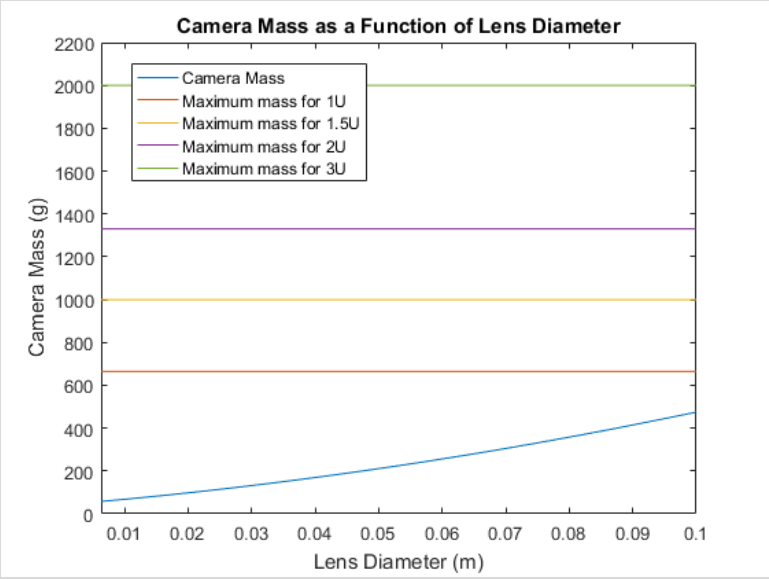

Figure 3.29 – Camera Mass as a Function of Lens Diameter

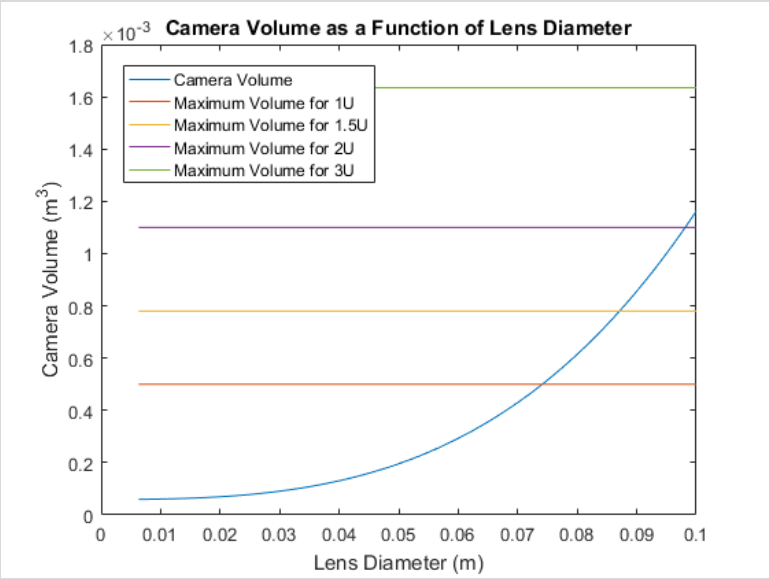

Figure 3.30 – Camera Volume as a Function of Lens Diameter

As seen in Figure 3.29 and Figure 3.30, the limiting factor on lens diameter is camera volume. The total mass of the camera at all diameters is less than 50% of the CubeSat maximum mass, but the volume limits the diameter of the lens for a 1,1.5, and 2 U CubeSat. These limits are at 7.41, 8.71, 9.81 cm respectively. All lenses can fit in a 3U CubeSat.

Based on the cost model presented, three components of the CubeSat are directly related to the size: 1) the structure, 2) the solar cells, and 3) the deployer cost. For all systems under 3U, if this penalty function is broken then the cost associated is simply the cost of the next size up CubeSat. However, if the system is a 3U CubeSat then the penalty to move to the next size is that of a 6U CubeSat as that is the next size up in common CubeSat architectures.

3.5 Summary of Proposed Model

From the driving mission requirements identified in Table 3.2, a set of 5 system models, 2 cost models, and 3 penalty functions were generated in order to determine the validity of a collection of CubeSats as a substitute mission architecture for the FireSat II mission and the associated performance gains.

From Chapter 2, there were 30 remaining subsystem drivers and factors. Table 3.21 below illustrates which of the 10 aspects of the mathematical model each driver or factor interacts with. The impact of these drivers and factors can vary; some explicitly impact the mathematical models and others were implicitly combined, and some were not considered.

"Mission Design" impacts all aspects of the mathematical model, after all it is the design of the mission that is being evaluated in the model. "Orbit" impacts each aspect of the mathematical model that is dependent on either the altitude or any of the other Keplerian elements. The "CubeSat Size" directly impacts the orbit model, satellite cost model, and the CubeSat size penalty. "External Torques" impact the orbit degradation of the satellite and thus impact the orbit model. "Payload" impacts anything that had to do with the camera; the ground sample distance model, the camera size model, the swath width model, the coverage penalty, and the CubeSat size penalty. "Solar Array Area" impacted the cost of the satellite. "Payload Accommodation" impacts the amount of space allotted for the payload and thus the CubeSat Size penalty. "Stability" was considered implicitly by including a tumbling factor into the coverage penalty. "Ground Station" was considered in the ground communications requirement and the possible range of orbit inclinations. "Layout," "Thermal Radiator Area," "Actuators," "Sensors," "Antenna," "Balance Mass," and "On Board Computer" were all considered implicitly when determining the percentage of the CubeSat the payload could occupy for the CubeSat Size penalty, as well as in the Cost Model of the Satellite as components.

"Bus Voltage," "Power Dissipated," "Center of Mass Offset," "Time in Eclipse," "Battery," "Thermal Environment," "Component Power," "Thermal Design," "Temperature Range," "Slew Rate Max," "Moment of Inertia," "Duty Cycle," "Data Rate and Distance," and "Orbit Average Power" were not considered in this mathematical model. Their inclusion is considered future work as further models need to be developed to handle these subsystems.

Table 3.21 – Direct Relationships between the Mathematical Model and the Subsystem Factors and Drivers

Subsystem Factor or Driver	**Mathematical Model Aspect**									
	Ground Sample Distance Model	*Camera Size Model*	*Orbit Model*	*Ground Track Model*	*Swath Width Model*	*Satellite Cost Model*	*Fire Cost Model*	*Mission Lifespan Penalty*	*Coverage Penalty*	*CubeSat Size penalty*
Mission Design	✓	✓	✓	✓	✓	✓	✓	✓	✓	✓
Orbit			✓	✓	✓			✓	✓	
CubeSat Size			✓			✓				✓
Bus Voltage										
External Torques			✓							
Layout										✓
Thermal Radiator Area										✓
Power Dissipated										
Center of Mass Offset										
Time in Eclipse										
Battery										
Thermal Environment										

Table 3.21 – Direct Relationships between the Mathematical Model and the Subsystem Factors and Drivers Continued

Subsystem Factor or Driver	**Mathematical Model Aspect**									
	Ground Sample Distance Model	*Camera Size Model*	*Orbit Model*	*Ground Track Model*	*Swath Width Model*	*Satellite Cost Model*	*Fire Cost Model*	*Mission Lifespan Penalty*	*Coverage Penalty*	*CubeSat Size penalty*
Component Power										
Thermal Design										
Temperature Range										
Payload	✓	✓			✓	✓			✓	✓
Solar Array Area						✓				
Payload Accommodation										✓
Moment of Inertia										
Stability									✓	
Actuators						✓				✓
Slew Rate Max										
Duty Cycle										

Ground Station			✓	✓						

Table 3.21 – Direct Relationships between the Mathematical Model and the Subsystem Factors and Drivers Continued

Subsystem Factor or Driver	**Mathematical Model Aspect**									
	Ground Sample Distance Model	*Camera Size Model*	*Orbit Model*	*Ground Track Model*	*Swath Width Model*	*Satellite Cost Model*	*Fire Cost Model*	*Mission Lifespan Penalty*	*Coverage Penalty*	*CubeSat Size penalty*
Data Rate and Distance						✓				✓
Sensors						✓				✓
Orbit Average Power										
Antenna						✓				✓
Balance Mass						✓				✓
On Board Computer						✓				✓

Based on this information and the derivations presented in this chapter, these 10 aspects of the mathematical model are combined to form the objective function used in the genetic algorithm. The relationships between these aspects are presented in Figure 3.31 below.

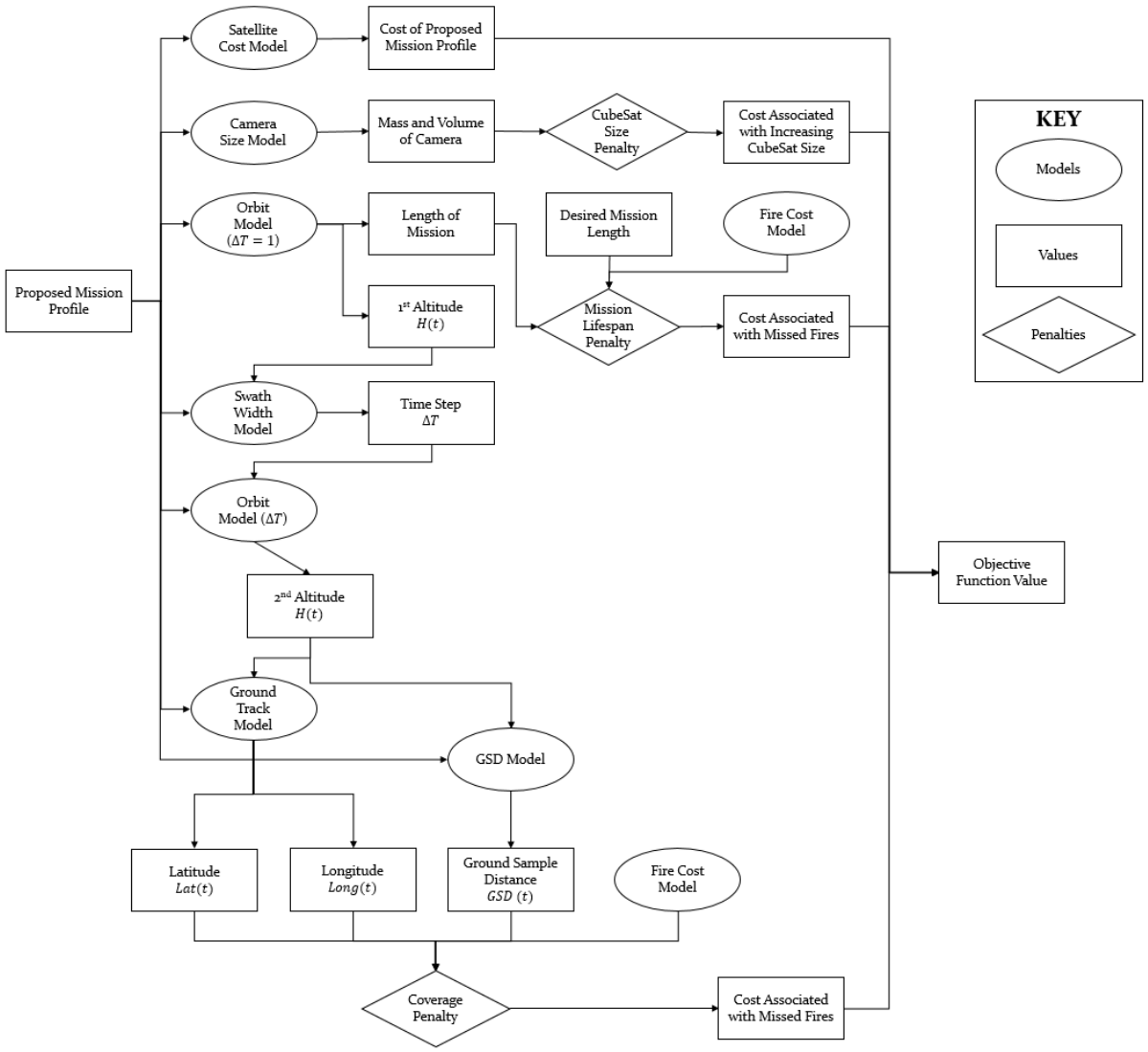

Figure 3.31 – Objective Function Flow

Where the rectangles represent values, the ovals are models, and the diamonds represent penalty functions. The costs of the penalty functions are added to the cost of the proposed mission to achieve the final objective function value. The genetic algorithm manipulates the design variables to minimize this value, and, in theory, eliminate any costs associated with system penalties. The following chapter will employ the mathematical model generated in this chapter to determine viable mission profiles based on the driving mission requirements.

4 MODEL IMPLEMENTATION

Using the mathematical model generated in Chapter 3, several different types of missions were run to prove the validity of the model and determine potential performance gains experienced by using a collection of CubeSats over a traditionally monolithic system. The first mission type tested aimed to check the feasibility of covering the target location for a single fire season. The second mission type tested looked to see if launching the same satellite repeated over the course of 8 years could comparably cover the target location over the course of the entire mission lifespan set forth in the mission requirements. Then, using the first mission type, potential requirement evolutions were examined to see the responsiveness of the CubeSat architecture to requirement changes.

4.1 Mission One: One Fire Season Mission

In using the CubeSat architecture to achieve the FireSat II mission, more than one satellite will have to be launched. Though they are a low cost solution to space access, CubeSats are not the most reliable of satellites, with 66.09% of CubeSats still functioning after 100 days in orbit [48]. Therefore, their lifespan was limited to one year for this work. This first mission type, the "One Fire Season Mission," examines the feasibility of the proposed system, and was used to determine whether or not it was possible to achieve the desired ground sample distance with a single CubeSat before moving forward and testing the possibility for longer missions. Assuming the success of this mission, the same satellite could be launched every year until the full, desired mission length. In preforming trials to achieve this mission type, all of the same requirements listed in Table 3.2 are used, but instead of a mission life of 8 years, this was performed for a desired mission life of one year. The general FireSat II requirements driving the mathematical model and the updated mission life requirement are presented in Table 4.1 below.

Table 4.1 – Driving Mission Requirements for the One Year Mission

ID	Requirements
R1.03	The mission shall be able to detect forest fires at up to 50 m in resolution
R1.04	The mission shall be able to determine forest fire locations within 1km geolocation accuracy
R1.05	The mission shall be able to cover specified forest areas within the US at least twice daily
R1.08a	The mission will last a minimum of 1 year
R1.14	The mission will have a recurring cost of less than $3M/year
R1.19	The mission will be interoperable through NOAA ground stations
R1.25	The mission must be able to monitor changes in the mean forest temperature to +/- 2C
R1.33	The mission will fit within a Standard CubeSat Size

Using the system models, cost models, and penalty functions developed in Chapter 3, the following results were obtained. The mission profiles presented below were the final, optimum candidate for each trial run of the genetic algorithm. Additionally, all of the final objective function values were equal to only the cost of the satellite, meaning that there were no remaining costs associated with the penalty functions, and thus all of the requirements had been satisfied.

Table 4.2 – Results from the One Fire Season Mission

One Year Mission									
Mission Cost	*Size*	*Initial Altitude (km)*	*Inclination (deg)*	*Longitude of the Ascending Node (deg)*	*Argument of the Periapsis (deg)*	*True Anomaly (deg)*	*Pixel Pitch (m)*	*Lens Diameter (cm)*	*f/n*
$71,905.32	1	354	38	95	329	352	12	6.98	1.2
$71,913.22	1	355	42	38	129	249	12	6.75	1.25
$71,907.61	1	352	138	218	124	109	12	6.00	1.4
$71,922.31	1	359	39	150	292	350	12	7.10	1.2
$71,902.76	1	352	137	156	325	109	12	6.96	1.2
$71,917.76	1	350	38	199	18	277	12	6.78	1.25
$71,971.09	1	373	40	333	348	299	12	5.96	1.5
$71,907.61	1	352	141	89	124	109	12	6.00	1.4
$71,922.31	1	359	39	150	292	350	12	7.10	1.2
$71,913.18	1	350	142	108	80	132	12	6.03	1.4
$71,899.89	1	352	41	267	184	175	12	5.55	1.5
$71,921.33	1	359	41	125	53	111	12	7.09	1.2

As seen in Table 4.2, all 12 of the resulting mission profiles used a single satellite to meet the requirements set forth for the One Fire Season Mission in Table 4.1 with 0.075% variation in the cost of the mission above the mean and 0.024% variation in the cost of the mission below the mean, where the mean mission cost is $71,917.03. The system was assumed to have reach convergence when the design strings homogenized and objective function values did not change after 20 generations. Figure 4.1 shows example convergence plots used to verify that each of the Trials completely eliminated the penalty functions and the costs and objective function values settled to a single value.

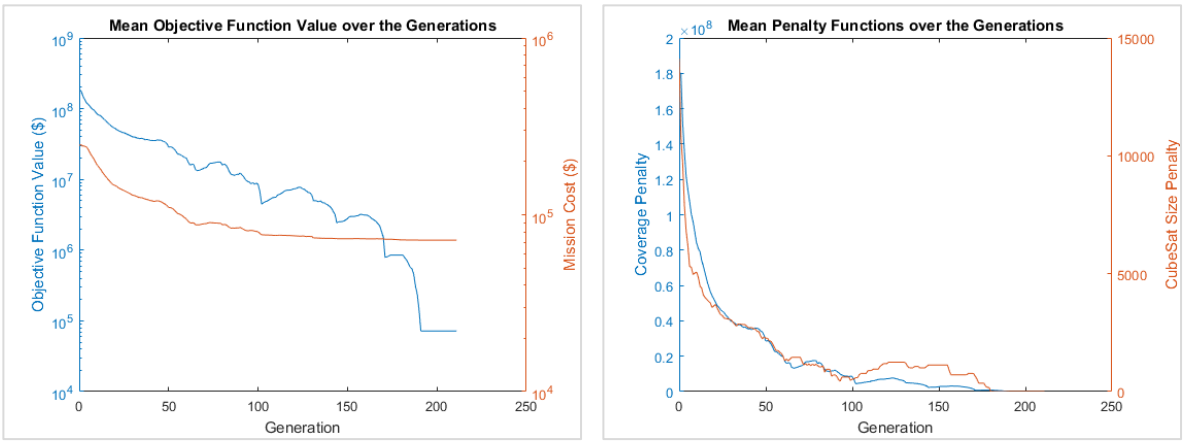

(a) Objective Function and Cost over the Generations

(b) The 3 Penalty Functions over the Generations

Figure 4.1 – Example Convergence Plots for Trial 7

The mission lifespan penalty was not included in part (b) of the figure above as this penalty function was never violated. Figure 4.2 below shows that all 12 of the mission profiles meet the desired mission length of one fire season. The two vertical lines in Figure 4.2 represent the first and last days of the fire season based on a launch day of April 28th. From work done by Westerling, fire seasons in this work have be defined as starting on the 120th day of the year (May 1, 2017) and ending on the 282nd day of the year (October 10, 2017) [40].

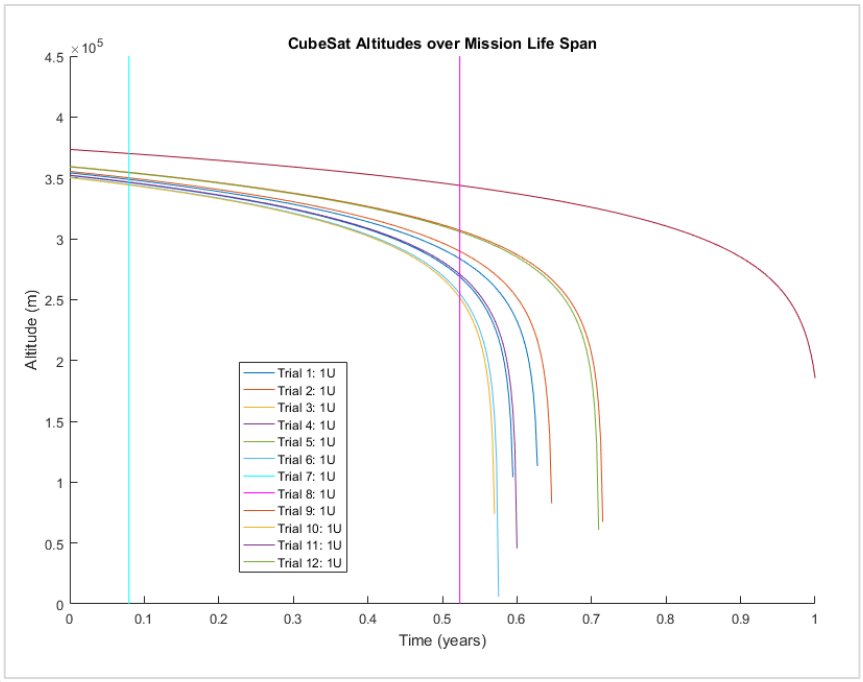

Figure 4.2 – Launch Altitudes, Size and Resulting Altitudes as a function of time for a One Fire Season Mission

All 12 mission profiles captured the entire fire season for 1 year, and only 1 satellite remained in orbit for the entire calendar year. Since there was no cost associated with initial launch altitude, it makes sense that these values can vary. As seen in Table 4.2, the launch altitudes ranged from 350 km to 373 km, where 373 was an outlier. The median was 353 km and average was 356 km, where 75% of the missions were launched between 351 km and 359 km. The distribution of the launch altitudes can be seen in Figure 4.3 below.

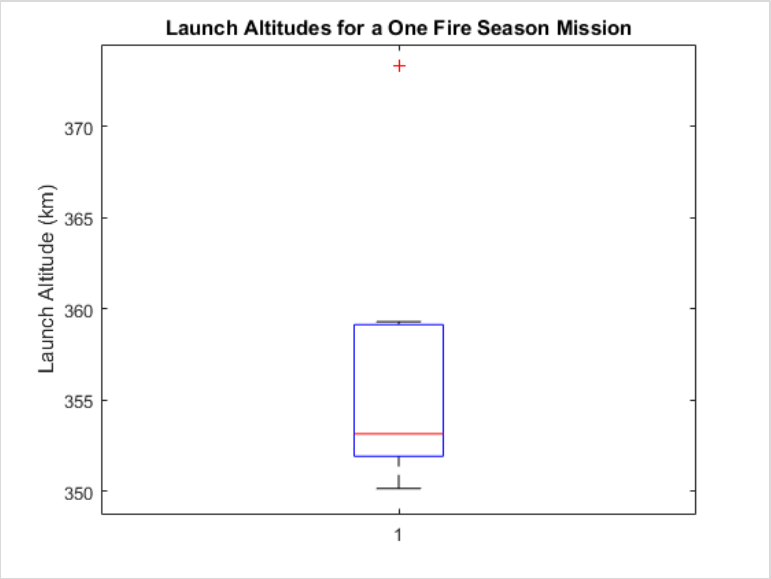

Figure 4.3 – Box and Whisker Plot representing the resulting Launch Altitudes for a One Fire Season Mission

These launch altitudes, coupled with four other orbital parameters, control the orbit of the spacecraft and determine whether or not the satellite achieves the desired coverage set forth in Requirement 1.05. The distribution of the other four orbital parameters can be seen in Figure 4.4 below.

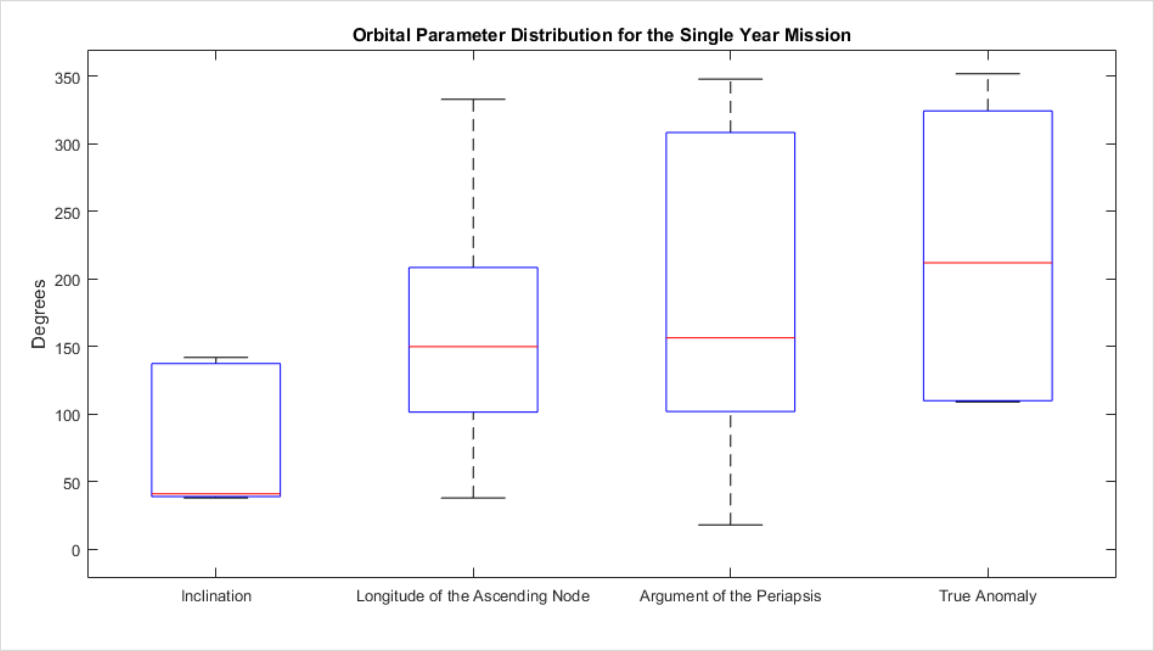

Figure 4.4 – Box and Whisker Plots of the resulting orbital parameters for a One Fire Season Mission

The inclination of the spacecraft was allowed to range from 28° to 145°, however, all of the resulting mission profiles fell within the 38° to 142° range. The average was 73°, while the median was 41°, and 50% of the data fell within the 39° to 137.5° range. The longitude of the ascending node, argument of the periapsis, and the true anomaly could all range from 0-360 degrees. As seen in Figure 4.4 above, the other orbital parameters were more varied. The Longitude of the Ascending Node for the resulting mission profiles ranged from 38° to 333°, where the mean is 161° and the median is 150°, and 50% ranged from 101.5° to 208.5°. The Argument of the periapsis for the resulting mission profiles ranged from 18° to 348°, where the mean is 192° and the median is 156°, and 50% ranged from 102° to 308.5°. The True Anomaly for the resulting mission profiles ranged from 109° to 352°, where the mean is 219° and the median is 212°, and 50% ranged from 110° to 324.5°. This shows that the four orbital parameters are not as restrictive as other elements in the design string, and there is no discernable correlation between these four orbital parameters and other variables in the design string.

Despite the varying orbital parameters, all of the mission profiles had successful orbits. Orbits were considered successful if they passed over the target location (Nevada) at least twice a day, as dictated by Requirement 1.05 in Table 4.1. Looking at the coverage maps of each Mission Profile, it can be seen that for all days in the fire season, the satellite passes over the target location at least twice a day, thus satisfying the coverage requirement. Figure 4.5 below is an example coverage over mission lifespan plot – this mission profile (Mission Profile 1) was chosen arbitrarily as this trial and all others met the desired coverage. The vertical lines represent the first and last fire season days, respectively.

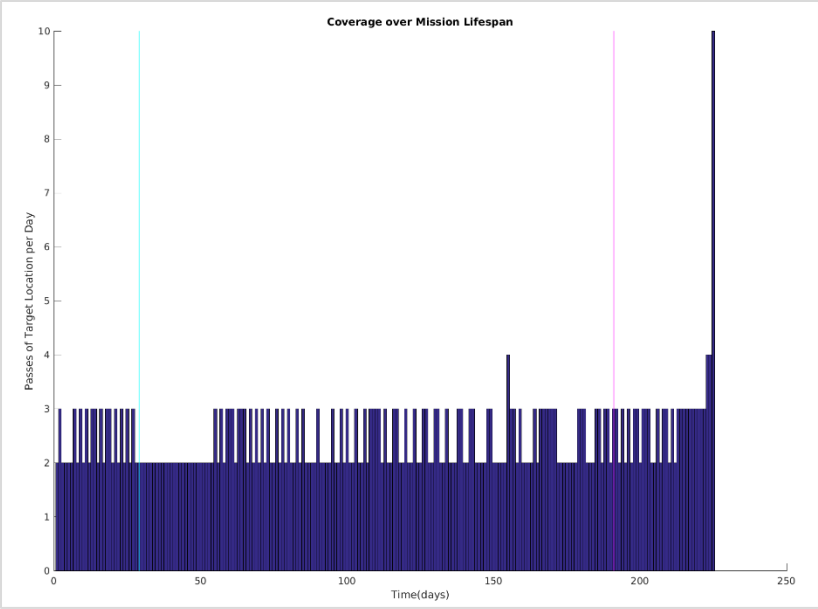

Figure 4.5 – Example Coverage Count for a One Fire Season Mission

Coverage was counted based on the number of times the satellite passed though the target location in a given day. Figure 4.6 below shows the time steps and location over the target area for a given day.

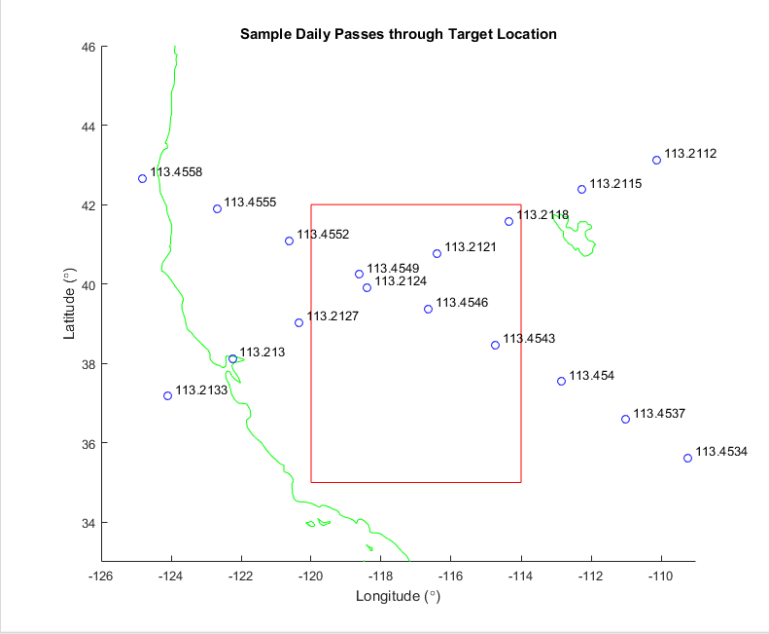

Figure 4.6 – Sample Daily Passes through the Target Location

As demonstrated by the two figures above, a single satellite, with the correct orbital parameters, passes over the state of Nevada more than twice a day and was easily able to meet this

requirement. The spike of coverage on in the final days is indicative of how quickly the orbits degrade towards the end of the CubeSat lifespan, this is also seen by the sharp taper in Figure 4.2.

In addition to passing over the target location at least twice a day, the success of the mission is also dependent on the ground sample distance of the camera. Figure 4.7 below shows that for the entire duration of the mission, the GSD for each of the satellites is under 50m. The colors and line styles used represent the pixel pitches and f/N numbers are included as Part (b) in Figure 4.7, and the lens diameters are included in the legend in Part (a). The horizontal line is the cut off for the required GSD.

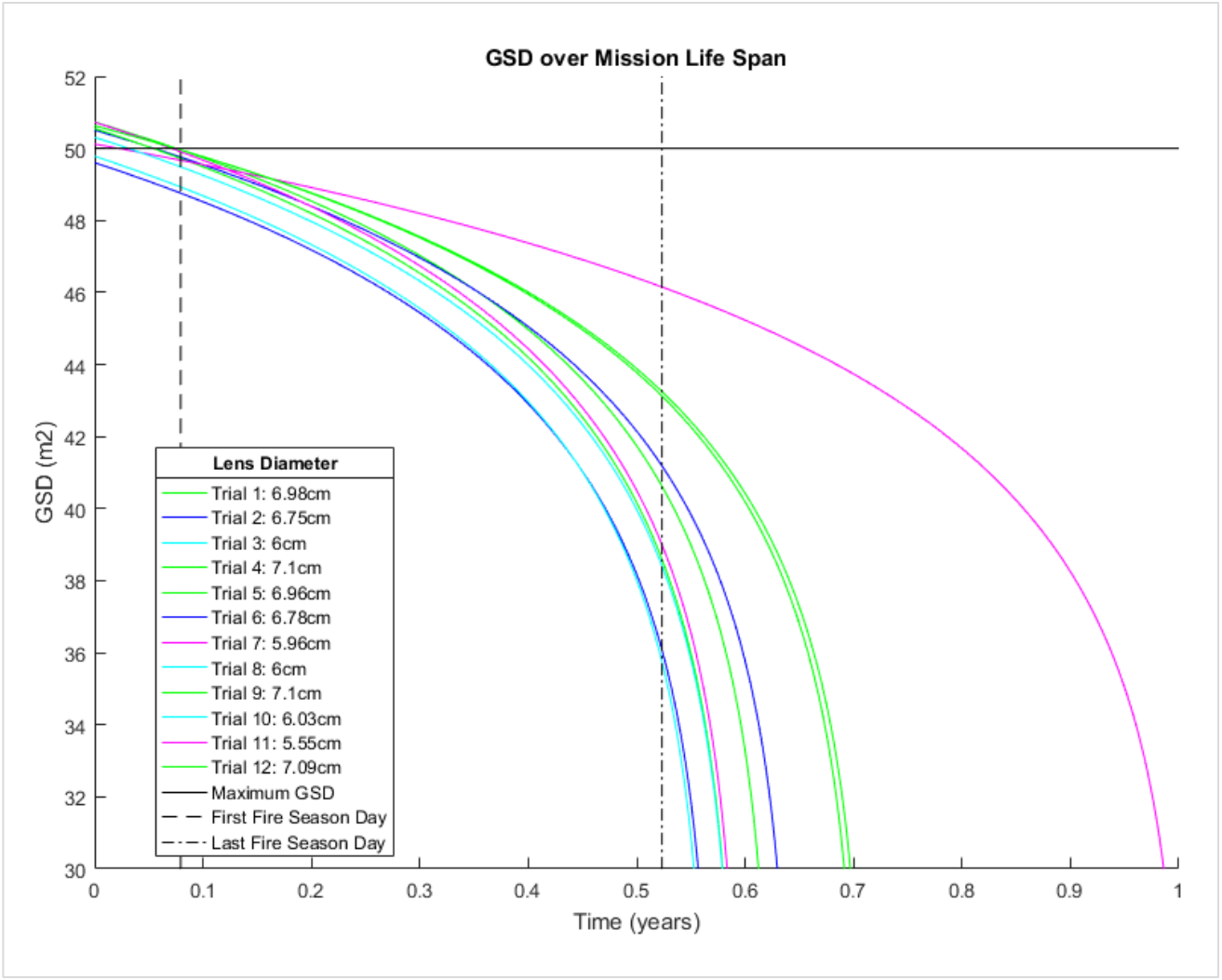

(a) Ground Sample Distances for a One Fire Season Mission

		Pixel Pitch (µm)
		12 *solid*
f/N	*1.2* *Green*	- (solid green)
	1.25 *Blue*	- (solid blue)
	1.4 *Cyan*	- (solid cyan)
	1.5 *Magenta*	- (solid magenta)
	1.6 *Black*	- (solid black)

(b) Matlab Line Styles Used to Distinguish Camera Information

Figure 4.7 – Ground Sample Distances for a One Fire Season Mission

This figure illustrates that all of the mission profiles generated meet the desired ground sample distance as set forth in Requirement 1.03. Similar to the varying altitudes presented in Table 4.2, there are multiple camera solutions which achieve the desired ground sample distance. However, unlike the orbital parameters, the pixel pitch, lens diameter, and f/N number of the camera do impact the cost model and ultimately the objective function value for each mission profile. Though pixel pitch is the same for all of the mission profiles presented in Table 4.2, f/N number and lens diameter vary as seen in Table 4.2 and Figure 4.7. Figure 4.8 below shows the distribution of the effective focal lengths of the camera – the product of the f/N number and the lens diameter.

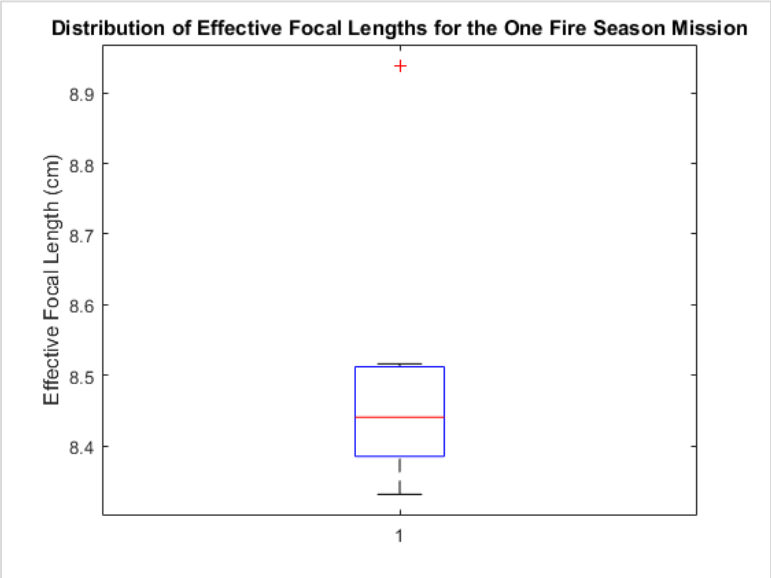

Figure 4.8 – Distribution of Effective Focal Lengths for the One Fire Season Mission

The effective focal lengths of the camera solutions range from 8.33 cm to 8.93 cm where 8.93 cm is an outlier and 75% of the effective focal lengths range from 8.38 cm to 8.51 cm. The mean is 8.47 cm and the median is 8.44. These effective focal lengths only exhibit a 5.5% variance above the mean and a 1.7% variance below mean. All of these lenses used to generate these effective focal lengths are under the size limit, satisfying Requirement 1.33, which states that the mission is able to fit in the prescribed CubeSat architecture.

Overall, the mission costs for the resulting mission profiles of the One Fire Season Mission Trials, range from $71,899.89 to $71,971.09 with a mean cost of $71,917.03. Overall, there is a 0.099% variation in the cost of the mission with 0.075% variation above the mean and a 0.024% variation below the mean. All of the mission profiles presented in Table 4.2 use a single 1U

CubeSat with a 12μm camera. Though the orbital parameters varied, they did not have an impact on the mission cost and therefor the variation exhibited in the mission cost is directly related to the cost of the camera lens. The overall cost of the mission is under the $3 million max, where the max cost is only 2% of the yearly cost of FireSat II.

Of the 12 unique mission profiles, all of them met each of the requirements set forth in Table 4.1. Though there were differences in the orbital parameters, and minor differences in the effective focal length of the camera, the overall cost of the mission converged. Having multiple successful sets of parameters which generate similar mission costs allows the designers choices when selecting the type of camera and provides flexibility when deploying the spacecraft. Despite having little to no effect on the cost of the system, having such wide ranges of orbital parameters that still produce viable solutions lends the mission to the CubeSat architecture as CubeSats are secondary payloads have little to no control over their point of deployment. Overall this set of One Fire Season Mission trials proved that it is possible to achieve the mission requirements of FireSat II for a significantly decreased cost. In conclusion, there are many solutions which can achieve the same mission requirements for a year of the FireSat II mission for a fraction of the cost. This next trial, looks to see if this trend continues when applied to an Eight Year Mission with a Single Satellite Design.

4.2 Mission Two: The Eight Year, Single Design Mission

This mission type is an expansion of the previous, "One Fire Season Mission." The goal of this second set of trials is to see if the resulting mission profiles generated from the optimization technique can achieve the desired full length of the mission, given the same satellite is launched repeatedly at a specified launch interval. In the previous mission type, the resulting mission profiles were 1U satellites with a 12μm pixel pitch camera with varying lens diameters and f/n number combinations. Additionally, in the "One Fire Season Mission" it was seen that a wide range of orbital parameters facilitated the desired coverage. In performing calculations for this mission type, the design variables were altered to ensure that the genetic algorithm was altering the pertinent design variables to achieve the optimum solutions. To do so, all of the orbital parameters, aside from Initial Altitude, were eliminated, and an additional variable, launch frequency, was added. From this the final design string was comprised of 7 variables: launch frequency, number of satellites, size of satellite, initial altitude, pixel pitch, lens diameter, and

f/n number. In this mission, all of the requirements listed in Table 3.2 were applicable, unlike the "One Year Mission" trial. These requirements are reiterated in Table 4.3 below.

Table 4.3 – Eight Year, Single Design Mission

ID	Requirements
R1.03	The mission shall be able to detect forest fires at up to 50 m in resolution
R1.04	The mission shall be able to determine forest fire locations within 1km geolocation accuracy
R1.05	The mission shall be able to cover specified forest areas within the US at least twice daily
R1.08	The mission will last a minimum of 8 years
R1.14	The mission will have a recurring cost of less than $3M/year
R1.19	The mission will be interoperable through NOAA ground stations
R1.25	The mission must be able to monitor changes in the mean forest temperature to +/- 2C
R1.33	The mission will fit within a Standard CubeSat Size

Using the cost models and penalty functions developed in Chapter 3, the following results were obtained. The mission profiles presented below were the final, optimum candidate for each trial run of the genetic algorithm. Additionally, all of the final objective function values were equal to only the cost of the satellite, meaning that there were no remaining costs associated with the penalty functions, and thus all of the requirements had been satisfied.

Table 4.4 – Results from the Eight Year, Single Satellite Mission

Eight Year, Single Satellite Mission								
Trial Number	*Mission Cost*	*Launch Freq. (months)*	*Number of Satellites*	*Size*	*Initial Altitude (km)*	*Pixel Pitch (μm)*	*Lens Diameter (cm)*	*f/n*
1	$377382.10	12	8	1	359	12	7.26	1.2
2	$377285.03	12	8	1	354	12	6.07	1.4
3	$377345.30	12	8	1	361	12	7.14	1.2
4	$377398.43	12	8	1	366	12	5.83	1.5
5	$377442.38	12	8	1	365	12	6.32	1.4
6	$377398.43	12	8	1	366	12	5.83	1.5
7	$377224.13	12	8	1	353	12	5.97	1.4
8	$377224.13	12	8	1	353	12	5.97	1.4

9	$377398.43	12	8	1	366	12	5.83	1.5
10	$377310.89	12	8	1	359	12	7.13	1.2

As seen in Table 4.4, all 10 of the resulting mission profiles used a single 1U satellite, launched yearly for eight years, to meet the requirements set forth for the Eight Year, Single Design Mission requirements set forth in Table 4.3 with 0.03% variation in the cost of the mission above the mean and 0.03% variation in the cost of the mission below the mean, where the mean mission cost is $377,340.90. The system was assumed to have reach convergence when the design strings homogenized and objective function values did not change after 30 generations. An example of the plots used to verify convergence are seen in Figure 4.9 below. In all 10 of the trials, the objective function and mission cost flat lined, and the penalty functions all ended with zero contribution to the objective function value.

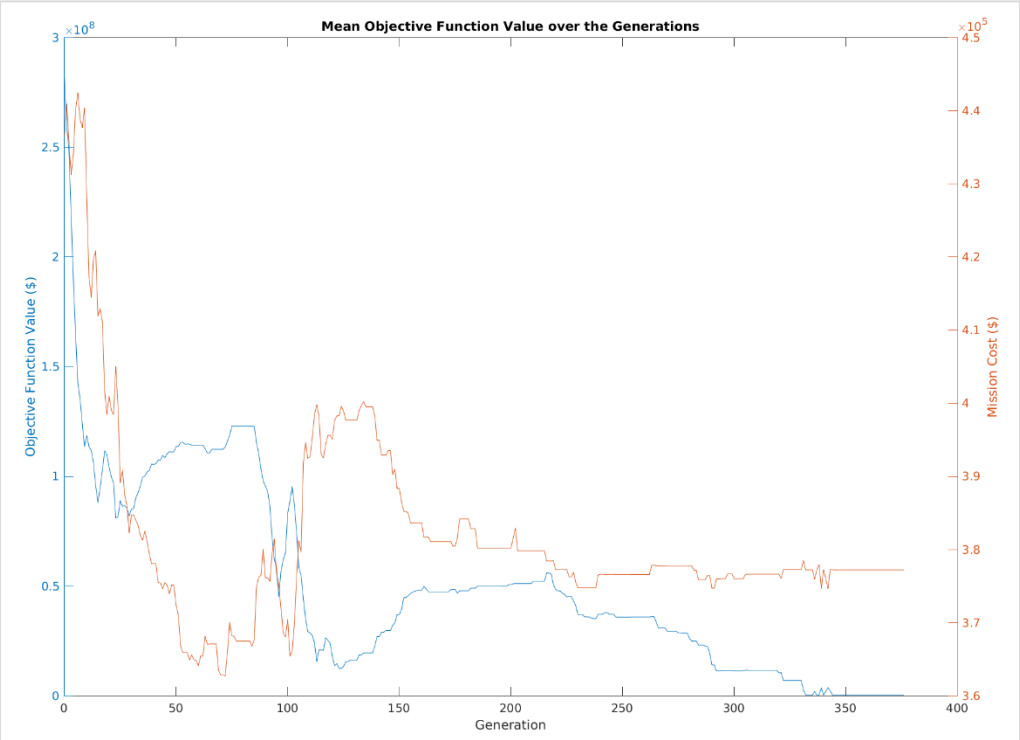

(a) Objective Function and Cost over the Generations

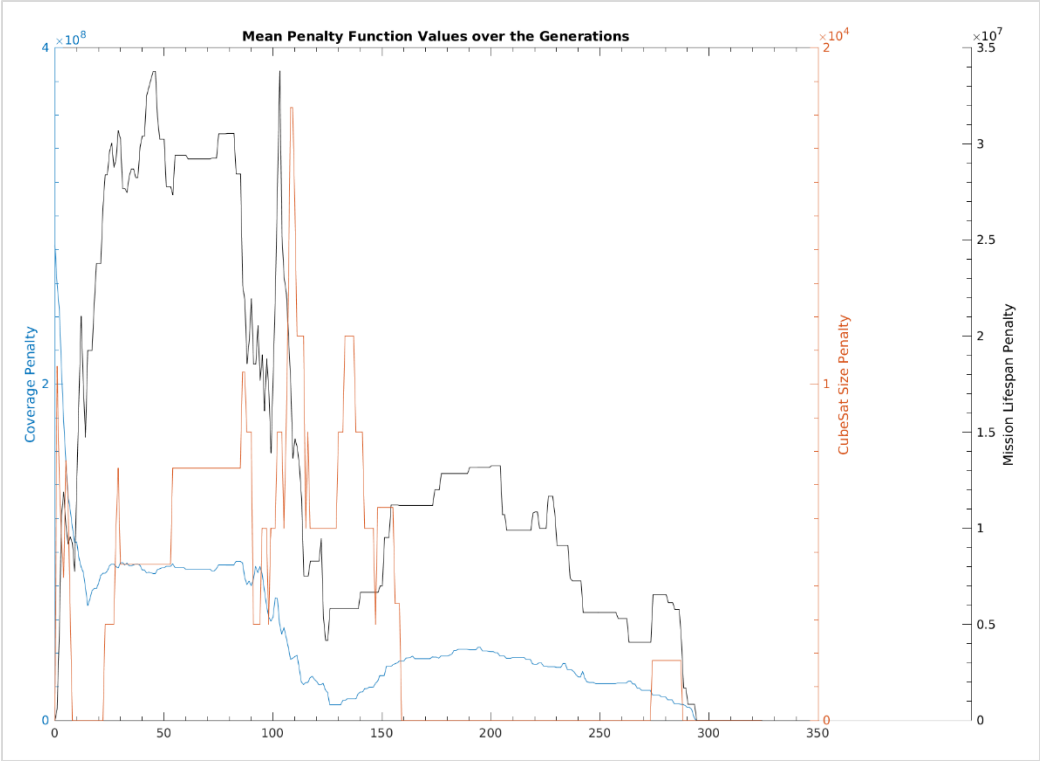

(b) The 3 Penalty Functions over the Generations

Figure 4.9 – Example Convergence plots for Trial 7, the cheapest solution

As seen in Figure 4.9, launch frequency, number of satellites, size of satellites, and pixel pitch are the same for all of the resulting mission profiles. The primary differences occur in the initial altitude of the spacecraft, the lens diameter, and the f/n number. Only two of which – the lens diameter and the f/n – directly impact the cost of the mission, and will be discussed more further on. The varying launch altitudes and the resulting orbit patterns for the 10 resulting mission profiles are presented in Figure 4.10 below.

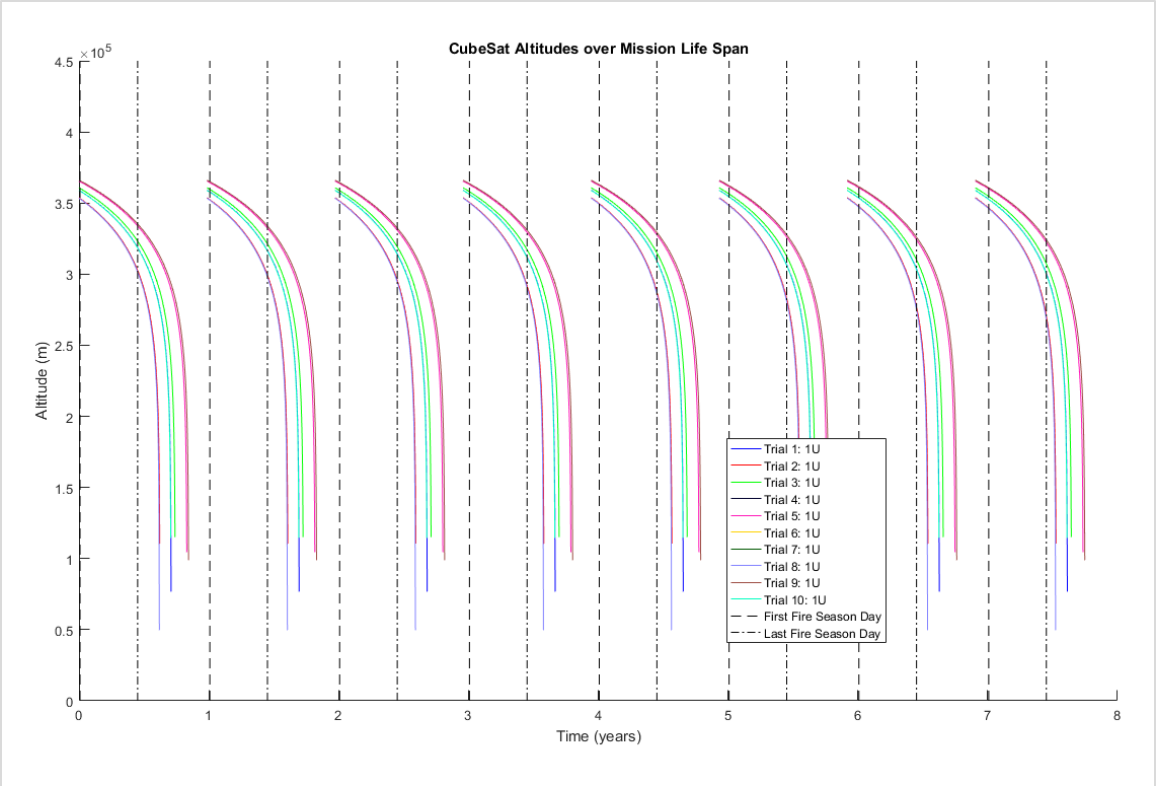

Figure 4.10 – Comparison of the Launch and Orbit Patterns of the resulting mission profiles from the Eight Year, Single Design Mission

The fire season for each year ranges from the first fire season day to the last fire season day as denoted by the cyan and the magenta lines respectively. Using this, it can be seen that each mission profile satisfies Requirement 1.08. All 10 mission profiles captured the entire fire season for each of the 8 years. However, since there is no cost associated with launch altitude, it makes sense that these values can vary. As seen in Table 4.4, the launch altitudes ranged from 353 km to 366 km. The median was 360 km and average was 360 km, where 100% of the missions were launched between 353 km and 360 km. The distribution of the launch altitudes can be seen in Figure 4.3 below.

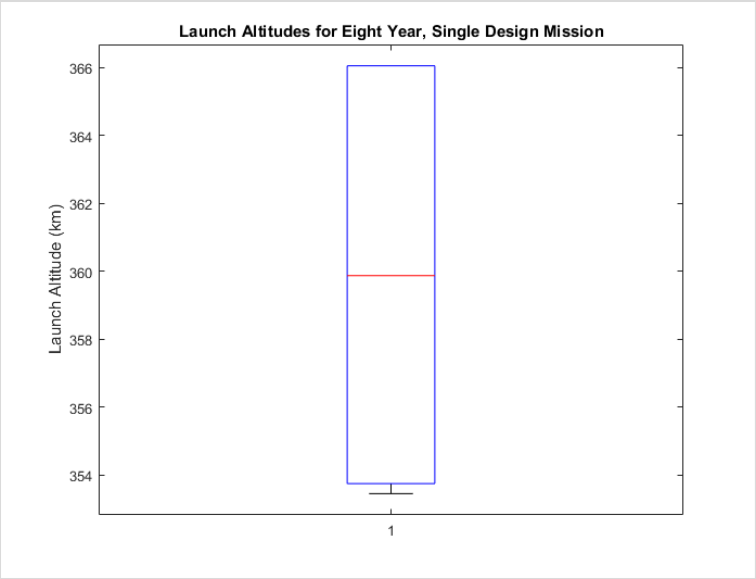

Figure 4.11 – Box and Whisker Plot representing the resulting Launch Altitudes for the Eight Year, Single Design Mission

These launch altitudes, coupled with four other orbital parameters, control the orbit of the spacecraft and determine whether or not the satellite achieves the desired coverage set forth in Requirement 1.05. Orbits were considered successful if they passed over the target location (Nevada) at least twice a day, as dictated by Requirement 1.05 in Table 4.3. Looking at the coverage maps of each Mission Profile, it can be seen that for all days in the fire season, the satellite passes over the target location at least twice a day, thus satisfying the coverage requirement. Figure 4.5 below is an example coverage over mission lifespan plot – this mission profile (Mission Profile 2) was chosen arbitrarily as this trial and all others met the desired coverage. The fire season for each year ranges from the first fire season day to the last fire season day represented by the vertical cyan and the magenta lines respectively.

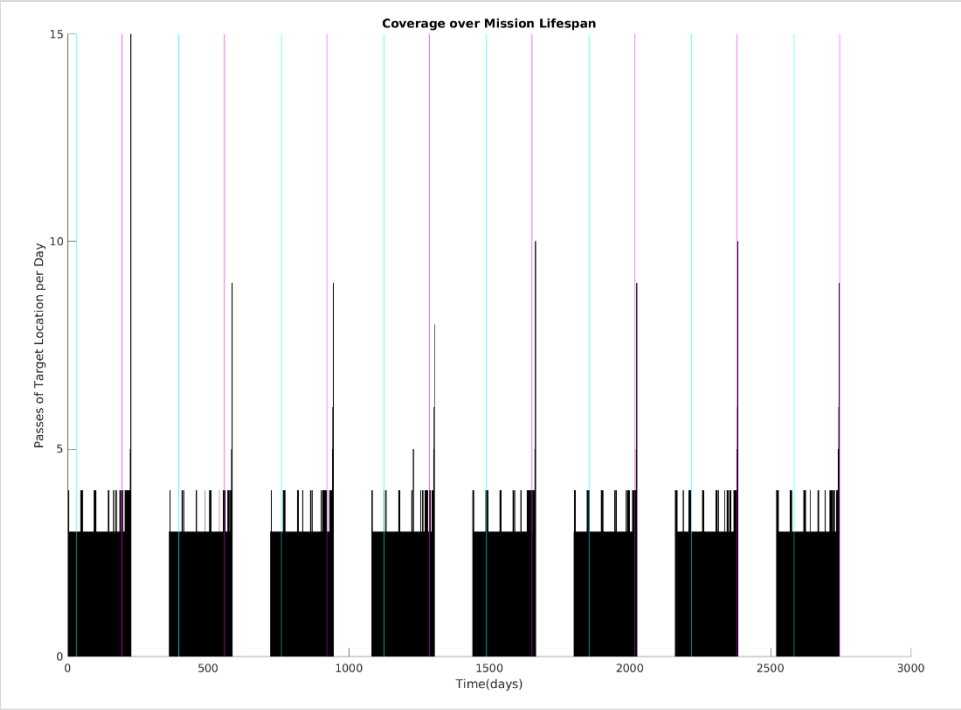

Figure 4.12 – Example Coverage Count for an Eight Year, Single Design Mission

Coverage was counted based on the number of times the satellite passed though the target location in a given day. In addition to passing over the target location at least twice a day, the success of the mission is also dependent on the ground sample distance of the camera. Figure 4.7 below shows that for the entire duration of the mission, the GSD for each of the satellites is under 50m. From work done in Chapter 3 it is known that the GSD of the satellite is a function of altitude, and camera parameters – pixel pitch, lens diameter, and f/n number. In this mission type, pixel pitch is constant across the 10 resulting mission profiles, but the f/n number and lens diameter vary. These two parameters – lens diameter and f/n number – are often combined and referred to as the effective focal length. The camera parameters used in the resulting mission profiles are presented in Table 4.5 below, as well as the calculated effective focal lengths for each camera.

Table 4.5 – Cameras Used for the Eight Year, Single Satellite Mission

Cameras Used				
Trial Number	*Pixel Pitch (μm)*	*Lens Diameter (cm)*	*f/n*	*Effective Focal Length (cm)*
1	12	7.26	1.2	8.71
2	12	6.07	1.4	8.49
3	12	7.14	1.2	8.57
4	12	5.83	1.5	8.75
5	12	6.32	1.4	8.85
6	12	5.83	1.5	8.75
7	12	5.97	1.4	8.36
8	12	5.97	1.4	8.36
9	12	5.83	1.5	8.75
10	12	7.13	1.2	8.55

These cameras, in conjunction with the altitude of the satellite at any given time provides the GSD of the spacecraft. The resulting GSDs are presented as a function of time in Figure 4.13 below. The colors and line styles used represent the pixel pitches and f/N numbers are included as Part (b) in Figure 4.7, and the lens diameters are included in the legend in Part (a). The horizontal line is the cut off for the required GSD, and the first and last fire season days are noted by a vertical dashed black line and a vertical dash-dot black line respectively.

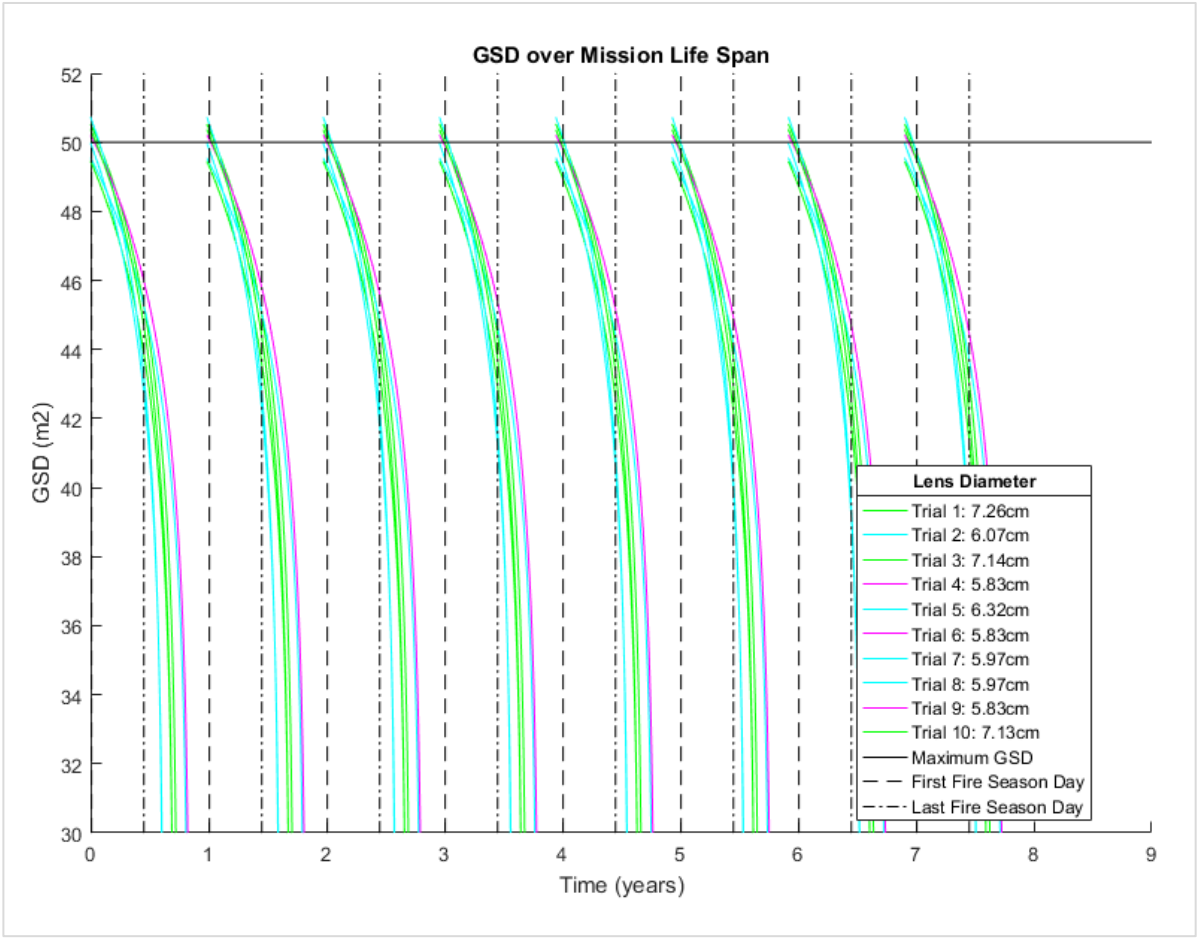

(a) Ground Sample Distances for a One Fire Season Mission

		Pixel Pitch (µm)
		12 *solid*
f/N	*1.2* *Green*	- (solid red)
	1.4 *Cyan*	- (solid cyan)
	1.5 *Magenta*	- (solid magenta)

(b) Matlab Line Styles Used to Distinguish Camera Information

Figure 4.13 – Ground Sample Distances for the Eight Year, Single Design Mission

In Figure 4.13, it can be seen that the GSD of the mission profiles decrease very quickly with the de-orbiting of the spacecraft – the higher the initial altitude the more consistent the GSD as a function of time. Originally, there was an upper limit set on the GSD, in order to properly identify the wildland fires, but upon further reflection and analysis, the lower the GSD the less geographic area covered. Future work includes placing a lower limit on the desired GSD – this, in theory, would decrease the number of feasible missions and help keep the data relayed to the ground consistent over the course of the mission. However, based on the set mission requirements and the current penalty function formulations, it is possible to meet the FireSat II mission requirements with the same satellite design launched over the 8 year mission life at under 1.5% of the cost of the traditional monolithic FireSat II mission.

From the 10 trials presented in Table 4.4, it can be seen that not only is it possible to capture the wildland fires in the target location using a series of CubeSats launched over the course of the mission lifespan, but that it is significantly cheaper to do so. With the cost of the fire season mission only 98.5% of the cost over the course of the entire 8 year mission lifespan, it is more than feasible to use CubeSats as an alternative mission architecture to achieve low earth orbit mission requirements. Additionally, with so much of the budget left over it would even be possible to redesign each subsequent CubeSat launched. This allows for the designers to update and improve their previous designs with the technology curve or to respond to unforeseen circumstances; indicating that the designers have choice and can adapt based on unforeseen restrictions or requirements not considered in this mathematical model. From this, the author would recommend further study to explore the full potential reach of the CubeSat architecture.

4.3 Mission Implementation Conclusions

The first mission type tested, the "One Fire Season Mission," aimed to check the feasibility of covering the target location for a single fire season. After performing 12 trials, this mission type yielded 12 unique solutions that converged around a single mission profile type; though there were differences in orbital parameters and combinations of lens diameters and f/n numbers, they were all 1U satellites that used a 12 μm pixel pitch. Even with these differences, the resulting mission profiles for the One Fire Season mission varied by no more than 0.075% from the mean. Form this it was seen that though the initial altitude and orbital parameters impacted the coverage obtained by the system, the orbital parameters still varied widely as they were not directly connected to the cost models used to determine the objective function values. The

second mission type, the “Eight Year, Single Design Mission” tested looked to see of the same satellite launched repeatedly could comparably cover the target location over the course of the entire 8 year mission. This too proved feasible with the proposed CubeSat architecture at under 1.5% the cost of a traditional monolithic satellite. Similar to the One Fire Season mission, the resulting mission profiles for the Eight Year, Single Design mission also used 1U CubeSats with a 12μm pixel pitch camera to meet the requirements placed on the system. Indicating that achieving the desired mission objectives is possible even with the smallest CubeSat size explored, and that the solution found in the One Fire Season Mission can be repeatedly launched to meet the requirements of the Eight Year, Single Design Mission. This means that increasing the size of the CubeSat only increases the capabilities of the system, and with such a low development and design cost, not only does the proposed architecture meet the requirements originally set forth, but the system is capable of something a traditional monolithic satellite is not: changing as the mission progresses.

5 CONCLUSION AND FUTURE WORK

The work in this thesis centered on the complexities involved in working with and designing complex engineered systems. These systems are composed of a larger number of components [1] whose overall structure and behavior are the direct result of the interactions of their components, [2] and whose systematic response is dependent on the interactions of these components [1]. In this thesis, a monolithic (integral) architecture – the hypothetical FireSat II mission – was decomposed into a series of modular, self-contained CubeSats and as a result met the initial mission requirements and exhibited the ability evolve based on historical system evolutions.

5.1 Research Review

The research conducted in this thesis went through three phases: 1) system decomposition, 2) mathematical model development, and 3) implementation and analysis of the mathematical model. The system decomposition phase – discussed in Chapter 2 – discusses the modifications and simplifications required to adapt a monolithic satellite to the CubeSat Architecture. After this, the requirements and constraints of the selected case studies were quantified and a mathematical model was created in Chapters 3 to represent the new, modular system. This phase served to create a framework by which system requirements could be manipulated to impact possible solutions generated by a genetic algorithm. The final phase, Chapter 4, brought together and implemented the system decomposition and resulting mathematical model to gain an understanding of the feasibility of using the CubeSat architecture on an Earth imaging mission and understand the ability of the new, modular architecture to respond to changing system requirements. In doing so this work attempted to address the following research question:

What are the performance gains of observing wildfires using a collection of CubeSats instead of a monolithic satellite?

The following sections review the major accomplishments of the work and tie it back to the research question highlighted above.

5.1.1 Chapter 2 Review

From identifying the driving factors and requirements for the FireSat II mission as illustrated in [31], using DSMs and system maps, as well as the CubeSat Design Specification [28], the number of influential drivers and factors was reduced from 87 to 30 as drivers and factors. In

performing these simplifications the system itself became less modular as more of the components became interconnected with each other. However, since the proposed mission involves a collection of CubeSats used to complete the specified mission requirements, each of the CubeSats can be seen as modules in the system that can be interchanged to meet changing needs and requirements. The final system map and DSM are reiterated in Figure 5.1 and Figure 5.2 below, respectively.

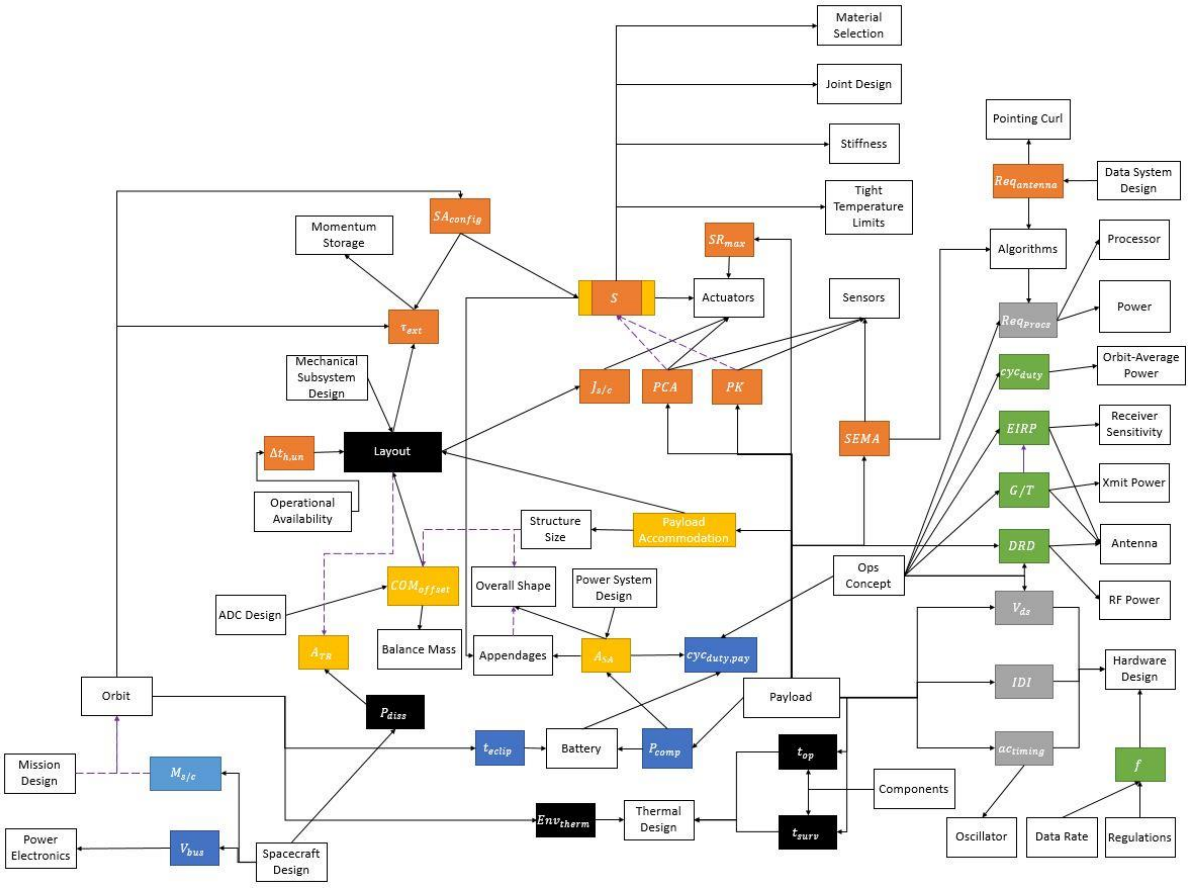

Figure 5.1 – Final System Map

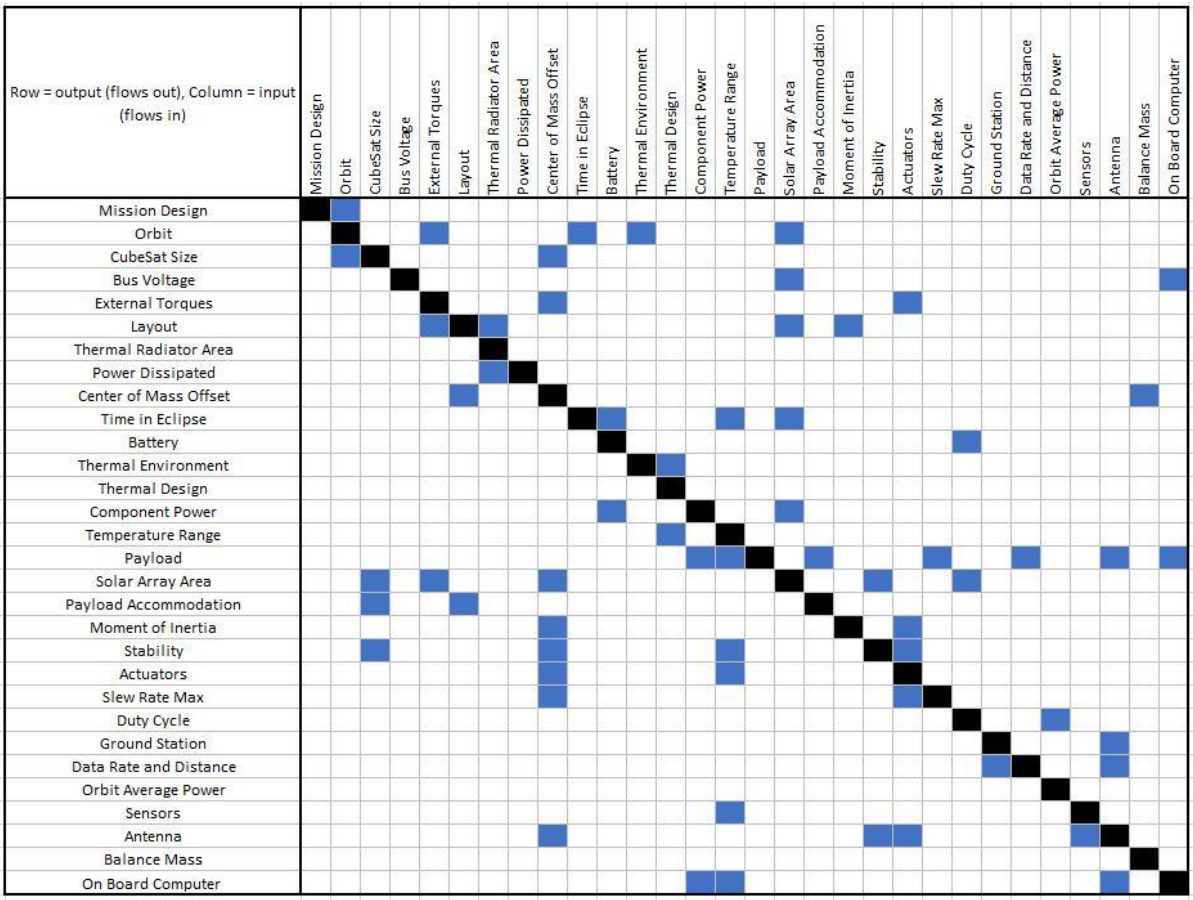

Figure 5.2 – Final System Design Structure Matrix

From this, it was determined that the payload of the system was one of the most impactful components in the simplified CubeSat system. It was with this in mind that the work in Chapter 3 moved forward with model development.

5.1.2 Chapter 3 Review

Building off of the system decomposition work done in Chapter 2, this section created a mathematical system model based on driving requirements identified from the FireSat II Level 1 requirements. This section took the 8 identified requirements and created 10 aspects which comprise the mathematical model presented in this thesis. 5 system models, 2 cost models, and 3 penalty functions were generated in order to model the FireSat II system as a series of CubeSats. The system models include 2 physical models representing the payload of the proposed CubeSats, and 3 interaction models that generated the orbit of the deployed CubeSat, mapped it back to a latitude and longitude on Earth, and how much of the Earth's surface was captured by the payload. The 2 cost models generated represented the cost to design, construct, and deploy the physical system as well a metric by which the success of the system could be

measured. The fire cost model allowed for identified requirements to be quantified in a meaningful way for use in a genetic algorithm as penalty functions. The fire cost model was used in conjunction with the 3 penalty functions developed. These models were tied together into the objective function used in the Genetic algorithm, reiterated in Figure 5.3 below.

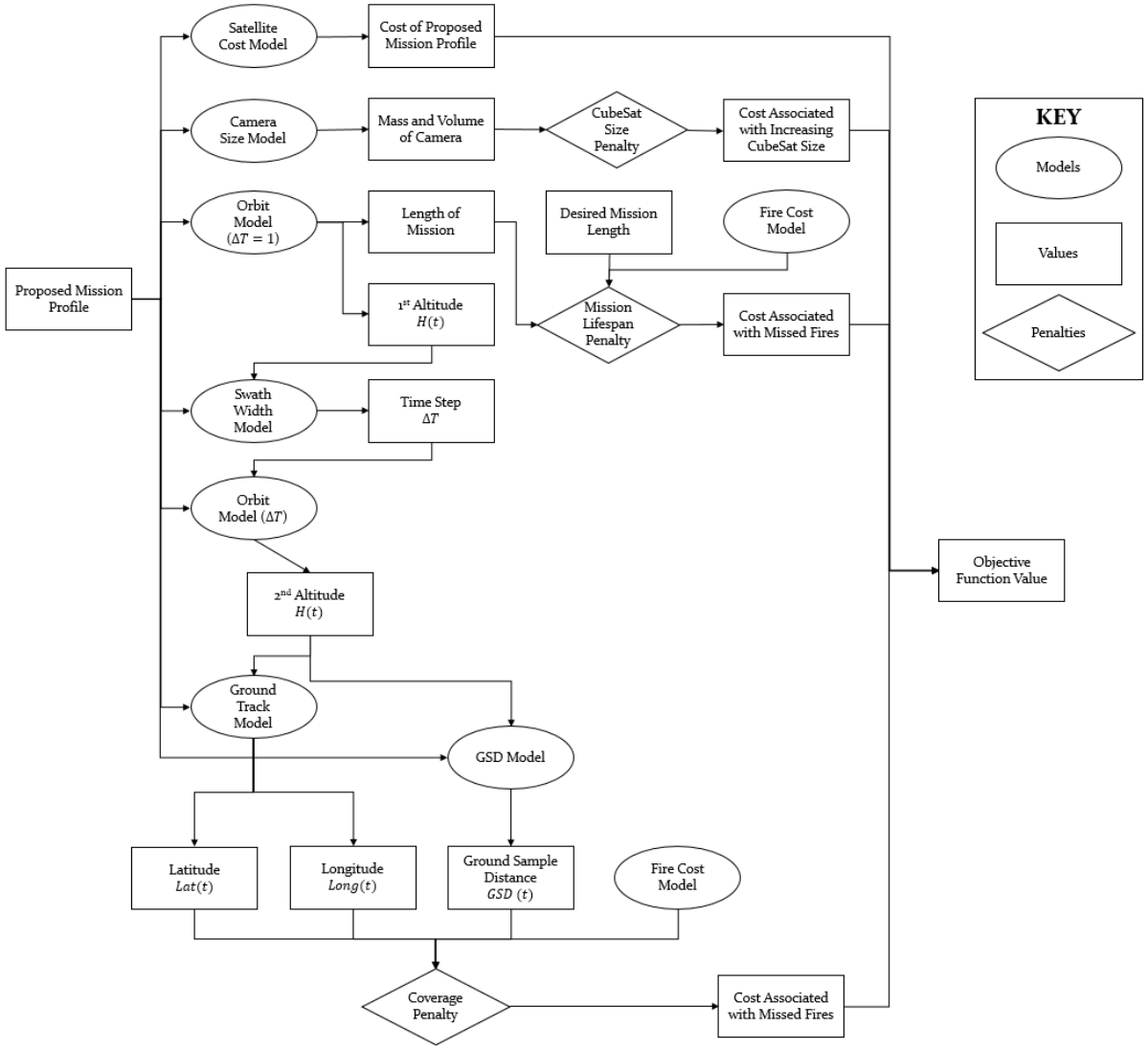

Figure 5.3 – Objective Function Formulation

Chapter 3 highlighted the way the driving system requirements were transformed into penalty functions and the models required to do so. This information was then applied in Chapter 4 to determine system viability and the performance gains exhibited by the proposed CubeSat architecture.

5.1.3 Chapter 4 Review

From Chapter 3 and the mathematical model generated, two different mission types were run, proving the validity of the model and determining performance gains experienced by using a collection of CubeSats instead of a traditionally monolithic system. The first mission type, the "One Fire Season Mission" proved that a single CubeSat was capable of achieving the desired ground sample distance during a single fire season. However, it also showed that by not associating each aspect of the design string to the cost model of the system certain variables were not consistent across the 12 resulting mission profiles. This mission type was not only a test bed for the system model but also for the general feasibility of using CubeSats in place of a traditionally monolithic satellite. Additionally, this mission type demonstrated which design variables were influential in determining the success of the mission.

Using the knowledge gained in the first mission type, the second mission type, the "Eight Year, Single Design Mission," explored the impact of launch frequency and the changing cost of technology in order to meet the specified requirements for the entire duration of the mission. Though this, it was confirmed that using a collection of CubeSats in place of a traditional monolithic satellite was a feasible solution over an extended period of time and presented even more cost savings than the single satellite mission.

5.2 Future Work

Future work in this area can primarily be categorized as further model development. There are a few minor things which should be taken into consideration when expounding upon the model used, and one area where there is potential for major model improvements. Some minor areas for future work include the addition of eccentricity into the de-orbit model. This part of the mathematical model was used throughout this work to generate the altitude of the spacecraft over time, however, it operated under the assumption that the satellite was maintaining a perfectly circular orbit. In reality, most orbits are not perfectly circular, and one area for future work involves the incorporation of eccentricity into the de-orbit model to obtain more accurate orbits. Additionally the resolution requirement could have a lower limit to provide more consistent imaging results over the lifespan of each modular satellite. If at the beginning of a satellite's life it is generating images with $50m^2$ resolution, and $30m^2$ by the end, this represents a significant change in the ground sample distance and could cause challenges when interpreting the data supplied by the system. Also a more comprehensive model for the satellite to NOAA LEO ground station communication could be included considering time

range for each of the LEO stations and their rates of communication. Doing so would develop an additional penalties and by increasing the number of penalties on the system then fewer number of possible solutions will be generated by the mathematical model.

Additionally, the "Bus Voltage," "Power Dissipated," "Center of Mass Offset," "Time in Eclipse," "Battery," "Thermal Environment," "Component Power," "Thermal Design," "Temperature Range," "Slew Rate Max," "Moment of Inertia," "Duty Cycle," "Data Rate and Distance," and "Orbit Average Power" drivers and factors were not considered in this mathematical model. Developing appropriate power and thermal system design models would lead to a more defined mathematical model by introducing further constraints into the system.

Another major area where there is room for improvement and future work is to better incorporate CubeSat reliability metrics. Previous work by Langer and Bouwmeester in [48] developed a MLE – 2 Weibull Mixture with PNZ which represents the reliability of CubeSats based on historical data. The first 100 CubeSats launched lasted an average of 200 days in orbit, [29] and only 80% of CubeSats function upon initial deployment, and then, after 2 years in orbit just under 60% are still functioning. [48] This trend is illustrated in Figure 5.4 below.

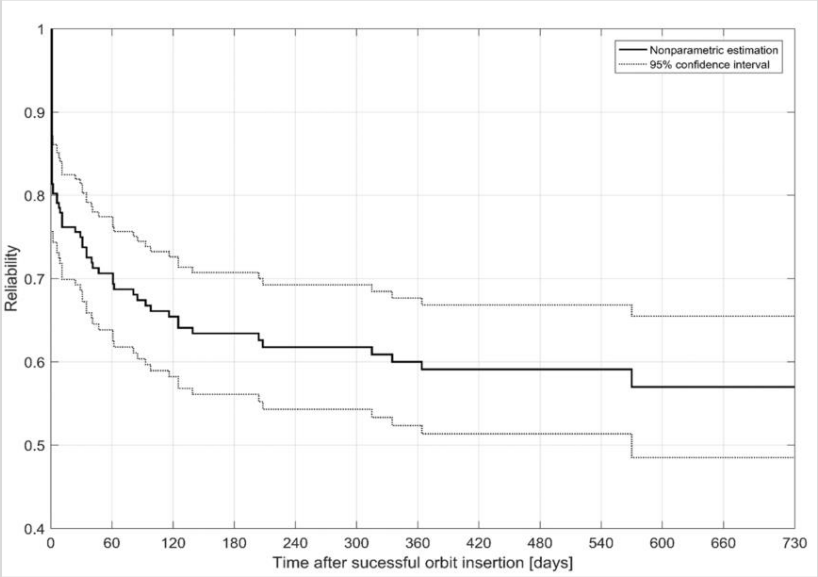

Figure 5.4 – CubeSat Reliability with 95% confidence interval – 2 years in orbit [48]

The equation and parameters used to model this CubeSat reliability function are taken from Langer and Bouwmeester's work, and are presented below.

$$R(t) = PNZ\ \alpha_1 \exp\left[-\left(\frac{t}{\theta_1}\right)^{\beta_1}\right] + \alpha_2 \exp\left[-\left(\frac{t}{\theta_2}\right)^{\beta_2}\right] \quad for\ t \geq 0 \tag{33}$$

Where $PNZ = 0.8146$, $\alpha_1 = 0.2115$, $\theta_1 = 57.9715$, $\beta_1 = 0.9017$, $\alpha_2 = 1 - \alpha_1 = 0.7885$, $\theta_2 = 4837.3947$, and $\beta_2 = 1.0710$. [48] By including this in the mathematical model, the number of satellites needed to achieve the mission should increase, increasing the impact of Requirement 1.14 – Cost on the system.

5.3 Conclusion

From the decomposition work in Chapter 2, to the model development and implementation in Chapters 3 and 4, respectively, it was discovered that it was indeed possible to not only decompose the monolithic satellite into a collection of CubeSats but also to meet and exceed the requirements set forth on the case study at 1.5% of the cost of a traditional monolithic satellite. This brings forth two main takeaways from this work: 1) it is possible to use a collection of modular satellites to meet the mission requirements of an integral satellite, and 2) doing so allows the designers the opportunity to evolve their mission with the launch of each additional modular satellite.

6 BIBLIOGRAPHY

[1] Norman, D., and Kuras, M., 2006, "Engineering complex systems," Complex Eng. Syst., pp. 206–245.

[2] Woodruff, M. J., Reed, P. M., and Simpson, T. W., 2013, "Many objective visual analytics: Rethinking the design of complex engineered systems," Struct. Multidiscip. Optim., **48**(1), pp. 201–219.

[3] Krus, D., and Grantham, K., 2011, "A step toward risk mitigation during conceptual product design: Component selection for risk reduction," J. Fail. Anal. Prev., **11**(4), pp. 432–445.

[4] "Monolithic System," Wikipedia [Online]. Available: https://en.wikipedia.org/wiki/Monolithic_system. [Accessed: 05-Dec-2016].

[5] "Distributed Computing," Wikipedia [Online]. Available: https://en.wikipedia.org/wiki/Distributed_computing. [Accessed: 05-Dec-2016].

[6] de Weck, O., 2015, "Modularity Fundamental Principles and Application to the Ara Platform."

[7] Holtta, K. M. M., and De Weck, O. L., 2011, "Degree of Modularity in Engineering Systems and Products with Technical and Business Constraints," Concurr. Eng. Res. Appl.

[8] Hölttä, K., Eun Suk, S., and de Weck, O., 2005, "Tradeoff Between Modularity and Performance for Engineered Systems and Products," Int. Conf. Eng. Des., **ICED 05 ME**, pp. 1–14.

[9] Kumar, A., 2004, "Mass Customization : Metrics and Modularity," Int. J. Flex. Manuf. Syst., **16**, pp. 287–311.

[10] "Evolvability," Nature.com [Online]. Available: http://www.nature.com/subjects/evolvability. [Accessed: 05-Dec-2016].

[11] Darwin, C., 2004, The Origin of Species, Barnes & Nobles Books, New York, NY.

[12] Tackett, M. W. P., Mattson, C. a., and Ferguson, S. M., 2014, "A Model for Quantifying System Evolvability Based on Excess and Capacity," J. Mech. Des., **136**(5), p. 51002.

[13] Hanisch, C., and Munz, G., 2008, "Evolvability and the intangibles," Assem. Autom., **28**, pp. 194–199.

[14] Collopy, P. D., and Hollingsworth, P. M., 2011, "Value-Driven Design," J. Aircr., **48**(3), pp. 749–759.

[15] Luo, J., 2015, "A simulation-based method to evaluate the impact of product architecture

on product evolvability," Res. Eng. Des., **26**(4), pp. 355–371.

[16] Ferster, W., 2015, "DARPA Cancels Formation-Flying Satellite Demo" [Online]. Available: http://spacenews.com/35375darpa-cancels-formation-flying-satellite-demo/#.UZbuE6KeCqE. [Accessed: 08-Oct-2015].

[17] Neill, M. G. O., and Yue, H., 2010, "Comparing and Optimizing the DARPA System F6 Program Value-Centric Design Methodologies," (September).

[18] "Cyclone Global Navigation Satellite System (CYGNSS) Fact Sheet."

[19] 2016, "CYGNSS," pp. 1–2 [Online]. Available: http://science.nasa.gov/missions/cygnss/. [Accessed: 08-Oct-2015].

[20] Cebrowski, A. K., and Raymond, J. W., "Operationally Responsive Space : A New Defense Business Model."

[21] Richards, M. G., Viscito, L., Ross, A. M., Hastings, D. E., Richards, M. G., Ross, A. M., and Hastings, D. E., 2008, "Distinguishing Attributes for the Operationally Responsive Space Paradigm."

[22] Maciuca, D., Chow, J., Siddiqi, A., de Weck, O., Alban, S., Dewell, L., Howell, A., Lieb, J., Mottinger, B., Pandya, J., Ramirez, J., Saenz-Otero, A., Yang, P., Zimdars, A., Saeed, S., Miller, D., and Hubbard, S., 2009, "A Modular, High-Fidelity Tool to Model the Utility of Fractionated Space Systems," AIAA Sp. 2009 Conf. Expo., (September), pp. 1–37.

[23] Mosleh, M., Dalili, K., and Heydari, B., 2014, "Optimal Modularity for Fractionated Spacecraft: The Case of System F6," Procedia Comput. Sci., **28**(Cser), pp. 164–170.

[24] Heiney, A., 2016, "Newly Launched CYGNSS Microsatellites to Shed Light on Hurricane Intensity," CYGNSS Hurric. Mission Blog [Online]. Available: https://blogs.nasa.gov/cygnss/2016/12/15/newly-launched-cygnss-microsatellites-to-shed-light-on-hurricane-intensity/. [Accessed: 01-May-2017].

[25] "What is the Largest Hurricane to Hit the United States," Geology.com [Online]. Available: http://geology.com/hurricanes/largest-hurricane/. [Accessed: 01-May-2017].

[26] Doggrell, L., 2006, "Defense Technical Information Center Compilation Part Notice Operationally Responsive Space A Vision for the Future of IMilitary Space."

[27] Toorian, A., Blundell Graduate Student, E., Puig Suari, J., and Twiggs, R., "CUBESATS AS RESPONSIVE SATELLITES."

[28] CalPoly, 2014, "Cubesat design specification (CDS)," p. 42.

[29] Swartwout, M., 2013, "The First One Hundred CubeSats : A Statistical Look," J. Small

Satell., **2**(2), pp. 213–233.

[30] Space Flight Now, "Launch Log" [Online]. Available: https://spaceflightnow.com/tracking/launchlog.html. [Accessed: 23-May-2017].

[31] Wertz, J. R., 2011, "Mission Objectives and Constraints (Step 1)," Space Mission Engineering: The New SMAD, J.R. Wertz, D.F. Everett, and J.J. Puschell, eds., Microcosm Press, Hawthorne, CA, pp. 45–60.

[32] Worland, J., 2016, "Climate Change Doubled the Size of Forest Fires in Western U.S., Study Says," Time [Online]. Available: http://time.com/4525178/climate-change-forest-fires/.

[33] 2016, "Total Wildland Fires and Acres (1960-2015)," Natl. Interag. Fire Cent. [Online]. Available: https://www.nifc.gov/fireInfo/fireInfo_stats_totalFires.html.

[34] "Global Warming and Wildfires," Natl. Wildl. Found.

[35] Flannigan, M., Cantin, A. S., De Groot, W. J., Wotton, M., Newbery, A., and Gowman, L. M., 2013, "Global wildland fire season severity in the 21st century," For. Ecol. Manage., **294**, pp. 54–61.

[36] NOAA National Centers for Environmental Information, 2017, State of the Climate: Global Analysis for Annual 2016.

[37] 2017, "Humans sparked 84 percent of US wildfires, increased fire season over two decades," Phys.org [Online]. Available: https://phys.org/news/2017-02-humans-percent-wildfires-season-decades.html. [Accessed: 01-Mar-2017].

[38] The Earth Institute, 2016, "Climate Change Has Doubled Western U.S. Forest Fires, Says Study," Columbia Univeristy [Online]. Available: http://www.earth.columbia.edu/articles/view/3343.

[39] Harvey, C., 2016, "Climate change has been makign western forest fires worse for decades, study says," Washington Post [Online]. Available: https://www.washingtonpost.com/news/energy-environment/wp/2016/10/10/climate-change-has-been-making-western-forest-fires-worse-for-decades-study-says/?utm_term=.8117d5bee850. [Accessed: 01-Mar-2017].

[40] Westerling, A. L., 2016, "Increasing western US forest wildfire activity: sensitivity to changes in the timing of spring.," Philos. Trans. R. Soc. Lond. B. Biol. Sci., **371**(1696), pp. 717–728.

[41] Browning, T. R., 2001, "Applying the design structure matrix to system decomposition

and Integration problems: a review and new directions," IEEE Trans. Eng. Manag., **48**(3), pp. 292–306.

[42] Holtta, K. M. M., and Salonen, M., 2003, "Comparing three modularity methods," Proc. ASME Des. Eng. Tech. Conf., p. 11.

[43] van Wie, M., Bryant, C. R., Bohm, M. R., Mcadams, D. A., and Stone, R. B., 2005, "A model of function-based representations," pp. 89–111.

[44] Grogan, P. T., and De Weck, O. L., 2015, "Interactive simulation games to assess federated satellite system concepts," IEEE Aerosp. Conf. Proc., **2015–June**.

[45] Brown, O., and Collopy, P., "Fractionated Spacecraft : Exploring Possible Futures of Space Systems," pp. 1–12.

[46] Huang, H., An, H., Wu, W., Zhang, L., Wu, B., and Li, W., 2014, "Multidisciplinary design modeling and optimizationfor satellite with maneuver capability," Struct. Multidiscip. Optim., **50**(5), pp. 883–898.

[47] Tafazoli, M., 2009, "A study of on-orbit spacecraft failures," Acta Astronaut., **64**(2–3), pp. 195–205.

[48] Langer, M., and Bouwmeester, J., 2016, "Reliability of CubeSats – Statistical Data, Developers' Beliefs and the Way Forward," AIAA/USU Conf. Small Satell.

[49] Wertz, J. R., 2011, "Space Mission Engineering," Space Mission Engineering: The New SMAD, pp. 45–60.

[50] Wertz, J. R., 2011, "Defining Alternative Mission Architechtures (Step 5) - Choosing the Pieces," Space Mission Engineering: The New SMAD, J.R. Wertz, D.F. Everett, and J.J. Puschell, eds., Microcosm Press, Hawthore, CA, pp. 61–66.

[51] Ploom, I., 2014, "Analysis of variations in orbital parameters of CubeSats," University of Tartu.

[52] Wertz, J. R., 2011, "Orbits and Astrodynamics," Space Mission Engineering: The New SMAD, pp. 197–234.

[53] FLIR, "Tau 2 Product Family Brochure."

[54] Everett, D. F., 2011, "Overview of Spacecraft Design," Space Mission Engineering: The New SMAD, pp. 397–438.

[55] Wood, J. S., 2011, "Launch Vehicles," Space Mission Engineering: The New SMAD, pp. 829–860.

[56] NASA, "Trajectories and Orbits" [Online]. Available:

https://www.hq.nasa.gov/pao/History/conghand/traject.htm. [Accessed: 29-Mar-2017].

[57] ISISpace, 2015, "CubeSat Structures," Online Store, pp. 2012–2014.

[58] ISISpace, "ISIS_CubeSat Structures_Brochure_v.7.11," pp. 11–12.

[59] CubeSatShop, "CubeSat Structures" [Online]. Available: https://www.cubesatshop.com/product-category/cubesat-structures/. [Accessed: 22-May-2017].

[60] IERS, 2004, General Definitions and Numerical Standards (1 June 2004).

[61] Snow, A., Buchen, E., and Olds, J. R., 2014, "Trends in Average Earth-Orbiting Spacecraft Launch Mass," (June), pp. 1–9.

[62] Brown, C. D., 1998, Spacecraft Mission Design Second Edition, American Institute of Aeronautics and Astronautics.

[63] Inter-Agency Space Debris Coordination Committee (IADC), 2010, "Space Debris Mitigation Guidelines of the Committee on the Peaceful Uses of Outer Space," p. 12.

[64] Starin, S. R., and Eterno, J., 2011, "Spacecraft Attitude Determination and Control Systems," Space Mission Engineering: The New SMAD, pp. 565–590.

[65] Glover Jr, D. R., 2001, "Dictionary of Technical Terms for Aerospace Use," NASA.

[66] "Moment of Inertia," Wikipedia [Online]. Available: https://en.wikipedia.org/wiki/Moment_of_inertia.

[67] CubeSpace, "CubeWheel."

[68] CubeSpace, "CubeTorquer & CubeCoil," p. 7600.

[69] Maryland Aerospace, "MAI-400."

[70] ISISpace, "Magnetorquer Board (iMTQ)."

[71] EXA, "MT01 Compact Magnetorquer."

[72] "CubeSat Attitude Actuators" [Online]. Available: https://www.cubesatshop.com/product-category/attitude-actuators/. [Accessed: 22-May-2017].

[73] Singh, R., Pentaleri, E., and Price, K. M., 2011, "Communications Payloads," Space Mission Engineering: The New SMAD, pp. 455–492.

[74] Helical Communication Technologies, "Helios Antenna."

[75] ISIS, "Antenna Systems."

[76] "CubeSat Antennas" [Online]. Available: https://www.cubesatshop.com/product-category/antenna-systems/. [Accessed: 22-May-2017].

[77] Ketsdever, A., “Lesson 2: Space Mission Geometry.”

[78] Hecht, H., 2011, “Reliability,” Space Mission Engineering: The New SMAD, pp. 753–767.

[79] Wertz, J. R., 2011, “Mission Concept Definition and Exploration,” Space Mission Engineering: The New SMAD, pp. 61–82.

[80] Norton, J. R., and Cloeren, J. M., 1994, “Precision quartz oscillators and their use aboard satellites,” Johns Hopkins APL Tech. Dig. (Applied Phys. Lab., **15**(1), pp. 30–37.

[81] “Duty Cycle,” Wikipedia [Online]. Available: https://en.wikipedia.org/wiki/Duty_cycle.

[82] ISISpace, 2015, “ISIS Ground Station Datasheet V2.2.”

[83] Spaceflight, 2017, “Ground Network Datasheet.”

[84] BridgeSat, “products/GROUND NETWORKS & SERVICES” [Online]. Available: http://www.bridgesatinc.com/products/#ground. [Accessed: 08-Mar-2017].

[85] Leaf Space, “Leaf Line” [Online]. Available: https://leaf.space/leaf-line/. [Accessed: 08-Mar-2017].

[86] Atlas Ground, “Space Operations as Service” [Online]. Available: http://www.atlasground.com/#about. [Accessed: 08-Mar-2017].

[87] Kongsberg Satellite Services, 2002, “Kongsberg Satellite Services,” (March), pp. 1–2.

[88] McDermott, J. K., and Schneider, J. P., 2011, “Power,” Space Mission Engineering: The New SMAD, pp. 641–662.

[89] GOMspace, 2012, “NanoPower Battery Datasheet,” p. 6.

[90] GOMSpace, “BPX Datasheet.”

[91] EnduroSat, “Electrical Power System (EPS) User Manual.”

[92] Burt, R., 2011, “Distributed Electrical Power System in Cubesat Applications.”

[93] Ismail, M. N., Bakry, A., Selim, H. H., and Shehata, M. H., 2015, “Eclipse intervals for satellites in circular orbit under the effects of Earth’s oblateness and solar radiation pressure,” NRIAG J. Astron. Geophys., **4**(1), pp. 117–122.

[94] EnduroSat, 2000, “Solar Panel,” p. 2010.

[95] GOMSpace, “NanoPower Datashee.”

[96] DHV Technology, “Solar Panels for Aerospace Applications.”

[97] Heidner, R., 2014, “Resolution Metrics for Space-Based Imagery Overview of Presentation.”

[98] Georgevic, R. M., 1971, “Mathematical Model of the Solar Radiation Force and Torques Acting on the Components of a Spacecraft,” pp. 33–494.

[99] Street, E., 2000, “Satellite Orbital Decay Calculations,” Flux.

[100] Alaska Aerospace, “Pacific Spaceport Complex - Alaska Range User’s Manual.”

[101] Virgina Space, “Space Access from Mid-Atlantic Regional Spaceport (MARS)” [Online]. Available: http://www.vaspace.org/index.php/space-access. [Accessed: 08-Mar-2017].

[102] Heyman, J., 2009, “FOCUS: CubeSats - A Costing + Pricing Challenge,” SatMagazine [Online]. Available: http://www.satmagazine.com/story.php?number=602922274. [Accessed: 07-Feb-2017].

[103] Zhang, M., and Berger, P., 2008, “The influence of technology evolution on technology adoption: a study of digital cameras,” Acadmey Manag. Conf.

[104] Balch, J. K., Bradley, B. A., Abatzoglou, J. T., Nagy, R. C., and Fusco, E. J., 2017, “Human-started wildfires expand the fire niche across the United States.”

[105] National Interagency Fire Center, 2016, “National Report of Wildland Fires and Acres Burned by State 2016.”

[106] Dale, L., 2010, “The True Cost of Wildfire in the Western U . S .,” West. For. Leadersh. Coalit., (April 2009), p. 18.

[107] National Interagency Fire Center, 2016, “Federal Firefighting Costs (Suppression Only).”

[108] National Interagency Fire Center, 2015, “National Report of Wildland Fires and Acres Burned by State 2015.”

[109] National Interagency Fire Center, 2014, “National Report of Wildland Fires and Acres Burned by State 2014.”

[110] National Interagency Fire Center, 2013, “National Report of Wildland Fires and Acres Burned by State 2013.”

[111] National Interagency Fire Center, 2012, “National Report of Wildland Fires and Acres Burned by State 2012.”

[112] National Interagency Fire Center, 2011, “National Report of Wildland Fires and Acres Burned by State 2011.”

[113] National Interagency Fire Center, 2010, “National Report of Wildland Fires and Acres Burned by State 2010.”

[114] National Interagency Fire Center, 2009, “National Report of Wildland Fires and Acres Burned by State 2009.”

[115] National Interagency Fire Center, 2008, “National Report of Wildland Fires and Acres Burned by State 2008.”

[116] National Interagency Fire Center, 2007, "National Report of Wildland Fires and Acres Burned by State 2007."

[117] National Interagency Fire Center, 2006, "National Report of Wildland Fires and Acres Burned by State 2006."

[118] National Interagency Fire Center, 2005, "National Report of Wildland Fires and Acres Burned by State 2005."

[119] National Interagency Fire Center, 2004, "National Report of Wildland Fires and Acres Burned by State 2004."

[120] National Interagency Fire Center, 2003, "National Report of Wildland Fires and Acres Burned by State 2003."

[121] National Interagency Fire Center, 2002, "National Report Wildland Fires and Acres Burned by State 2002."

[122] NOAA, "LEOSAR Satellite Coverage" [Online]. Available: http://www.cospas-sarsat.int/?option=com_content&view=article&id=196&catid=29&Itemid=154&lang=en. [Accessed: 11-Apr-2017].

[123] Arora, J. S., 2004, Introduction to Optimum Design, Iowa City Academic Press.

[124] Thompson, R., Colombi, J., and Black, J., 2014, "Computer-aided architecting of disaggregated space systems," IEEE Aerosp. Conf. Proc., (April 2016).

[125] Larson, W., and Wertz, J., eds., 1999, Space Mission Analysis and Design, Microcosm Press, El Segundo, CA.

[126] Fernandes, J., Henriques, E., Silva, A., and Moss, M. a., 2014, "Requirements change in complex technical systems: an empirical study of root causes," Res. Eng. Des., **26**(1), pp. 37–55.

7 APPENDICES

7.1 General Mission Requirements

Table 7.1 – Level 0 Mission Requirements

Level 0 Mission Requirements	
0	Decompose a monolithic spacecraft into a distinct set of two or more modules. Each of the modules should carry out one or more unique spacecraft system support functions that are shared and utilized by all other nodes while using SMAD's FireSat as a case study
ID	*Primary Objectives*
0.1	Modules must be comprised of CubeSats
0.2	Modules must be able to be deployed by the PPOD deployer
0.3	To detect, identify, and monitor forest fires throughout the United Sates, including Alaska and Hawaii, in near real time and at a low cost
ID	*Secondary Objectives*
0.4	To demonstrate to the public that positive action is underway to contain forest fires
0.5	To collect statistical data on the outbreak and growth of forest fires
0.6	To monitor forest fires for other countries
0.7	To collect other forest management data

In the table below, the struck out mission requirements are requirements that were eliminated when the mission changed from FireSat to FireSat II.

Table 7.2 – Level 1 Mission Requirements

Level 1 Mission Requirements	
ID	*Requirement*
1.01	All modules must abide by the appropriate CubeSat Standards as referenced in CubeSat Design Specification Rev. 13
~~1.02~~	~~The mission will be able to operate at 4 temperature levels.~~
1.03	The mission shall be able to detect forest fires at up to 50 m in resolution
1.04	The mission shall be able to determine forest fire locations within 1km geolocation accuracy
1.05	The mission shall be able to cover specified forest areas within the US at least twice daily
~~1.06~~	~~The mission will be able to send registered mission data within 30 min to 50 users~~
~~1.07~~	~~The mission will be able to operate at 4 temperature levels for pest management~~
1.08	The mission will last a minimum of 8 years
1.09	The mission must be operational 95% of the time excluding the weather
1.1	The mission will have a maximum 24 downtime
1.11	The mission is expected to survive natural environments only (not radiation belts)
1.12	The mission will be able to distribute data to up to 500 fire-monitoring offices and 2,000 rangers worldwide with a maximum of 100 simultaneous users
1.13	The mission will collect the location and extent in latitude and longitude for local plotting of fires in average temperature for each 40 m2 section
1.14	The mission will have a recurring cost of less than $3M/year
1.15	The mission will be operational within 3 years of initial launch
~~1.16~~	~~The mission will be at final operating capability within 6 years~~
~~1.17~~	~~The mission will adhere to all regulations that apply to NASA missions~~
1.18	The mission will be responsive to the public demand for action
1.19	The mission will be interoperable through NOAA ground stations
~~1.20~~	~~The mission will launch on STS or expendable launch vehicles~~
~~1.21~~	~~The mission will require no unique operations people at data distribution nodes~~
1.22	The mission will be able to work though light clouds
1.23	The mission will be able to identify an emerging forest fire within 8 hours with less than 10% false positives
1.24	The mission will send interpreted data to the end user within 5 min
1.25	The mission must be able to monitor changes in the mean forest temperature to +/- 2C
1.26	The mission will be commandable within 3 min of events
1.27	The mission will download units of stored coverage areas
1.28	The mission user will have a 10 x 20 cm display with zoom and touch controls as well as a built in GPS Quality Map
1.29	The mission will have a nonrecurring cost of less than $10 M
1.3	The mission must have higher than a 90% probability of success
1.31	The mission will adhere to all orbital debris regulations
1.32	The mission will adhere to all civil program regulations
1.33	The mission will fit within a Standard CubeSat Size

7.2 Sampled Cameras from FLIR

Table 7.3 – Sampled Cameras Used to Create Models

Sampled Cameras Used to Create Models												
Camera Name	*Array Format*	*Pixel Pitch (m)*	*f/N*	*HFOV (°)*	*VFOV (°)*	*iFOV (mRad)*	*Effective Focal Length (m)*	*Thermal Sensitivity (K)*	*Length (m)*	*Diameter (m)*	*Camera Weight (g)*	*Weight (g) {Camera + Lens}*
Boson 1	320x256	1.20E-05		92			2.30E-03	6.00E-02			7.5	
Boson 2	320x256	1.20E-05		50			4.30E-03	6.00E-02			7.5	
Boson 3	320x256	1.20E-05		34			6.30E-03	6.00E-02			7.5	
Boson 4	320x256	1.20E-05		24			9.10E-03	6.00E-02			7.5	
Boson 5	320x256	1.20E-05		16			1.40E-02	6.00E-02			7.5	
Boson 6	320x256	1.20E-05		12			1.80E-02	6.00E-02			7.5	
Boson 7	320x256	1.20E-05		6.1			3.60E-02	6.00E-02			7.5	
Boson 8	320x256	1.20E-05		4			5.50E-02	6.00E-02			7.5	
Boson 9	640x512	1.20E-05		50			8.70E-03	6.00E-02			7.5	
Boson 10	640x512	1.20E-05		32			1.38E-02	6.00E-02			7.5	
Boson 11	640x512	1.20E-05		24			1.80E-02	6.00E-02			7.5	
Boson 12	640x512	1.20E-05		18			2.50E-02	6.00E-02			7.5	

Table 7.3 – Sampled Cameras Used to Create Models Continued

Camera Name	*Array Format*	*Pixel Pitch (m)*	*f/N*	*HFOV (°)*	*VFOV (°)*	*iFOV (mRad)*	*Effective Focal Length (m)*	*Thermal Sensitivity (K)*	*Length (m)*	*Diameter (m)*	*Camera Weight (g)*	*Weight (g) {Camera + Lens}*
Boson 13	640x512	1.20E-05		12			3.60E-02	6.00E-02			7.5	
Boson 14	640x512	1.20E-05		8			5.50E-02	6.00E-02			7.5	
Boson 15	640x512	1.20E-05		5.5			7.30E-02	6.00E-02			7.5	
Tau 2 640 1	640x512	1.70E-05	1.40E+00	90	69	2.267	7.50E-03	5.00E-02	1.90E-02	2.90E-02		7.10E+01
Tau 2 640 2	640x512	1.70E-05	1.40E+00	69	56	1.889	9.00E-03	5.00E-02	1.90E-02	2.90E-02		7.20E+01
Tau 2 640 3	640x512	1.70E-05	1.25E+00	45	37	1.308	1.30E-02	5.00E-02	1.90E-02	2.90E-02		7.00E+01
Tau 2 640 4	640x512	1.70E-05	1.25E+00	32	26	0.895	1.90E-02	5.00E-02	1.90E-02	2.90E-02		7.00E+01
Tau 2 640 5	640x512	1.70E-05	1.10E+00	25	20	0.68	2.50E-02	5.00E-02	3.00E-02	4.20E-02		1.12E+02
Tau 2 640 6	640x512	1.70E-05	1.20E+00	18	14	0.486	3.50E-02	5.00E-02	3.90E-02	4.20E-02		1.50E+02
Tau 2 640 7	640x512	1.70E-05	1.20E+00	12.4	9.9	0.34	5.00E-02	5.00E-02	6.20E-02	5.80E-02		280
Tau 2 640 8	640x512	1.70E-05	1.25E+00	10.4	8.3	0.283	6.00E-02	5.00E-02	6.20E-02	6.10E-02		2.00E+02

Tau 2 640 9	640x512	1.70E-05	1.60E+00	6.2	5	0.17	1.00E-01	5.00E-02	1.10E-01	8.20E-02		479

Table 7.3 – Sampled Cameras Used to Create Models Continued

Camera Name	*Array Format*	*Pixel Pitch (m)*	*f/N*	*HFOV (°)*	*VFOV (°)*	*iFOV (mRad)*	*Effective Focal Length (m)*	*Thermal Sensitivity (K)*	*Length (m)*	*Diameter (m)*	*Camera Weight (g)*	*Weight (g) {Camera + Lens}*
Tau 2 336 1	336x256	1.70E-05	1.25E+00	45	35	2.267	7.50E-03	5.00E-02	1.90E-02	2.90E-02		7.10E+01
Tau 2 336 2	336x256	1.70E-05	1.25E+00	35	27	1.889	9.00E-03	5.00E-02	1.90E-02	2.90E-02		7.20E+01
Tau 2 336 3	336x256	1.70E-05	1.25E+00	25	19	1.308	1.30E-02	5.00E-02	1.90E-02	2.90E-02		7.00E+01
Tau 2 336 4	336x256	1.70E-05	1.25E+00	17	13	0.895	1.90E-02	5.00E-02	1.90E-02	2.90E-02		7.00E+01
Tau 2 336 5	336x256	1.70E-05	1.10E+00	13	10	0.68	2.50E-02	5.00E-02	3.00E-02	4.20E-02		1.12E+02
Tau 2 336 6	336x256	1.70E-05	1.20E+00	9.3	7.1	0.486	3.50E-02	5.00E-02	3.90E-02	4.20E-02		1.50E+02
Tau 2 336 7	336x256	1.70E-05	1.20E+00	6.5	5	0.34	5.00E-02	5.00E-02	6.20E-02	5.80E-02		280
Tau 2 336 8	336x256	1.70E-05	1.25E+00	5.5	4.2	0.283	6.00E-02	5.00E-02	6.20E-02	6.10E-02		2.00E+02
Tau 2 336 9	336x256	1.70E-05	1.60E+00	3.3	2.5	0.17	1.00E-01	5.00E-02	1.10E-01	8.20E-02		479
Tau 2 324 1	324x256	2.50E-05	1.25E+00	63	50	3.333	7.50E-03	5.00E-02	1.90E-02	2.90E-02		7.10E+01
Tau 2 324 2	324x256	2.50E-05	1.25E+00	49	39	2.778	9.00E-03	5.00E-02	1.90E-02	2.90E-02		7.20E+01

Tau 2 324 3	324x256	2.50E-05	1.25E+00	35	28	1.923	1.30E-02	5.00E-02	1.90E-02	2.90E-02		7.00E+01
Tau 2 324 4	324x256	2.50E-05	1.25E+00	24	19	1.316	1.90E-02	5.00E-02	1.90E-02	2.90E-02		7.00E+01

Table 7.3 – Sampled Cameras Used to Create Models Continued

Camera Name	*Array Format*	*Pixel Pitch (m)*	*f/N*	*HFOV (°)*	*VFOV (°)*	*iFOV (mRad)*	*Effective Focal Length (m)*	*Thermal Sensitivity (K)*	*Length (m)*	*Diameter (m)*	*Camera Weight (g)*	*Weight (g) {Camera + Lens}*
Tau 2 324 5	324x256	2.50E-05	1.10E+00	18	15	1	2.50E-02	5.00E-02	3.00E-02	4.20E-02		1.12E+02
Tau 2 324 6	324x256	2.50E-05	1.20E+00	13	10	0.714	3.50E-02	5.00E-02	3.90E-02	4.20E-02		1.50E+02
Tau 2 324 7	324x256	2.50E-05	1.20E+00	9.3	7.3	0.5	5.00E-02	5.00E-02	6.20E-02	5.80E-02		280
Tau 2 324 8	324x256	2.50E-05	1.25E+00	7.7	6.1	0.417	6.00E-02	5.00E-02	6.20E-02	6.10E-02		2.00E+02
Tau 2 324 9	324x256	2.50E-05	1.60E+00	4.6	3.7	0.25	1.00E-01	5.00E-02	1.10E-01	8.20E-02		479